CHEMICAL REVIEWS

pubs.acs.org/CR

Review

Emerging Engineered Wood for Building Applications

Yu Ding, Zhenqian Pang, Kai Lan, Yuan Yao, Guido Panzarasa, Lin Xu, Marco Lo Ricco, Douglas R. Rammer, J. Y. Zhu, Ming Hu, Xuejun Pan, Teng Li, Ingo Burgert, and Liangbing Hu*

Cite This: *Chem. Rev.* 2023, 123, 1843−1888

Read Online

ACCESS | Metrics & More | Article Recommendations

ABSTRACT: The building sector, including building operations and materials, was responsible for the emission of ∼11.9 gigatons of global energy-related CO_2 in 2020, accounting for 37% of the total CO_2 emissions, the largest share among different sectors. Lowering the carbon footprint of buildings requires the development of carbon-storage materials as well as novel designs that could enable multifunctional components to achieve widespread applications. Wood is one of the most abundant biomaterials on Earth and has been used for construction historically. Recent research breakthroughs on advanced engineered wood products epitomize this material's tremendous yet largely untapped potential for addressing global sustainability challenges. In this review, we explore recent developments in chemically modified wood that will produce a new generation of engineered wood products for building applications. Traditionally, engineered wood products have primarily had a structural purpose, but this review broadens the classification to encompass more aspects of building performance. We begin by providing multiscale design principles of wood products from a computational point of view, followed by discussion of the chemical modifications and structural engineering methods used to modify wood in terms of its mechanical, thermal, optical, and energy-related performance. Additionally, we explore life cycle assessment and techno-economic analysis tools for guiding future research toward environmentally friendly and economically feasible directions for engineered wood products. Finally, this review highlights the current challenges and perspectives on future directions in this research field. By leveraging these new wood-based technologies and analysis tools for the fabrication of carbon-storage materials, it is possible to design sustainable and carbon-negative buildings, which could have a significant impact on mitigating climate change.

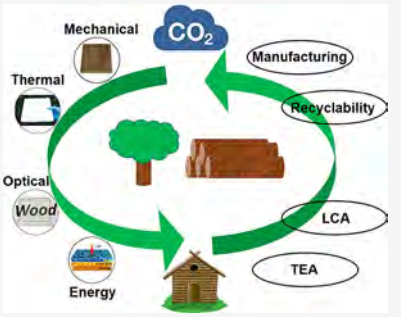

CONTENTS

Special Issue: Sustainable Materials

Received: June 29, 2022
Published: October 19, 2022

https://doi.org/10.1021/acs.chemrev.2c00450
Chem. Rev. 2023, 123, 1843−1888

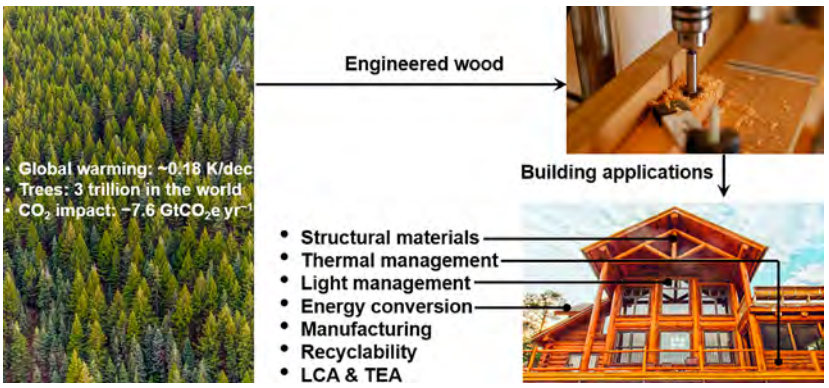

Figure 1. Carbon impact of using wood for building applications. There are around 3 trillion trees on earth, which can give rise to the carbon impact of $-7.6\ GtCO_2e\ yr^{-1}$ by estimation and alleviate the global warming issue. Modified wood products can not only be used as structural materials but also for thermal management, light management, and energy conversion applications. Moreover, manufacturing, recyclability, LCA, and TEA should be considered to meet the requirement within the context of building applications.

1. INTRODUCTION

Climate change due to anthropogenic emissions of greenhouse gases is posing a mounting threat to human welfare and the health of the planet. Global CO_2 emissions total ~36 billion metric tons every year, primarily from the burning of fossil fuels.[1] As a result, the global annual average temperature has risen by over 0.7 °C between 1986−2016 in comparison to the period of 1901−1960.[2] Furthermore, petroleum-based materials are nonrenewable, forcing the chemicals and materials industry to pivot to renewable resources. Addressing these daunting challenges toward a sustainable future requires immediate action via the development and use of renewable materials with low or even negative carbon footprints. Wood features promising structural and functional properties with added environmental benefits. As such, it provides a multifaceted solution to sustainability challenges.

Trees are abundant and globally planted, with ~3 trillion trees on Earth (equivalent to ~400 trees/person, Figure 1).[3] It is estimated that 1.8 kg of CO_2 can be removed from the atmosphere per kg of dry wood via photosynthesis.[4] Therefore, both the Intergovernmental Panel on Climate Change (IPCC) reports and Paris Agreement underscore the importance of promoting forest conservation and enhancing forest carbon stocks to realize net zero anthropogenic emissions.[5] Between 2001 and 2019, global forests annually absorbed ~15.6 billion metric tons of CO_2 from the Earth's atmosphere.[6] However, deforestation, wildfires, and other disturbances emitted ~8.1 billion metric tons of CO_2 each year.[6] Improving the performance of wood products to match or even outperform traditional nonrenewable counterparts could promote the use of renewable wood sources and improve forest management.[1]

In addition to the superior carbon sequestration capability, wood is attractive for structural applications, as it has a unique hierarchical structure made of ~40% cellulose embedded in a matrix of hemicelluloses and lignin.[7] The cellulose elementary fibrils in wood, with diameters of ~3 nm, exhibit outstanding material properties for a broad range of applications,[8] for example, demonstrating a tensile strength as high as 7.5 GPa in the crystalline form, which is higher than most metals and alloys.[9] However, conventional bottom-up approaches for extracting cellulose fibrils from wood and other plant biomass require significant energy, chemicals, and water, ultimately challenging the sustainability of the material.[10,11] Alternatively, the top-down in situ modification of the natural wood structure (e.g., selectively removing lignin and/or hemicelluloses by chemical treatment) is a less energy and resource-intensive process to transform natural wood into strong structural materials. This approach can also open nanopores within the cell walls and between the cellulose molecular chains while still maintaining the overall anisotropic structure of wood, and such a special structure enables a broad range of applications. Therefore, the top-down engineering method makes it possible to fabricate unique wood-based structures for a new class of sustainable, advanced structural materials that feature exceptional properties, especially in terms of mechanical performance for construction applications (Figure 1).[12,13]

Historically, wood was one of the earliest structural materials employed by humans and has remained a widely used, biodegradable construction material, with annual consumption increasing from 5.2 million metric tons in the 1950s to 6.4 million metric tons in the 1990s.[14] Currently, novel engineered wood products continue to be developed and introduced into the construction marketplace, spurred by the globally increasing demand for sustainable and economical housing. Innovative engineered wood products with superior performance make it possible to build even high-rise buildings.[14] For example, the 25-story Ascent building, recently constructed in Milwaukee, features 18 stories of mass timber framing on top of 7 stories of a concrete parking structure, reaching a height of 86.56 m. This ranks among the tallest mass timber structures in the world and makes Ascent the tallest residential tower mostly

https://doi.org/10.1021/acs.chemrev.2c00450
Chem. Rev. 2023, 123, 1843−1888

constructed of wood. It is projected that the annual demand for engineered wood products could reach >20 million metric tons in 2030.[14]

In this review, we discuss novel modified wood products for construction applications along with ways modified wood can be incorporated into engineered wood products for improved performance. For clarity in this paper, an engineered wood product (EWP) is defined as wood product that is manufactured by gluing or fixing the strands, particles, fiber, veneers, or boards of wood together. EWPs are fabricated and tested according to approved national or international specifications or standards to ensure durable, structural performance. With scaled-up production, chemically and mechanically modified wood has the potential to enhance performance, decrease costs, and therefore boost economics. Besides economy, the eco benefits of durable wood building products enable smaller carbon footprints of construction and facilitate net negative carbon emission objectives. Herein, we explore recent progress in the field of how modified wood is used within the context of carbon storage in buildings. Our fundamental understanding of the intrinsic properties of wood is discussed to highlight examples of multiscale structural design, processing, and applications. Moreover, insights from modeling across multiscales are covered to guide the optimization of new wood-based products in terms of mechanics. Subsequently, we critically analyze various chemical modification approaches to fabricating modified wood by following the principles of green chemistry. The resulting performance of modified wood in terms of mechanical, thermal, optical, and electrochemical properties is elaborated as well. We then discuss the carbon and environmental impacts of engineered wood products based on life cycle assessment (LCA) studies, especially recent development in dynamic LCAs, which track temporal changes of carbon flows associated with forest ecosystems and buildings. Furthermore, we analyze the existing techno-economic analysis (TEA) of engineering wood products and highlight the main factors driving economic feasibility. Finally, current challenges and future perspectives are discussed. We hope that this timely review will not only provide a guideline to design advanced wood products incorporating modified wood for building applications but also promote more interest to build a sustainable future.

2. MECHANICS OF MODIFIED WOOD: INSIGHTS FROM MODELING ACROSS SCALES

In natural wood, cellulose, hemicelluloses, and lignin are the three major building blocks. They play different roles in the resulting mechanical properties of the wood. A cellulose molecule is a linear chain of tens of thousands of anhydroglucose units connected by β-1,4 glycosidic bond.[15,16] The cellulose elementary fibrils contain both crystalline and paracrystalline regions. The crystalline region is conserved by stacked parallel cellulose chains to each other and bound via inter- and intrahydrogen bonding. In the paracrystalline region, abundant twists and distortions exist in between cellulose chains that alter the ordered arrangement. Failure of wood materials often derives from the sliding of these molecular chains.[17,18] Thus, the length or the degree of polymerization of the cellulose chains plays an important role in dictating the strength and toughness of wood.[19] Hemicelluloses consist of numerous branched polysaccharides.[15] Softwood is rich in galactoglucomannans, while hardwood mainly contains glucuronoxylan.[20] Lignin is one of the three major components of wood, with a content of 15−30%, depending on the species. Lignin plays critical biological and structural roles in plants. It is part of the plant defensive system protecting against degradation by insects, pathogens, and UV radiation. Lignin also provides the cell wall with hydrophobicity, preventing water permeation and thus helping wood tissue to transport water, nutrients, and photosynthesis products. In addition, lignin functions as a binder holding the cells (fibers) together to form a strong and tough wood matrix. These three roles of lignin confer to plant biomass strong resistance against chemical and enzymatic degradation. Lignin is an amorphous polymer composed of three building units (guaiacyl, syringyl, and *p*-hydroxyphenyl).[21] Syringyl units dominate in hardwood lignin, while guaiacyl units in softwood lignin.[19,21,22] Furthermore, lignin is usually covalently bound with hemicelluloses and forms lignin−carbohydrate complexes.[22−24] It has been confirmed that there are eight different types of lignin−carbohydrate (L−C) bonds, including benzyl ether, benzyl ester, glycosidic or phenyl glycosidic, hemiacetal or acetal linkages, and ferulate or diferulate esters that are linked to lignin at 4-OH and 4-O positions.[23,25,26] The matrix of intertwined hemicelluloses and lignin, namely lignin−carbohydrate complex (LCC), gives rise to the abundance of hydrogen bonds and thus results in high adhesion energy with cellulose microfibrils. Their synergistic interaction determines the strength and stiffness of cell wall fibril.[16,27−29] Overall, the isolated and collective mechanical behavior of these three building blocks, as well as the interactions between them, directly affect the mechanical properties of natural wood and modified wood.

However, it remains a challenge to use experimental methods to directly characterize and visualize the internal interaction in the building blocks of wood materials, the evolution process of bonding and failure within and in between the building blocks under loading conditions, and the transition states between original natural wood and modified wood that is chemically treated, especially at small scales (e.g., the molecular- and nanoscale). To this end, computational modeling is widely utilized to resolve such a challenge. This section mainly summarizes the research progress on understanding and tailoring the mechanical properties of natural and engineered wood through multiscale modeling (Figure 2): at the molecular scale (by density functional theory (DFT) simulation), fibrillar scale (by classic molecular dynamic (MD) simulation), micro-/mesoscale (by coarse-grained (CG) MD simulation), and macroscale (by finite element models (FEM)), with a special focus on the interactions between the building blocks at such scales.

2.1. Molecular Scale

This subsection focuses on the fundamental mechanisms that govern the interactions in cellulose, hemicelluloses, and lignin at the molecular scale, as revealed by DFT and MD simulations of the basic units of these three building blocks of wood materials. Hemicelluloses have been barely studied at the molecular scale.[30] Thus, this subsection will review mainly cellulose and lignin.

Cellulose is the most abundant component in wood and forms the main framework of the wood nanostructure. Thus, a better understanding of the interaction and behaviors among its building blocks (anhydroglucose units) is crucial in understanding the mechanical properties of modified wood. The cellulose chains are mainly bonded together via hydrogen bonds between the hydroxyl groups in neighboring glucose units. The

https://doi.org/10.1021/acs.chemrev.2c00450
Chem. Rev. 2023, 123, 1843−1888

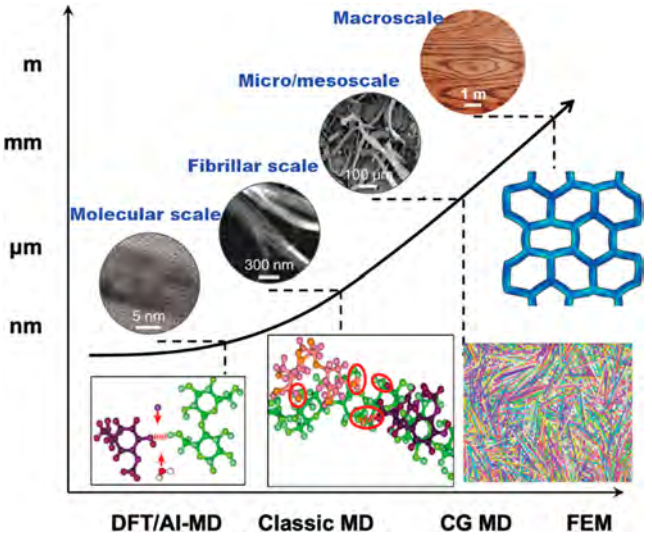

Figure 2. Hierarchical structure of natural and modified wood, and the corresponding multiscale modeling strategies: at the molecular scale (by density functional theory (DFT) simulations), fibrillar scale (by classic molecular dynamic (MD) simulations), micro-/mesoscale (by coarse-grained (CG) MD simulations), and macroscale (by finite element models (FEM) simulations).

sliding failure process of a wood material nanostructure involves a cascade of events of hydrogen bond formation, breaking, and reformation in neighboring cellulose chains (Figure 3A), which can be captured by the energy variation of the molecular simulation model.[31] For example, the decrease and increase of energy correspond to the breaking and reformation of hydrogen bonds, respectively. The peak of the energy curve indicates that the hydrogen bonds are stretched to the maximum. Then these hydrogen bonds break, as indicated by the drop in the energy. But new hydrogen bonds can readily form when the new hydroxyl groups come close to each other upon further sliding deformation, as evidenced by the rise of the energy curve from a local trough. Such a cascade of events of breaking and reformation of the hydrogen bonds gives rise to the zigzag profile of the energy curve, revealing a unique toughening mechanism in modified wood and cellulose-based materials.[31,37]

Given the hydrophilic nature of cellulose and the polarity of water molecules, water plays a crucial role in the bonding between cellulose chains. Figure 3B shows the hydrogen bonds along the cellulose interfaces without and with water molecules.[32] Water molecules increase the distance between neighboring cellulose fibrils but facilitate the formation of cellulose−water−cellulose hydrogen bonds. Even though the single hydrogen bond between cellulose and water is weaker than that between the cellulose chains, the significant increase in the number of hydrogen bonds (cellulose−water−cellulose) effectively enhances the bonding, as evidenced by the increased index values of the average energy barriers in sliding (Figure 3C). As a result, the average strength of the newly formed hydrogen bonds is 306% higher than that of the hydrogen bonds in the structure without water (as indicated by the red and blue dashed lines in Figure 3C).

Ion intercalation is another efficient method to enhance intrinsic interaction between carboxylated cellulose molecules in chemically treated engineered wood. Carboxylated cellulose intercalated with monovalent ions is less stable than that with divalent ions.[38] However, Williams et al. found that the ion valency is not sufficient to explain the trends of the interaction between carboxylated cellulose and metallic ions (Figure 3D).[33] In their DFT simulations, transition metal cations that intercalate between carboxylated cellulose nanofibrils can form coordination-covalent bonds with multiple carboxylate $-COO^-$ groups on opposite fibrils, which is hard to form between the other metallic ions and fibrils. This is mainly because of the unfilled valence *d* orbitals in the transition metal elements. In addition, Ca^{2+} can bond tightly with both $-COO^-$ groups and $-OH$ groups of carboxylated cellulose chains (Figure 3E),[34] which results in a much higher binding energy of the cross-linked cellulose foam (Figure 3F). The higher binding energy endows a cellulose-based composite foam with better stability and much higher compressive strength. Such an enhancement effect is also found in the gelation of cellulose solutions.[35] In the process of physical gelation, the cellulose chains self-associate with each other and form a heterogeneous network with "thick" walls, as shown in the sketch in Figure 3G. Chemical gelation can perturb cellulose chain self-association and decrease the crystallinity of cellulose (Figure 3H), as well as increase swelling in water and forming a more porous structure,[39] which results in better toughness.

The main functional groups in three basic units of lignin include methoxyl ($-OCH_3$), phenolic and aliphatic hydroxyl ($-OH$), and carbonyl ($-C{=}O$) groups.[40,41] Modifying the interactions between these groups is shown to be effective to enhance the mechanical stability of modified woods. Jeong et al.[36] proposed three possible binding sites of different alkaline earth metals on the lignin units and obtained the associated binding energy values (Figure 3I). They found that the metal ions linked O (C_β) and O (methoxy), defined as Model 2 in Figure 3I, has the highest binding energy of the complex structure. The lignin intercalated with alkaline earth metals forms the half-sandwich structure, which is difficult to decompose and requires higher activation energy. These results open the opportunities through introducing alkali and alkaline earth metals to obtain a stable lignin-based structure.

2.2. Fibrillar Scale

Modeling at the fibrillar scale can be used to investigate the dynamic evolution of the structures and analyze the interaction among the fibers in modified wood. Modeling at this scale can be implemented through the classic MD simulations to predict the mechanical responses and underlying mechanisms that govern the mechanical properties (e.g., strength and toughness) of modified wood.

The tensile failure of natural and modified wood often originates from the relative sliding between the aligned cellulose fibrils in the wood (Figure 4A).[42] Cellulose fibrils are constituted of crystalline cellulose chains, and the shearing interface often occurs between the (110) crystal plane of one cellulose fibril and the (110) crystal plane of another cellulose fibril (termed as (110)−(110) interface). Therefore, it is important to understand the sliding behavior of neighboring cellulose fibrils, in particular, the shearing behavior on the (110)−(110) interface. Figure 4A shows the evolution of hydrogen bonds along with the (110)−(110) interface as a function of the shearing distance. During continuous shearing at the (110)−(110) interface, the −OH groups are alternatively aligned (locations 1 and 3 of insert in Figure 4A) and misaligned (location 2 of insert in Figure 4A). When the cellulose chains are aligned across the interface, it corresponds to the local maximum number of hydrogen bonds formed at the interface (locations 1 and 3 as in Figure 4A). When

https://doi.org/10.1021/acs.chemrev.2c00450
Chem. Rev. 2023, 123, 1843−1888

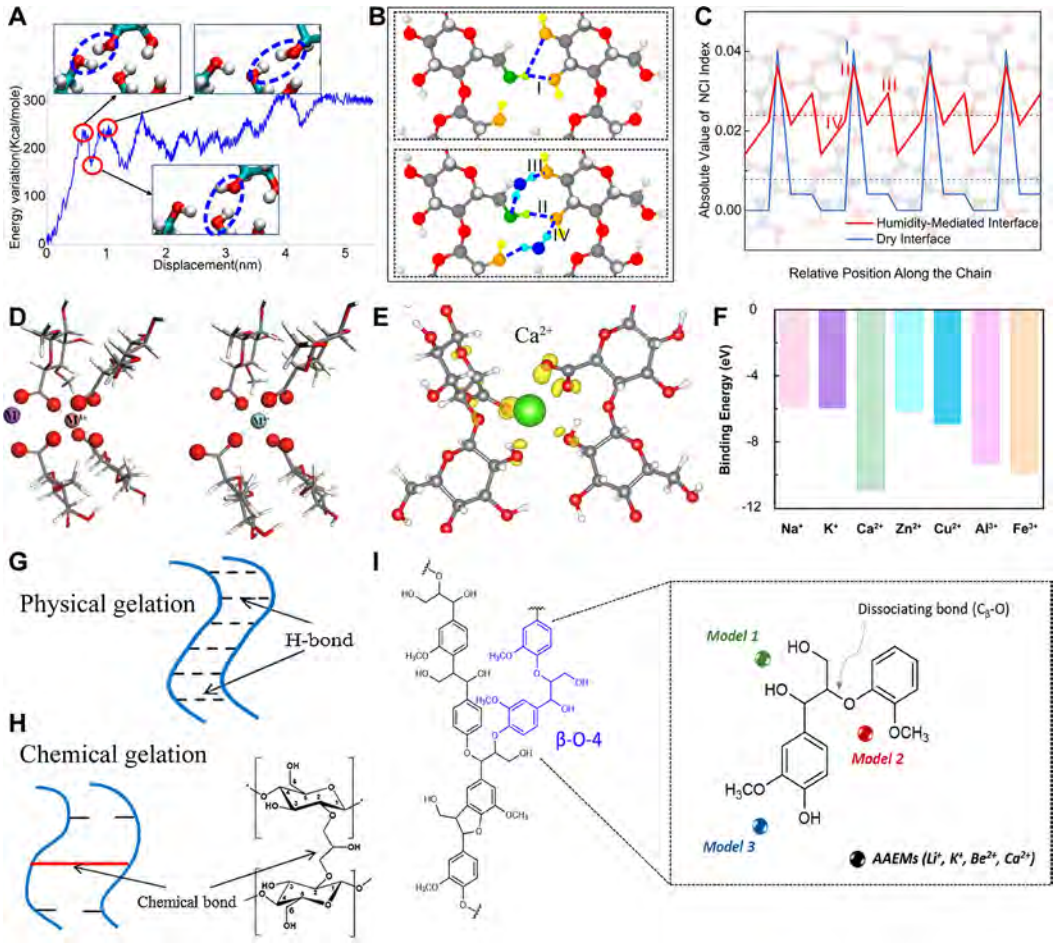

Figure 3. Internal interactions in cellulose, hemicellulose, and lignin in modified wood at the molecular scale. (A) Energy variation of cellulose molecules as the function of the sliding displacement between cellulose molecules.[31] Reproduced with permission from ref 31. Copyright 2015 U.S. National Academy of Sciences. (B) The hydrogen bonds along the cellulose interfaces without and with water molecules.[32] Reproduced with permission from ref 32. Copyright 2021 American Chemical Society. (C) The index values of the energy barriers in the process of sliding.[32] Reproduced with permission from ref 32. Copyright 2021 American Chemical Society. (D) The interaction between metal cations and cellulose chains.[33] Reproduced with permission from ref 33. Copyright 2013 Elsevier. (E) Charge density differences of Ca^{2+} ions-intercalated cellulose. The yellow region represents the gain of electrons.[34] Reproduced with permission from ref 34. Copyright 2022 American Chemical Society. (F) The binding energy between cellulose and different metal ions.[34] Reproduced with permission from ref 34. Copyright 2022 American Chemical Society. (G) The schematic of physical gelation formation in the cellulose solution.[35] Reproduced with permission from ref 35. Copyright 2003 American Chemical Society. (H) The schematic of chemical gelation formation in the cellulose solution.[35] Reproduced with permission from ref 35. Copyright 2003 American Chemical Society. (I) Three possible binding sites of different alkaline earth metals on the lignin units.[36] Reproduced with permission from ref 36. Copyright 2020 American Chemical Society.

the cellulose chains become misaligned (from location 1 to 2), a few original hydrogen bonds break and the left cellulose chains (inset in Figure 4A) begin to reform the new hydrogen bonds with the next cellulose on the right chains, resulting in a number decrease in the whole hydrogen bonds (location 2 of Figure 4A) in the system. This dynamic variation in the number of hydrogen bonds, corresponding to the continuous breaking and reformation of hydrogen bonds, aids in the resistance to failure.

Water molecules can form hydrogen bonds with different cellulose chains and influence the breaking and reformation behaviors of the hydrogen bonds in wood under mechanical loading. Thus, the water content in wood plays a crucial role in the shearing behaviors of the cellulose fibrils. When water molecules were introduced at the interface of the cellulose fibrils (Figure 4B), Young's modulus of the cellulose nanocrystal-based hierarchical structure is almost a constant as the change of interfacial water content,[32] which is due to the initial linear elastic stage of interlayer sliding. However, the fracture energy and peak stress increase significantly with the increase in water content. But the enhancement of the strength and toughness are limited by a reasonable range. When the water content is larger than 3.75 H_2O/nm^2, the interfacial interaction is weakened by the hydrogen bonds between water molecules, which results in lower fracture energy. Recent experimental research successfully obtained strong and tough wood by a three-step process of delignification, drying-induced assembly, and water molecules-induced hydrogen bonding under compression. The resulting wood has a densified structure with improved mechanical properties (2.4 times increase in tensile strength, 2.7 times increase in Young's modulus, and 1.4 times increase in density) in comparison with natural wood.[46]

To better understand the deformation mechanism of the shearing behavior of wood materials, Jin et al.[43] built a sandwich model of the wood cell wall with cellulose, hemicellulose, and lignin (Figure 4C). The cellulose sheets form the bottom and top layers, while the hemicellulose and lignin fill the gap in

https://doi.org/10.1021/acs.chemrev.2c00450
Chem. Rev. 2023, 123, 1843−1888

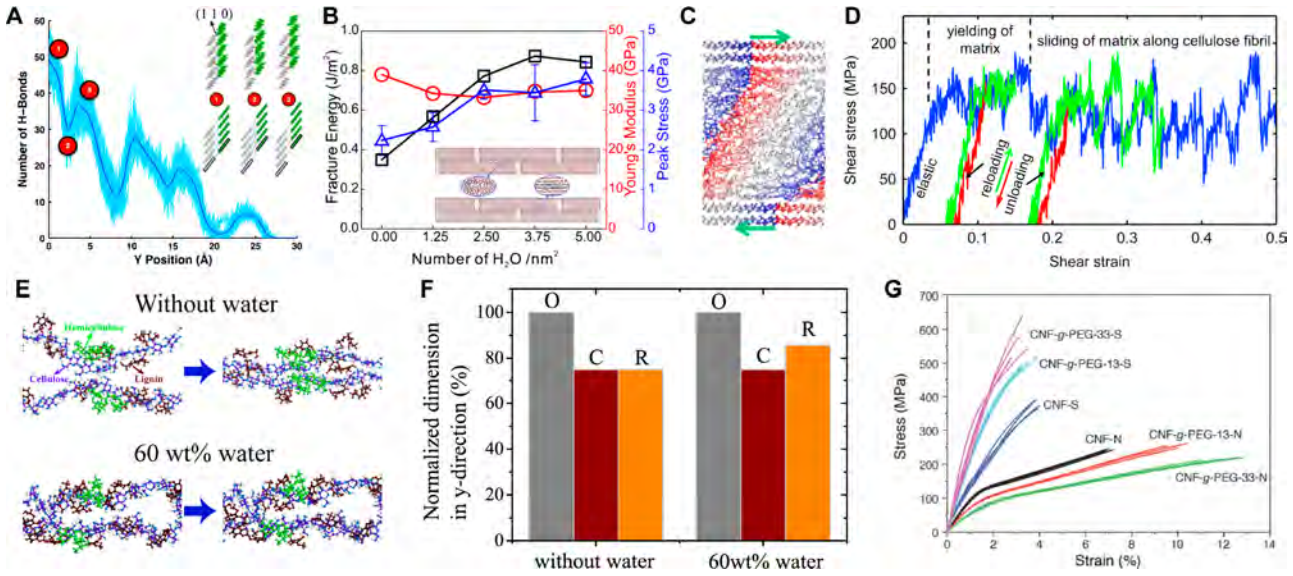

Figure 4. Mechanical response and enhancement of modified wood at the fibrillar scale. (A) Hydrogen bonds along with the (110)−(110) interface as a function of the distance the fibrils have been sheared during simulation.[42] Reproduced with permission from ref 42. Copyright 2015 Elsevier. (B) Summarized mechanical properties of the nanocellulose model with a (010) crystal plane as a function of the number of H_2O molecules.[32] Reproduced with permission from ref 32. Copyright 2021 American Chemical Society. (C) The sandwich model of the wood cell wall with cellulose (outmost layer), hemicellulose (secondary outer layer), and lignin (middle layer).[43] Reproduced with permission from ref 43. Copyright 2015 Elsevier. (D) A representative stress−strain response of the sandwich model in Figure 3C.[43] Reproduced with permission from ref 43. Copyright 2015 Elsevier. (E) Morphological derivation of elastic wood without and with 60 wt % water in the process of compression and release.[44] Reproduced with permission from ref 44. Copyright 2020 American Chemical Society. (F) Normalized dimension of the models in (E) in the *y*-direction before compression, after compression, and after the release of the compression.[44] Reproduced with permission from ref 44. Copyright 2020 American Chemical Society. (G) Stress−strain curves of the nonstretched (−N) and stretched (−S) cellulose ribbons of CNF, CNF-*g*-PEG-13, and CNF-*g*-PEG-33.[45] Reproduced with permission from ref 45. Copyright 2015 John Wiley and Sons.

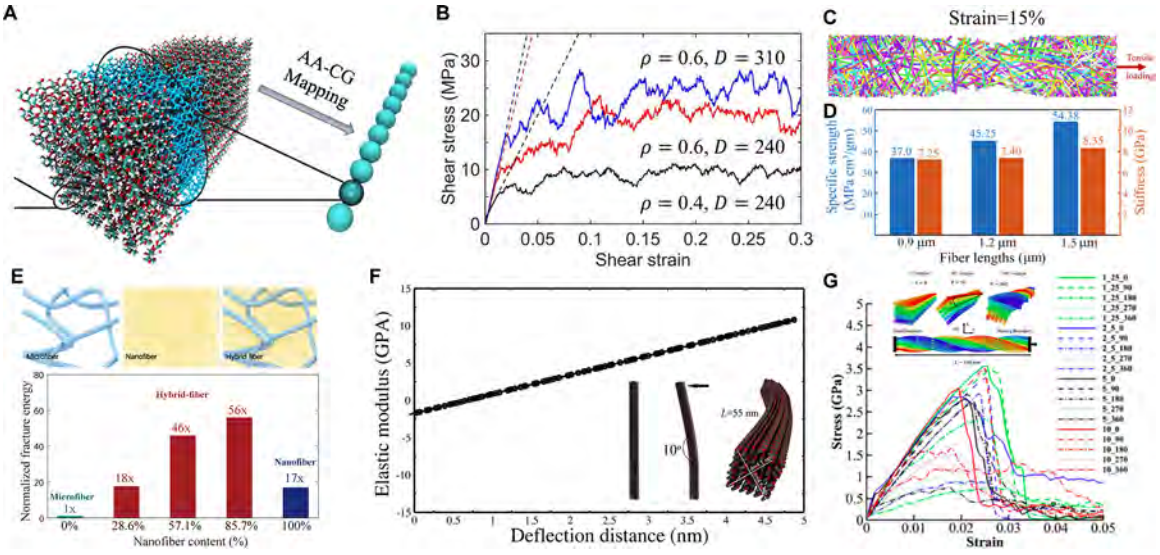

Figure 5. Mechanical response of modified wood at micro-/mesoscale. (A) CG modeling of the cellulose nanocrystals.[47] Reproduced with permission from ref 47. Copyright 2020 Elsevier. (B) Representative shear stress−strain response of bulk CNCs for different densities and cohesive interaction.[47] Reproduced with permission from ref 47. Copyright 2020 Elsevier. (C) The deformation snapshots of a CG model of cellulose fiber network under a tensile strain = 15%.[48] Reproduced with permission from ref 48. Copyright 2021 Springer. (D) Comparisons of the specific strength and stiffness of the cellulose fiber network with varying fiber lengths.[48] Reproduced with permission from ref 48. Copyright 2021 Springer. (E) Schematic morphology and normalized fracture energy of cellulose films made of microfibers, nanofibers, and hybrid fibers.[17] Reproduced with permission from ref 17. Copyright 2020 John Wiley and Sons. (F) Elastic modulus of a CG microfiber as a function of deflection distance.[49] Reproduced with permission from ref 49. Copyright 2015 American Chemical Society. (G) Stress−strain curves for different bundle sizes and twist angles.[50] Reproduced with permission from ref 50. Copyright 2019 MDPI.

between. The stress−strain curves of the model under shear loading are illustrated in Figure 4D and can be divided into three regimes: an initial elastic regime and two plastic regimes. The first plastic regime is dominated by the yielding of the matrix, and the second one is derived from the "self-healing" interface. Additionally, the self-healing behavior in wood materials can

https://doi.org/10.1021/acs.chemrev.2c00450
Chem. Rev. 2023, 123, 1843−1888

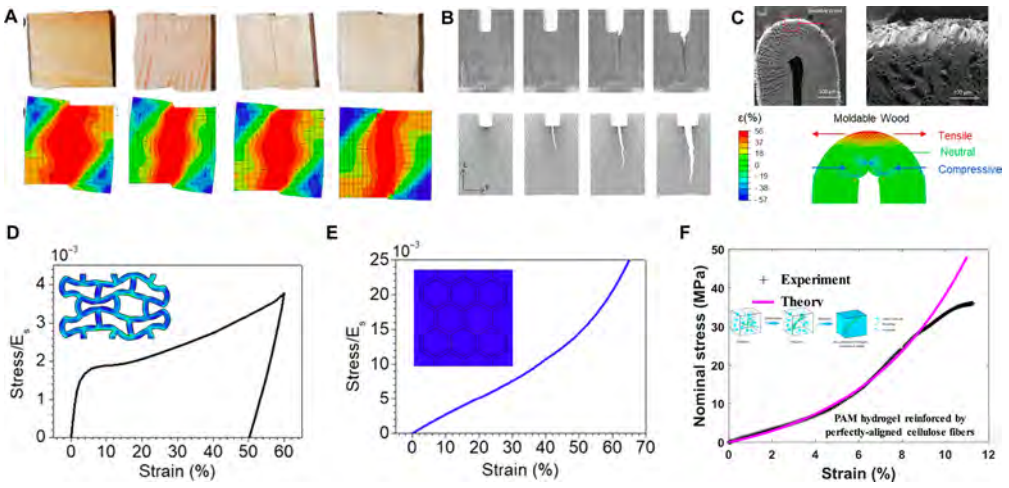

Figure 6. Mechanical response of natural and modified wood at the macroscale. (A) Mechanical response of natural wood under shearing test. The panels from left to right represent the shearing perpendicular to the fibers in the tangential plane and radial plane and along the fibers in the radial plane and tangential plane, respectively. The bottom panel are responding to stress distribution at the elastic−plastic range of wood in the FEM simulation.[55] Reproduced with permission from ref 55. Copyright 2021 MDPI. (B) Crack initiation and propagation of the engineered wood in the experimental test and FEM simulations.[56] Reproduced with permission from ref 56. Copyright 2018 Springer. (C) SEM and stress distribution of engineered wood under folding.[57] Reproduced with permission from ref 57. Copyright 2021 American Association for the Advancement of Science. Loading−unloading curve of the natural wood (D) and wood-based gel (E).[44] Reproduced with permission from ref 44. Copyright 2020 American Chemical Society. (F) A theoretical model can predict the stress−strain relation of cellulose-fiber-reinforced PAM hydrogels under uniaxial tension, which agrees well with experimental results.[58] Reproduced with permission from ref 58. Copyright 2020 Elsevier.

also be influenced by water molecules.[44] Chen et al. fabricated a highly elastic wood via chemical treatment and freeze-drying. This elastic wood can, after hydration, sustain a compressive strain of up to 70% with negligible plastic deformation and a small energy loss coefficient. However, dehydrated elastic wood cannot self-heal. To understand the mechanism of the self-healing behavior, they constructed the fibrillar modeling of wood framework with and without water, as shown in Figure 4E. Subject to compression, the cellulose chains without water come close and form new hydrogen bonds between one chain to another chain. Water molecules in between the cellulose chains can limit the formation of the new hydrogen bonds between the cellulose chains and help to push the chains to their original location. The two scenarios of the simulations elaborated for the recovery behavior of the elastic wood are illustrated in Figures 4E,F.

Due to the hydroxyl groups on the surface of cellulose, CNFs can also be modified by polymers, which results in stronger cross-linking under loading. Tang et al.[45] prepared CNF grafted with polyethylene glycol (CNF-*g*-PEG) from pulp fibers and then tested their stress−strain curve under tension (Figure 4G). The prestretched (−S) and nonstretched (−N) cellulose ribbons were prepared by drying the stretched and nonstretched hydrogel stripes of CNF-*g*-PEG nanofibrils. As shown in Figure 4G, the stretched cellulose ribbons have a higher strength as well as a lower failure strain than the nonstretched ones, which is because the stretched ribbons prevent the interfibrillar debonding and slippage of nanofibrils. An increased grafted amount of the PEG in the stretched CNFs leads to an increase in the strength of the cellulose ribbons, which can be attributed to the enhanced interfibrillar interaction. The above understanding of the enhanced strength of cellulose ribbons made of polymer grafted CNFs offers insight into guiding the design of engineered wood with improved mechanical performance.

2.3. Micro-/Mesoscale

The length of the cellulose fibers in wood materials is in the range of several nanometers to several millimeters. The superlarge scale and cross-scale simulations of these fibrils make classic MD simulations prohibitive in terms of required time and resources. Therefore, coarse-grained (CG) MD simulations emerge as effective methods to solve the limitation and reveal the mechanism of the interfibrillar interaction at the micro-/mesoscale.[47,48]

Li et al.[47] represented the cellulose nanocrystal (CNC) units with the 36 chain as a CG bead (Figure 5A) and calculated the shear behavior of the bulk CNC random network (Figure 5B). The shear modulus and yield strength of the bulk system increase as significantly as the increase of density and cohesive energy between CNCs. However, such CG modeling is restricted to the specific diameter of the fibrils. Recently, a scalable CG scheme based on atomistic simulations[48] was used to model CNC where the mapping and interaction potentials are scaled on three different levels (levels 1−3). The level 1 bead represents 1 glucose unit, and then six level 1 beads are mapped into one level 2 bead. Subsequently, seven level 2 chains form one level 3 bead. Random networks of cellulose fibers made of level 3 CG beads are constructed to analyze their mechanical response and failure behavior. When a uniaxial tension is applied, the randomly oriented cellulose fibers start to slide apart from each other. As the tensile strain increases, cracks initiate at the edges and result in stress concentration and localized deformation (Figure 5C,D). The specific strength of the network increases as the cellulose fiber length increases. It means that longer cellulose fibers can resist more tensile deformation as higher energy is required to cause the failure of the random network of cellulose fibers. The CG modeling is also applied to understand the mechanical behaviors of cellulose films (Figure 5E).[17] It shows that the fracture energy of a cellulose film made of nanofibers is 17 times higher than that of a cellulose film made of microfibers. The film made of microfiber

https://doi.org/10.1021/acs.chemrev.2c00450
Chem. Rev. 2023, 123, 1843−1888

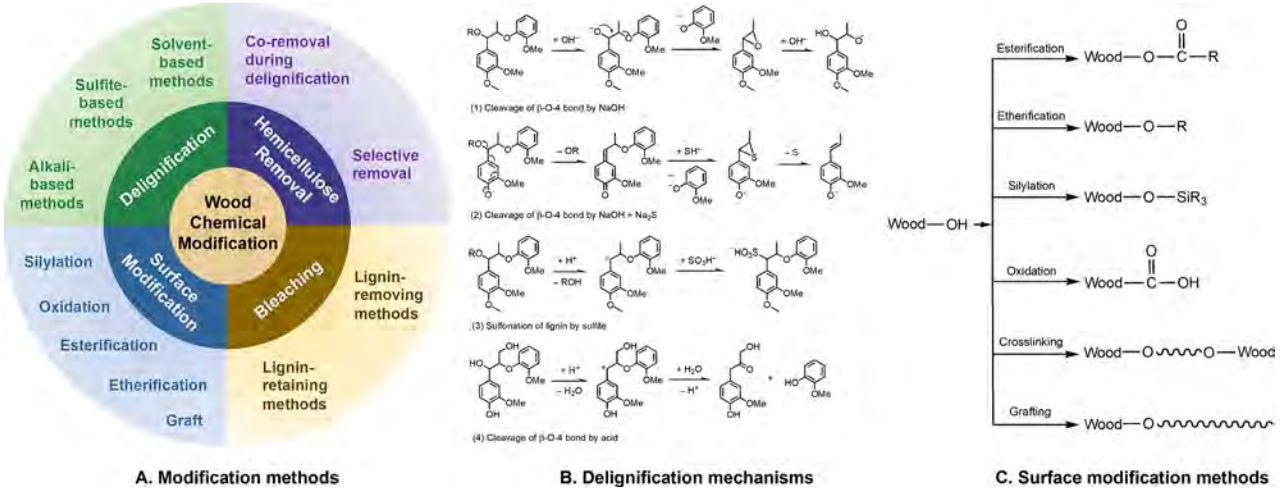

Figure 7. Chemial modifications of wood. (A) Modification methods, (B) delignification mechanisms, and (C) surface modification methods.

and nanofiber hybrids is shown to have even higher fracture energy, which can be attributed to the increased sliding distance among the fibers.

CG modeling parametrized by the MARTINI force field is also widely used in the analysis of the mechanical bending and twisting of the cellulose microfibers. Even though the modeling is limited to microscale, the MARTINI CG modeling sustains more interaction information among cellulose microfibers due to the parametrization based on the functional groups in cellulose. Experimentally, atomic force microscopy and Raman spectroscopy measurements are widely used techniques to measure the bending stiffness of cellulose fibers with various diameters. The measuring scales are in the range of microfibrillated cellulose sheets to cellulose macrofibers, with the measured bending stiffness ranging from 29 to 150 GPa.[51−53] A cellulose fibril with a smaller scale might likely have a lower bending stiffness, but these existing experimental measurements become unrealistic at such a small scale. López et al. use the MARTINI CG modeling to obtain the elastic modulus of a 36-chain cellulose fibril, as shown in Figure 5F.[49] External bending forces are loaded on one side of the cellulose microfiber, and the bending stiffness is estimated to be around 10 GPa. The results from the CG modeling verify the speculation and suggests a feasible method to measure the bending stiffness of ultrafine cellulose fibers. To extend the research of individual CNCs and CNC−CNC interfacial properties, Shishehbor and Zavattieri[54] developed the MARTINI CG modeling and found that the elastic modulus of the CNC bundle increases but the toughness decreases with the increase of the cohesive (interfacial) interactions between the CNCs. Based on the developed MARTINI CG modeling, Ramezani[50] investigated the effects of the bundle size and the twist on the mechanical response for bundles of CNCs (Figure 5G). The increase in bundle size and twist angle leads to the increase in hydrogen bonds breaking among the outer fibers, thus decreasing the strength and failure strain of the CNCs.

2.4. Macroscale

Products made of natural wood and engineered wood are often of sizes of centimeters to meters. To understand the mechanical response of such wood products at the macroscale, continuum scale models, such as FEM, and phenomenological constitutive models, are often used to predict the stress distribution (especially the region of stress concentration) and reveal the possible failure mode of these products under various types of mechanical loading, which, in turn, can be used to design wood structures.

The mechanical response of wood materials depends strongly on the loading direction, given the anisotropic nature of wood. Figure 6A shows the experimental shear tests of wood in different directions compared with the stress distribution in the FEM models.[55] FEM models present the stress distribution in the wood samples. Additionally, FEM is used to analyze the crack initiation and propagation in wood materials. Figure 6B compares the crack growth in a wood sample with a rectangular notch under three-point bending measured by an experimental test (upper panel) and predicted by FEM (bottom panel).[56] FEM can accurately predict the stress distribution and failure behavior of the wood samples. FEM is also used to understand the stress distribution in engineered wood under severe folding (Figure 6C), which offers critical insight into designing highly moldable wood.[57]

Besides, FEM simulations are also used to analyze the mechanical response of wood-based composites. Parts D and E of Figure 6 illustrate the stress−strain curves of a wood material and a wood-based gel during a compressive loading and unloading process, respectively.[44] The wood framework without water is easy to buckle severely under compressive loading, which leads to partial failure of the framework. Upon unloading, only a small fraction of the compressive strain (∼10%) can be recovered. By contrast, the wood-based gel can sustain severe compressive loading (>60%) without fracture, largely resulting from the hyperelastic nature of the structure due to the water contained inside the wood channels. Upon unloading, the wood-based gel can fully recover its original shape. Figure 6F presents the comparison of the experimental test and the prediction of a constitutive model of microfiber reinforced anisotropic hydrogels on the wood-based polyacrylamide (PAM) hydrogels under uniaxial tension, suggesting a reasonable agreement with each other.[58] Such a constitutive model can be further implemented into FEM (e.g., via a user subroutine to define material properties), so that the mechanical response of wood-based hydrogels of any other dimensions and geometries can be readily studied.

https://doi.org/10.1021/acs.chemrev.2c00450
Chem. Rev. 2023, 123, 1843−1888

3. CHEMICAL MODIFICATIONS FOR ADVANCED AND FUNCTIONALIZED WOOD PRODUCTS

Wood modification aims to overcome one or more disadvantages or weaknesses of native wood by altering wood's chemical and physical structures and properties. The wood's mechanical strength, dimensional stability, biodegradation resistivity, optical transparency, and other properties can be substantially improved through physical and chemical modifications. Chemical modification of wood includes, but is not limited to, selectively removing wood components (such as lignin and/or hemicelluloses), changing chemical structures of wood components, or introducing new functional groups. Based on their objectives, the important chemical modification methods are summarized in Figure 7A.

3.1. Delignification

Lignin is an aromatic polymer biosynthesized from three precursors (*p*-coumaryl, coniferyl, and sinapyl alcohols) by radical coupling. The radical coupling results in diverse linkages between the building units and a complex structure of lignin. The three building units are primarily linked by C-*O*-C (ether) bonds and C−C (carbon to carbon) bonds. The arylglycerol-*β*-aryl ether (*β*-*O*-4) bond is the most abundant (50−80%) linkage in native lignin. Other ether bonds include arylglycerol-*α*-aryl ether (*α*-*O*-4), diaryl ether (5-*O*-4), and resinol ether (*α*-*O*-*γ*) linkages. The primary C−C linkages in lignin are phenylcoumaran (*β*-5), biphenyl (5−5), 1,2-diarylpropane (*β*-1), and resinol (*β*−*β*).

Delignification is an operation to selectively remove or separate lignin from wood via depolymerization followed by dissolution and can be accomplished using different chemicals at an elevated temperature. Depolymerization of lignin entirely depends on the cleavage of ether linkages, whereas the carbon-to-carbon linkages are essentially stable. Among the ether linkages, only the cleavage of *β*-*O*-4 linkage can lead to depolymerization of lignin, as other ether linkages are either not directly linking lignin building units or are less abundant. It should be noted that condensation reactions (formation of new carbon-to-carbon linkages, or repolymerization) occur in most delignification processes, retarding lignin removal.

Delignification chemistry and processes have been well-established in the paper industry for chemical pulping and in the biorefining research for chemical fractionation/pretreatment to remove lignin-induced recalcitrance to enzymatic hydrolysis of cellulose. Depending on the chemicals used, delignification can be classified into alkali, sulfite, and solvent processes.

In alkali delignification, bases (e.g., NaOH) are used to depolymerize lignin. As shown in Figure 7B (1), hydroxyl ion (OH^-) cleaves *β*-*O*-4 in nonphenolic structures via an oxirane intermediate. However, because OH^- is a weak nucleophile, this reaction is slow and cannot extensively depolymerize lignin. Therefore, "soda pulping" (NaOH alone) is less effective for wood, especially for softwood. The addition of Na_2S in kraft (NaOH + Na_2S) pulping can significantly catalyze lignin depolymerization. Because of its strong nucleophilicity, SH^- can effectively cleave *β*-*O*-4 in phenolic structures by the mechanism shown in Figure 7B (2) via a quinone methide intermediate. For this reason, the kraft process has dominated wood chemical pulping in the paper industry. Anthraquinone is an alternative sulfur-free catalyst for soda pulping, but it is less effective than Na_2S. Oxygen is another efficient and sulfur-free reagent for delignification under alkali conditions. However, this system is quite unselective. Oxygen attacks not only lignin but also cellulose. Other ether linkages (e.g., *α*-*O*-4) can be cleaved too under alkaline conditions, but it does not directly lead to significant depolymerization of lignin. However, the formation of phenolic hydroxyl groups from the *α*-*O*-4 cleavage promotes the cleavage of *β*-*O*-4 by HS^- (Figure 7B (2)) and increases the hydrophilicity and thereby the solubility of lignin in alkaline solutions.

In sulfite processes, sulfite is used to remove lignin from wood. Sulfite delignification can be conducted in a wide range of pH from acidic to alkaline range. Different from that in alkaline processes, the delignification in sulfite processes is mainly attributed to the enhanced solubility due to lignin sulfonation at the *α* position to result in lignosulfonate, as shown in Figure 7B (3). The *β*-*O*-4 linkages are not significantly cleaved in low-pH sulfite processes, although the acid-induced *β*-*O*-4 cleavage shown in Figure 7B (4) could occur. The *β*-*O*-4 linkages can be cleaved in neutral and alkaline sulfite processes via the quinone methide intermediate, but it is insignificant and not the key cause of the delignification. As a result, lignosulfonate usually has a lower content of phenolic hydroxyl (due to limited cleavage of *β*-*O*-4 linkages) and higher molecular weight (because of insufficient depolymerization) than alkali lignin (such as kraft lignin).

In solvent-based processes, lignin is depolymerized and then dissolved in a solvent, such as organic solvents (ethanol, methanol, acetone, formic acid, acetic acid, *γ*-valerolactone (GVL), tetrahydrofuran (THF)),[59−64] ionic liquids (IL),[65,66] deep eutectic solvents (DES),[67,68] and acid hydrotropes.[69−71] Acid is usually used as a catalyst in most solvent-based processes. As shown in Figure 7B (4), the cleavage of *β*-*O*-4 linkages by acid is initiated by the protonation of benzyl alcohol, and the following dehydration generates an *α*-carbocation intermediate. The *α*-carbocation is then transformed to *β*-carbocation, and the hydrolysis of the latter leads to the cleavage of *β*-*O*-4 linkage, generating Hibbert's ketone and guaiacol moiety. It should be noted that the reactive *α*-carbocation intermediate can attack the electron-rich positions on benzene rings of lignin and lead to intramolecular and intermolecular condensation. This is the reason why the lignin from acidic processes usually contains more C−C linkages (condensed).

Chlorite is another effective delignification reagent. Under acidic conditions, chlorite can selectively destruct lignin without significantly affecting cellulose and hemicelluloses. Therefore, it has been frequently used at the laboratory scale for the selective removal of lignin to bleach wood or pulp. However, due to the cost and environmental concerns, chlorite is not feasible for wood delignification on a large, industrial scale.

Size reduction of wood to chips (or smaller) is usually a prerequisite in chemical pulping and pretreatment to promote mass and heat transfer during wood delignification. The delignification leads to wood fiberization (destruction of the wood cell wall into individual fibers). The fiberization, however, is not desired for many engineered wood products (such as superwood,[72] transparent wood[73]), which need to maintain the continuous cellular structure and fiber orientation of original wood for enhanced structural strength and stiffness. Alternative delignification processes for these special-performance applications are necessary to avoid breaking the inherent wood structure of continuous fibers but selectively remove lignin to increase the bonding of cellulose fibers, remove the lignin-induced color, and improve optical stability, or simply create pores for a porous structure. Therefore, delignification of wood blocks and panels is different from traditional wood pulping or

https://doi.org/10.1021/acs.chemrev.2c00450
Chem. Rev. 2023, 123, 1843−1888

pretreatment using wood chips because the much larger physical dimensions of wood panels or boards require an extensive predelignification impregnation process, and the requirement to keep the physical integrity of wood for structural materials can be challenging.[57,72,74]

3.2. Removal of Hemicelluloses

Hemicelluloses are another major component of lignocellulosic materials (20−40%), and they are a group of heterogeneous polysaccharides composed of multiple sugar units. The sugar units and the structures of hemicelluloses vary greatly among plant species. For example, in grasses and hardwood, *O*-acetyl-4-*O*-methylglucurono-D-xylan (glucuronoxylan or simply xylan) is the principal hemicellulose structure, in which the β-1,4 linked D-xylopyranose units form the backbone with the branches of 4-*O*-methyl-D-glucopyranosyluronic acid α-1,2-linked to xylose units and the acetyl group linked to xylose units at C2 or C3. Hemicelluloses in softwood are predominately galactoglucomannans with a small amount of arabinoglucuronoxylan. The former has the backbone of β-1,4 linked D-glucopyranose and D-mannopyranose units with the side chains of α-1,6 linked D-galactopyranose unit and acetyl group attached to the backbone at C2 or C3 of the D-glucopyranose and D-mannopyranose unit.

Hemicelluloses can be separated and removed from wood using different chemicals and processes.[75−77] The most effective method is to hydrolyze and dissolve hemicelluloses using an acid. The acetyl groups on hemicelluloses are easily cleaved under hydrothermal conditions and released as acetic acid, which can catalyze the hydrolysis of hemicelluloses. In addition, hemicelluloses can be simultaneously dissolved and/or hydrolyzed during wood delignification processes. Removing hemicelluloses is required or beneficial in many cases, such as dissolving pulp production and biomass pretreatment.[78] The removal of hemicelluloses is also beneficial or desired when producing engineered wood products. For example, dissolving hemicelluloses contributed to the formation of the porous structure of highly porous wood or aerogel materials.[79,80] Partial removal of hemicelluloses also played an important role when preparing ultrastrong densified wood.[72]

3.3. Bleaching

The color of wood due to the absorbance of visible light is mainly from lignin, attributed to the chromophoric structures and groups (such as benzene ring, quinonoid, vinyl, phenolic hydroxyl, and carbonyl groups) in lignin. These chromophoric units can form comprehensive conjugated systems (such as coniferaldehyde structures, *ortho*-and *para*-quinonoid units, and quinone methide intermediates) to result in a darker color. In addition, chemical treatment of wood (e.g., delignification) can lead to the formation of new chromophores from both lignin depolymerization and lignin condensation reactions.

There are two strategies to remove the color and increase the whiteness of wood or wood products: removing lignin and bleaching (decoloring) lignin. In the lignin-removing strategy, strong chemicals, such as chlorine-containing chemicals (chlorine, hypochlorite, and chlorine dioxide) and oxidants (oxygen, ozone, and peroxide), are used to completely destruct and dissolve lignin. In lignin-bleaching methods, moderate reductive (hydrosulfite) or oxidative (hydrogen peroxide) chemicals are commonly used to alter or remove the chromophoric groups and systems of lignin, selectively decoloring (bleaching) lignin while retaining its macrostructure. These strategies have been practiced in the paper industry for chemical pulps and high-yield (lignin-retaining) pulps (such as mechanical and chemimechanical pulps), respectively.[81]

These chemicals and technologies have been used for bleaching wood blocks and panels when preparing advanced wood products. For example, in the study of preparing transparent wood composite,[74] wood block was first delignified using NaOH and Na_2SO_3 and then bleached using H_2O_2 to completely remove residual lignin. In another study, the wood block was delignified and bleached using acidic chlorite before epoxy infiltration to fabricate aesthetic transparent wood.[82] In addition to removing lignin, a lignin-bleaching strategy was used to prepare transparent wood.[83] Lignin in the wood panel was bleached using H_2O_2, which did not significantly remove lignin but decolored the lignin by breaking the chromophoric groups and structures of the lignin. After epoxy infiltration, the obtained transparent wood composite had a high transmittance (>90%) and high haze (>60%).

Recently, a so-called solvent-controlled encapsulation (SCE) method was reported that can permanently whiten lignin and convert brown lignin into a white powder.[84] In a mixture of water, ethanol, and/or acetone, a nonchromophoric group was introduced into lignin by a condensation reaction between lignin hydroxy groups and an isocyanate. By carefully controlling the polarity (ratio of water to ethanol/acetone) of the solvent, the isocyanate-modified lignin forms spheric nanoparticles in which chromophoric lignin is encapsulated within the particle core, while the nonchromophoric groups introduced by the isocyanate are located on the surface of the particles. The whitened lignin can be cast into a transparent film and used as a colorless adhesive or filler in composite materials.

3.4. Surface Modification

Wood surface modification can improve the binding strength, optical properties, performance, stability, hydrophobicity, reactivity, and other properties of wood. Chemical modifications are conducted almost exclusively via the reactions of hydroxyl groups of cellulose, hemicelluloses, or lignin, such as esterification, etherification, oxidation, silylation, cross-linking, and grafting,[85] as summarized in Figure 7C.

Esterification is accomplished by the reaction between hydroxyl groups and inorganic or organic acids (or anhydrides). The most important inorganic ester of cellulose is cellulose nitrate, prepared with a mixture of nitric acid and sulfuric acid, which can be used for explosives and plastics, depending on the degree of substitution. Many organic acid anhydrides (linear and cyclic) have been used for wood esterification. The acetylation of wood with acetic anhydride is the most extensively studied approach. Acetylation can confer wood unique properties, such as solubility in organic solvents, plasticity, hydrophobicity, dimensional and biological stability, and compatibility in polymeric composites.[86]

Etherification can be conducted by treating cellulose or wood with the reagents like alkyl/aryl halides and alkene oxides.[87] Most important cellulose ethers include methylcellulose, ethylcellulose, carboxymethylcellulose, hydroxyethylcellulose, and cyanoethylcellulose, and they have been used in many areas.[88] Wood etherification has been used to improve its interface compatibility in wood plastic composites.[89]

Silylation of hydroxyl groups of cellulose and wood by chlorosilanes, silazanes, and other silylation agents can dramatically change their surface properties, such as compatibility, thermal and oxidative stability, hydrophobicity, and permeability.[90−94] For example, silane coupling agents have

https://doi.org/10.1021/acs.chemrev.2c00450
Chem. Rev. 2023, 123, 1843−1888

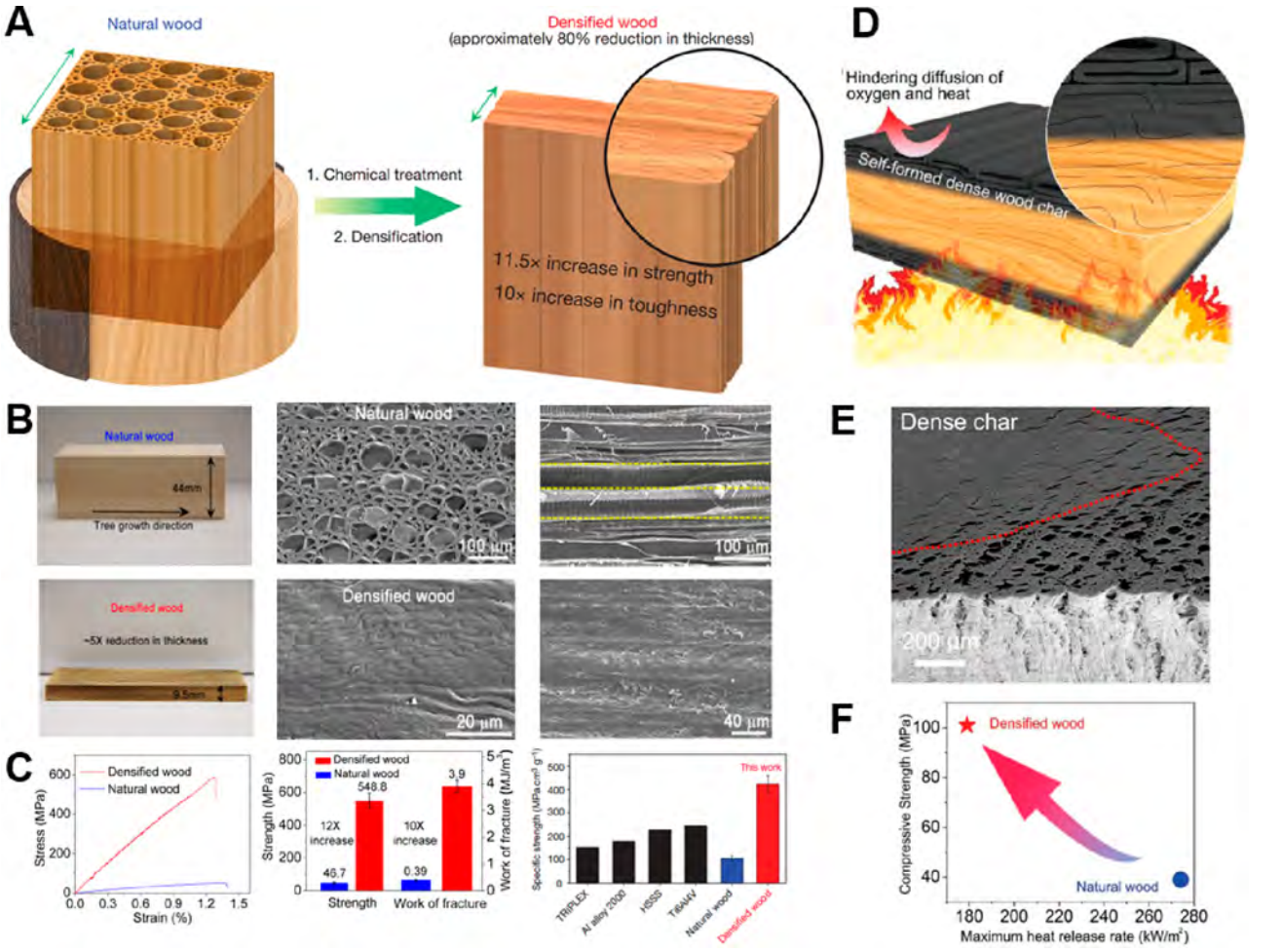

Figure 8. (A) Schematic of the processing of densified wood (super wood), which is comprised of aligned cellulose nanofibers with reinforced hydrogen bonds.[72] Reproduced with permission from ref 72. Copyright 2018 Springer Nature. (B) Photographs and SEM images of the natural and densified wood samples in the direction perpendicular to the tree growth.[72] Reproduced with permission from ref 72. Copyright 2018 Springer Nature. (C) Comparison of specific strength between densified wood and typical structural materials.[72] Reproduced with permission from ref 72. Copyright 2018 Springer Nature. (D) Schematic representation demonstrating the working principle of the self-formed wood char layer of densified wood for fire resistance.[115] Reproduced with permission from ref 115. Copyright 2019 John Wiley and Sons. (E) SEM image of the densified wood after combustion. Reproduced with permission from ref 115. Copyright 2019 John Wiley and Sons. (F) The compressive strength of densified wood is higher than natural wood, and the maximum heat release rate of the densified wood is significantly lower than natural wood. Reproduced with permission from ref 115. Copyright 2019 John Wiley and Sons.

been widely used for cellulose surface modification. Silane coupling agents have dual reactivity. At one end, they have an alkoxyl silane group capable of reacting with a hydroxyl-rich surface (such as cellulose), and at the other end, they can have a large number of functional groups which can be tailored. Silane coupling agents were used to introduce new functional groups onto polymers[95] and cellulose.[96−98]

Oxidation can introduce carboxyl and carbonyl groups to cellulose and wood. For example, the oxidation of primary hydroxyl groups at C6 by TEMPO, persulfate, and other oxidants has been used to produce cellulose nanocrystals and nanofibers because the surface charge induced by the carboxylic groups facilitates the dispersion of the cellulose nanoparticles.[99−102] Periodate oxidation is a unique reaction to produce dialdehyde cellulose (DAC). Periodate can regioselectively oxidize the vicinal hydroxyl groups at C2 and C3 in anhydroglucose units of cellulose into two aldehyde groups.[103] The aldehyde groups in DAC can be further oxidized to acids or converted to the Schiff base (imine) by reacting with an amine to synthesize functionalized cellulose derivatives.[104,105]

Chemical cross-linking is an effective way to improve the strength and dimensional stability of structural cellulose and wood products. The cross-linking creates bridge linkages between molecules of cellulose, hemicelluloses, and lignin via the reactions between hydroxyl groups and cross-linking reagents such as maleic anhydride, diacid, epoxy resin, isocyanate, and silane.[106−108] Cross-linking is also an important strategy to fabricate cellulose and hemicellulose hydrogels. For example, citric acid, dialdehyde, diisocyanate, divinyl sulfone, epichlorohydrin, and glutaraldehyde have been used to cross-link cellulose in hydrogel preparation.[109,110]

Grafting is an approach to grafting polymers onto cellulose and wood, which provides or improves the properties such as dimensional stability, resistance to abrasion and wear, wrinkle recovery, oil and water repellence, elasticity, ion exchange capabilities, temperature responsiveness, thermal resistance, and resistance to microbiological attack. The grafting can be accomplished by free radical polymerization, ionic and ring-opening polymerization, and living radical polymerization via

https://doi.org/10.1021/acs.chemrev.2c00450
Chem. Rev. 2023, 123, 1843−1888

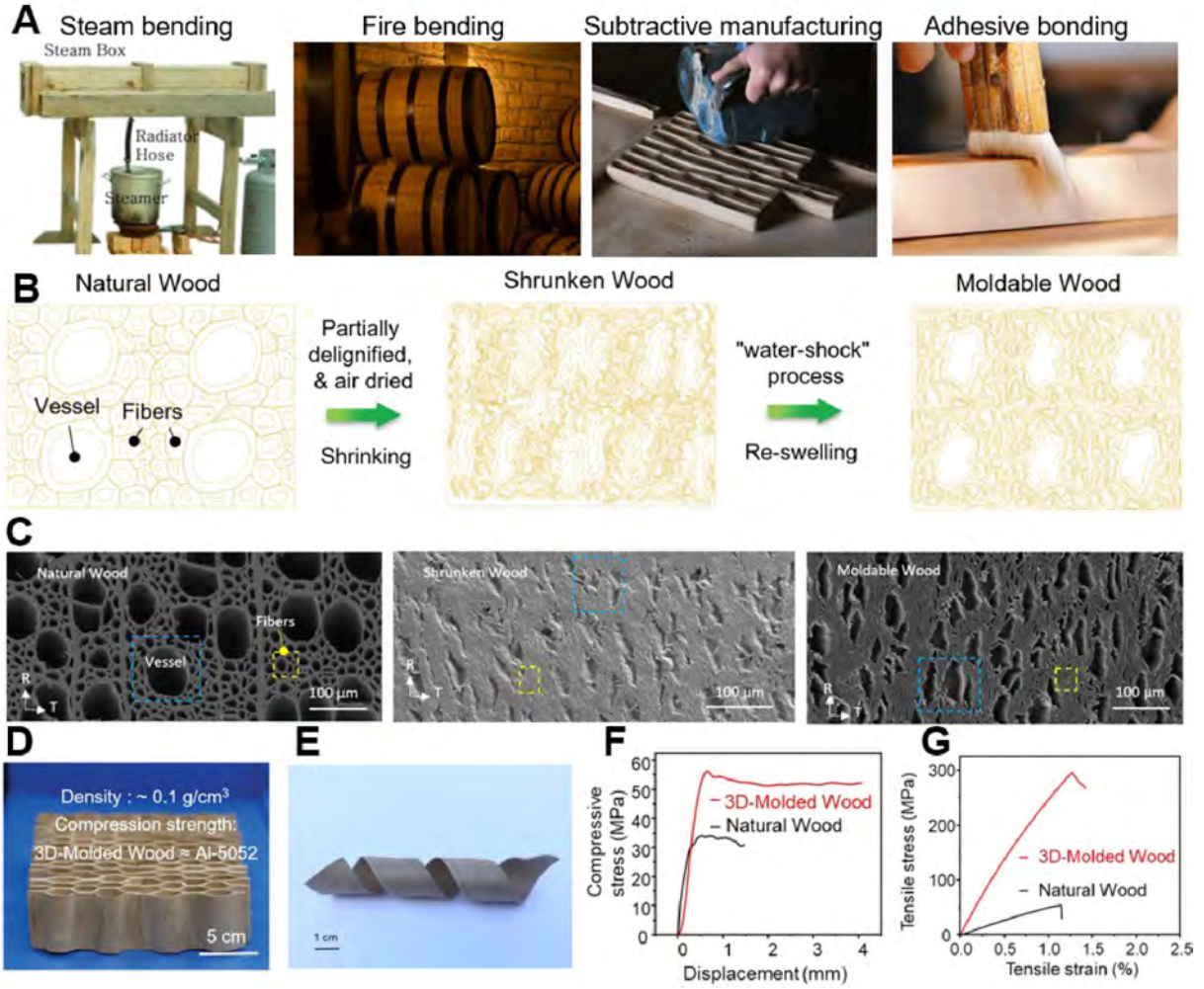

Figure 9. (A) Conventional methods to fabricate complex wood shapes and structures. (B) Schematic of the processing of 3D wood by the cell wall engineering strategy.[57] Reproduced with permission from ref 57. Copyright 2021 American Association for the Advancement of Science. (C) SEM image of the natural wood, shrunken wood, and moldable wood samples in the direction perpendicular to the tree growth. Reproduced with permission from ref 57. Copyright 2021 American Association for the Advancement of Science. (D,E) Photograph of the 3D-molded wood honeycomb core material and helical structured wood. Reproduced with permission from ref 57. Copyright 2021 American Association for the Advancement of Science. (F,G) Mechanical properties of the natural wood and 3D-molded wood. Reproduced with permission from ref 57. Copyright 2021 American Association for the Advancement of Science.

the approaches of grafting-to, grafting-from, and grafting-through cellulose.[111]

3.5. Chemical Recovery

Chemical recovery and waste treatment are very important considerations in using chemicals for wood modification to develop engineered wood products. When using low dosages of low-cost chemicals, chemical recovery may not be necessary, but the waste streams (solids and liquid) containing the chemicals need to be treated for discharge or reuse. For example, bleaching chemicals are not recovered in commercial pulp mill operations. Depending on the chemicals used, the waste streams are treated with various technologies to meet chemical oxygen and biological oxygen demands to minimize environmental impact. On the other hand, chemical recovery is necessary when chemical dosages for wood processing are relatively high. Conventional alkaline chemical recovery is a mature commercial process and has been in industry operation for more than 80 years, however, involves expensive capital investment. Sulfite chemical recovery is relatively difficult. Only when expensive magnesium is used as the base in sulfite pulping, complete chemical recovery is possible. Because chemical recovery is the make or break of any chemical process, it should be a critical consideration in choosing or developing a new wood chemical modification process. Another issue that is also important to biorefinery is the utilization of removed lignin and hemicelluloses which can improve process economics. There have been plenty of reviews on the subject but with limited commercial success.[112]

4. MODIFIED WOOD MATERIALS FOR ENHANCED EWPS

4.1. Ultra-Strong Densified Wood

The manufacturing of construction materials alone gave rise to 3.2 gigatons of CO_2 in 2020, accounting for 10% of total CO_2 emissions among all sectors.[113] Therefore, it is urgent to develop carbon-negative materials to nullify embodied greenhouse gas emissions, meanwhile transforming buildings into net carbon storage structures on a life cycle basis. The mechanical strength of structural materials is of primary importance to achieving widespread implementation in building applications. Metals,

https://doi.org/10.1021/acs.chemrev.2c00450
Chem. Rev. 2023, 123, 1843−1888

such as steel, are ubiquitously used in structural applications due to their high magnitude and consistent mechanical strength, stiffness, ductility properties, and processability into various shapes and sizes. However, there have been increasing calls for the development of more sustainable materials as metal processing and fabrication are energy intensive. Wood, as a renewable structural material, is mechanically strong, lightweight, and could be a sustainable alternative to metals. The mechanical properties of wood vary widely due to its natural origin. And the density of wood, varying with species, correlates well with its strength. Despite the abundance, renewability, and sustainability, the mechanical performance of natural wood cannot compete with steel, which has been used for diverse and advanced applications as structural materials.

By reducing the pores and voids between cell walls, the densification of wood has been demonstrated as an efficient approach to optimizing the mechanical strength of low-density wood.[114] Nevertheless, most of the reported densification procedures rely on pretreatment using steam, heat, ammonia, or cold rolling, leading to incomplete densification and dimensional instability, especially in some harsh environments.[114] In 2018, Hu et al. reported a facile yet effective top-down approach that can directly process natural wood into an ultrastrong structural material with exceptional mechanical properties (Figure 8A).[72] Distinguished from conventional densification methods, the pretreatment of partial delignification, removing partial lignin and hemicelluloses, makes it possible to fully densify the natural wood structure with an approximately 80% reduction in thickness (Figure 8B). The porous natural wood structure contains lumina with tubular channels along the wood growth direction (Figure 8B); in contrast, the densified wood is mainly composed of fully collapsed wood cell walls, which are closely intertwined and densely packed (Figure 8B). In such a unique microstructure of densified wood, the cellulose nanofibers are highly oriented, akin to natural wood, but much more tightly packed, giving rise to remarkably enhanced hydrogen bonding between neighboring nanofibers. On the other hand, the highly densified wood with minimized vessels and pits can effectively alleviate the adverse influence of such defects on the mechanical strength. Residual lignin in the delignified wood also plays a key role, as a binder, in enhancing the mechanical performance. The demonstrated tensile strength can reach 587 MPa for densified wood, a more than 10-fold increase in comparison with natural wood, which also exceeds many metal-based structural materials (Figure 8C).[72]

Fire resistance is another important consideration for EWPs, as natural wood is combustible. The fire-retardant properties of densified wood can be remarkably improved owing to the eliminated space between cell walls to block the infiltration of oxygen and reduce the transport of heat (Figure 8D).[115] Moreover, it is noteworthy that a dense and insulating layer of wood char can be generated on the surface, further inhibiting the diffusion of oxygen and heat (Figure 8E). Considering these synergistic effects, a 2.08-fold increase in the ignition time can be achieved experimentally, as well as a 34.6% decrease in the maximum heat release rate versus natural wood (Figure 8F), paving a new path toward the fire-resistant and mechanically strong structural EWPs that incorporate densified wood.

4.2. 3D Moldable Wood

Wood is primarily fabricated as rectangular boards or flat sheets, which need further manufacturing to be utilized where more complex shapes are required. Several methods have been adopted to fabricate wood into various desired shapes. For instance, steam bending or chemical impregnation has been used, followed by clamping in a mold and drying to fix the form (Figure 9A);[116] in traditional wine barrel manufacturing, each barrel is warmed over an open fire to bend the staves into the desired shape without breaking the wood followed by a toasting process (Figure 9A). Alternatively, adhesive bonding of timber sections, namely, wood chips, flakes, veneer, and other elements, has also been adopted to fabricate larger and more complex structural sections (Figure 9A). These engineering approaches, based on the modifications at a bulk scale, do not change the intrinsic microstructure/properties of wood and rely primarily on adhesive bonding to enhance mechanical properties. While adhesive polymers make good use of wood byproducts and facilitate the lamination or pressing of complex 3D forms, engineered wood products without continuous wood fibers might lack stiffness for high-performance structural applications where the thickness of the shell must remain thin yet strong and stiff.[114] Therefore, the formability and mechanical properties of wood must be improved so that engineered wood can serve as a good substitute for applications requiring complex shapes and structures.

As reported by Hu et al., a cell wall engineering approach was adopted to render wood moldable while simultaneously boosting its mechanical performance, endowing wood with fabrication versatility previously limited to metals and plastics.[57] Such a new process enables flat sheets of wood to be shaped into versatile 3D structures with significantly improved mechanical performance. In the fabrication process, wood is first softened by in situ chemical delignification, followed by air-drying to close the hollow wood vessels and fibers that form a highly aligned channel structure (Figure 9B). The shrunken wood is then partially reswollen in a "water-shock" process that specifically expands the wood vessels. The resulting wrinkled cell wall makes it possible to mold the foldable wood into any target shapes, which can then be locked into place by air drying (Figure 9C−E). The resulting wood material has a compressive strength of ∼55 MPa and a tensile strength of ∼300 MPa, both of which are much higher than the starting natural wood and comparable to some of the popular structural materials, such as Al alloys or some reinforced polymer composites (Figure 9F,G). This unique cell-wall-oriented, nanoengineering approach to shaping wood into lightweight, strong, and tough 3D structures allows molding wood into efficient structures that could compete with metal products. This capability opens the possibility of wood building products with both complex geometries and improved mechanical properties.

5. THERMAL MANAGEMENT WOOD

5.1. Thermally Insulating Wood and Thermal Energy Storage Wood

In 2020, global CO_2 emissions from buildings operations reached 8.7 gigatons, accounting for 27% of total emissions in the world.[113] Additionally, global building operations consumed 127 EJ of energy, indicating a global share of 31%.[113] It is noted that building operations alone, taking no account of the manufacturing of construction materials, is the majority shareholder for both global energy demand and emissions. Accordingly, the development of high-performance building insulation panels is crucial in achieving the emission reduction and energy conservation targets set out in the Paris Agreement.[5] There are several disadvantages to some of the widely used

https://doi.org/10.1021/acs.chemrev.2c00450
Chem. Rev. 2023, 123, 1843−1888

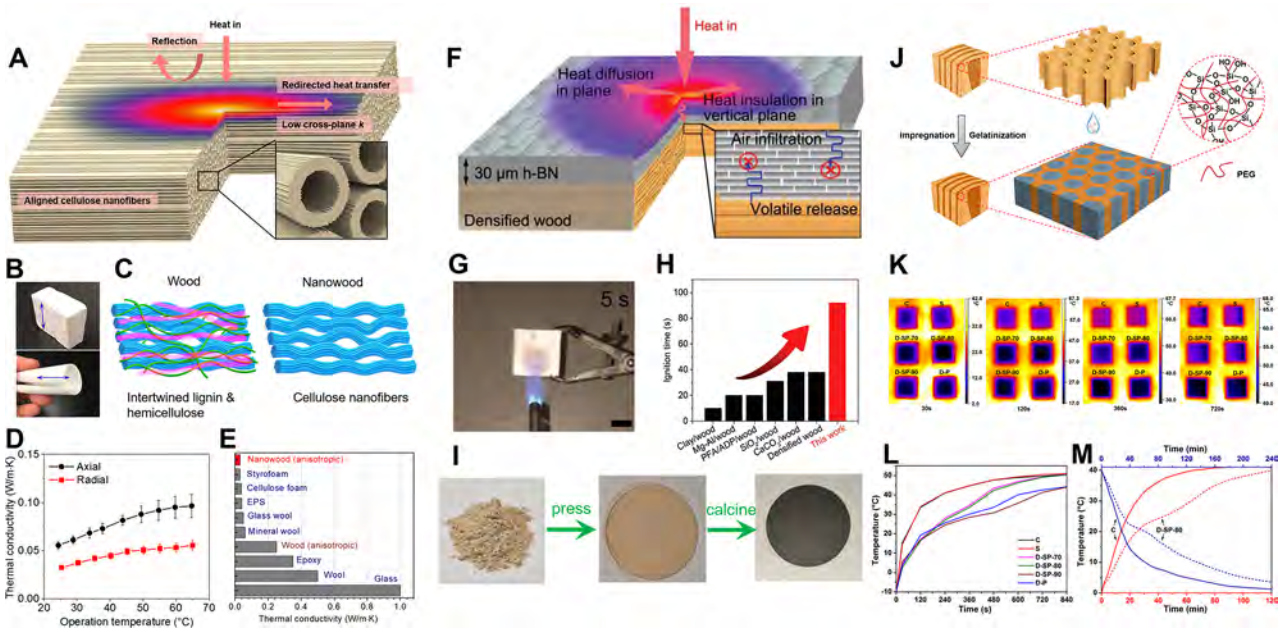

Figure 10. (A) Schematics of thermally insulating properties of nanowood.[118] Reproduced with permission from ref 118. Copyright 2018 American Association for the Advancement of Science. (B) Photograph of the thermally insulating wood. Reproduced with permission from ref 118. Copyright 2018 American Association for the Advancement of Science. (C) Schematics of the aligned cellulose nanofibrils in the nanowood before and after delignification. Reproduced with permission from ref 118. Copyright 2018 American Association for the Advancement of Science. (D,E) Measured thermal conductivity of the nanowood and comparison with existing thermally insulating materials. Reproduced with permission from ref 118. Copyright 2018 American Association for the Advancement of Science. (F) Schematic of the thermal conductivity and heat insulating properties of the BN-coated densified wood.[119] Reproduced with permission from ref 119. Copyright 2020 John Wiley and Sons. (G) The burning behavior of the BN-densified wood under the propane flame. Reproduced with permission from ref 119. Copyright 2020 John Wiley and Sons. (H) Comparison of the calculated ignition delay time of this work with other reported fire-resistant wood results in an external heat flux of 50 kW m^{-2}. Reproduced with permission from ref 119. Copyright 2020 John Wiley and Sons. (I) Fabrication of thermally insulating wood foams derived from sawdust.[120] Reproduced with permission from ref 120. Copyright 2022 Elsevier. (J) Schematic illustration of the fabrication process of the thermal energy storage wood.[121] Reproduced with permission from ref 121. Copyright 2020 Elsevier. (K–M) Thermal infrared images and corresponding temperature–time curves of the thermal energy storage wood samples. Reproduced with permission from ref 121. Copyright 2020 Elsevier.

construction materials, namely, concrete, steel, and brick-based systems. (1) These materials' low thermal resistance can cause energy leaks, especially during winter and summer. (2) Concrete and steel production can also be responsible for significant CO_2 and other harmful emissions. (3) Steel cladding panels dent upon impact with vehicles, hail, and windborne debris. (4) Precast concrete architectural cladding is heavy, placing high demands on structural support and the thermal mass can contribute to urban heat island effects, if not actively managed.[117] As a result, developing innovative building envelope solutions is urgently needed to reduce wasted energy, improve occupant comfort, and reduce environmental impacts.

In 2018, Hu et al. proposed an effective "top-down" method to fabricate natural wood into an anisotropic, thermally insulating material named "nanowood" (Figure 10A).[118] The delignification process not only gets rid of thermally conductive lignin components but also creates nanopores to impede phonon transport, resulting in largely reduced thermal conductivity of wood. What's more, the nanowood inherits a similar anisotropic structure from natural wood composed of highly aligned cellulose fibers (Figure 10B,C), giving rise to anisotropic thermal conductivity. The thermal conductivity is ~0.06 W/m·K along the cellulose alignment direction, while a considerably low value of ~0.03 W/m·K can be achieved in the perpendicular direction (Figure 10D). When compared with synthetic, nonrenewable structures (e.g., styrofoam), the thermal insulation nanowood possesses a similarly low thermal conductivity but significantly higher mechanical strength and stiffness (Figure 10E).

Alternatively, the thermal management of wood can also be achieved via the surface coating of anisotropic thermally conductive boron nitride (BN) nanosheets, which maintains the thermal conductivity of 390 and 2 W/m·K in the in-plane and through-plane directions, respectively.[119] The BN-coated densified wood can facilitate in-plane thermal diffusion while blocking the heat conduction in the vertical direction (Figure 10F). Meanwhile, BN can serve as an oxygen barrier upon exposure to fire. These synergistic effects of BN coating resulted in a 2-fold increase in the ignition delay time of densified wood (Figure 10H). Such a method provides a viable solution to fabricating high-performance structural materials in terms of mechanical properties, thermal management, and fire resistance (Figure 10G). In addition to delignified wood and densified wood samples, the thermally insulating wood products can be prepared by using sawdust, a waste byproduct from wood processing, as the starting material.[120] The lightweight, cost-effective, sustainable, and insulating wood foam derived from sawdust is promising to substitute for ubiquitous polystyrene foams in modern construction (Figure 10I).

To further reduce building energy consumption, thermal energy storage wood can be prepared with temperature-conditioning functions.[121] Considering the relatively low heat capacity of the wood itself, the impregnation of phase change materials into the porous wood structure has been adopted. For example, polyethylene glycol (PEG) is regarded as a versatile

https://doi.org/10.1021/acs.chemrev.2c00450
Chem. Rev. 2023, 123, 1843–1888

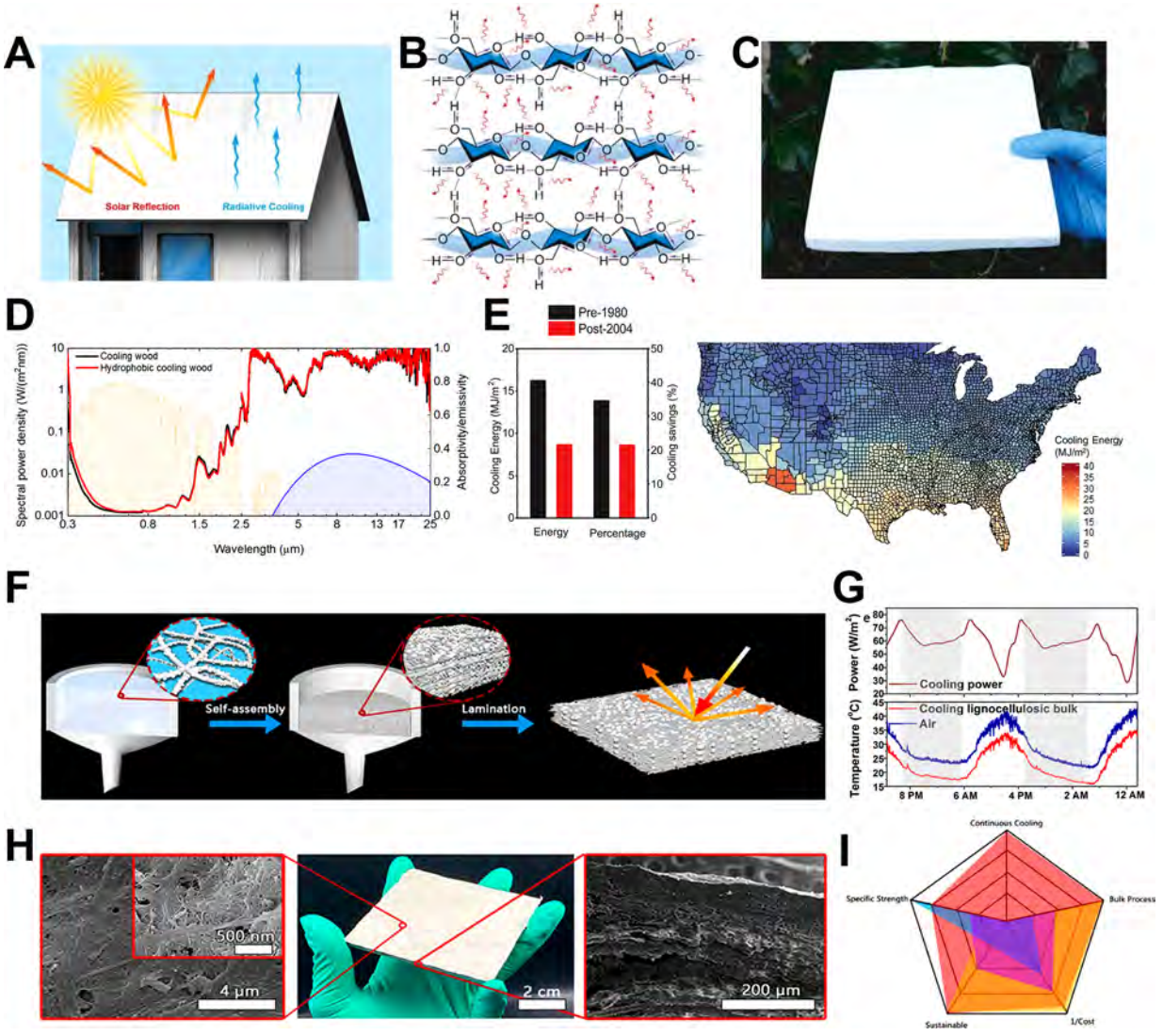

Figure 11. (A) Schematic of the cooling wood showing strongly scattering solar irradiance.[123] Reproduced with permission from ref 123. Copyright 2019 American Association for the Advancement of Science. (B) Schematic of infrared emission by molecular vibration of the cellulose functional groups. Reproduced with permission from ref 123. Copyright 2019 American Association for the Advancement of Science. (C,D) Photograph of the cooling wood, and its emissivity before and after the hydrophobic treatment. Reproduced with permission from ref 123. Copyright 2019 American Association for the Advancement of Science. (E) Average cooling energy savings and percentage among all 16 cities and total predicted cooling energy savings of midrise buildings extended for all U.S. cities. Reproduced with permission from ref 123. Copyright 2019 American Association for the Advancement of Science. (F) The fabrication process of the cooling lignocellulosic bulk.[124] Reproduced with permission from ref 124. Copyright 2021 American Chemical Society. (G) Continuous measurement of the ambient temperature and the surface temperature of a cooling lignocellulosic bulk under direct thermal testing. Reproduced with permission from ref 124. Copyright 2021 American Chemical Society. (H,I) SEM images and photographs of the cooling lignocellulosic bulk and the radar plot show a comparison among different materials. Reproduced with permission from ref 124. Copyright 2021 American Chemical Society.

organic phase change material with high latent enthalpy, stability, and a highly tunable phase transition temperature. To boost the thermal reliability of wood, Xu et al. infused silica-stabilized PEG into the pores of wood via vacuum infiltration (Figure 10J).[121] The infiltrated functional material can store or release large amounts of heat during the phase transition process to keep the indoor temperature stable. As presented in the thermal infrared images in Figure 10K, the surface temperature of PEG-modified wood is lower than the control sample, showing the capability of PEG to absorb heat during phase change and slow the temperature variation of the environment (Figure 10L,M). To fulfill the promise of reducing greenhouse gas (GHG) emissions through embodied and operational energy savings, the great challenge of upscaling these chemical processes to produce construction-size panels is on the horizon.

5.2. Radiative Cooling Wood

Cooling of buildings based on conventional air conditioners not only consumes substantial amounts of energy but also engenders a serious greenhouse effect due to ozone-depleting coolants. Therefore, efficient, eco-friendly, and cost-effective approaches with net cooling capability are demanded to replace traditional cooling systems. Passive radiative cooling involves high solar reflectance and infrared radiation passing through the atmospheric transparent window with zero energy consumption. However, sophisticated emissive coatings, such as metamaterials and nanophotonic structures, are typically required, and it is

https://doi.org/10.1021/acs.chemrev.2c00450
Chem. Rev. 2023, 123, 1843−1888

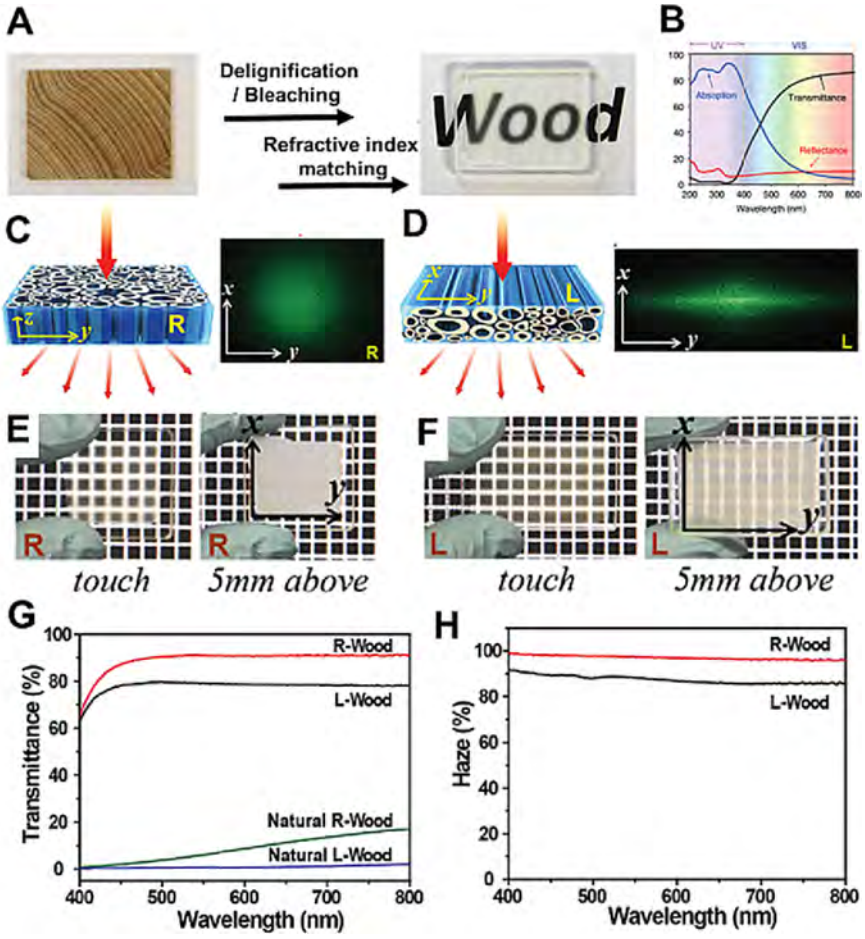

Figure 12. (A) Representative pictures of native and transparent wood.[74] Reproduced with permission from ref 74. Copyright 2016 John Wiley and Sons. (B) Typical optical properties of transparent wood.[82] Reproduced with permission from ref 82. Copyright 2020 Springer Nature. (C,D) Schematic representation and experimental verification of light scattering by transparent wood along (R-wood) and perpendicular (L-wood) to the wood fiber. (E,F) Photographs showing optical differences between transparent R-wood and L-wood. For the L-wood, the vertical white lines are more visible than the parallel white lines due to the anisotropic scattering. Transmittance (G) and haze (H) spectra for native R-wood, native L-wood, transparent R-wood, and transparent L-wood. (C−H) Reproduced with permission from ref 74. Copyright 2016 John Wiley and Sons.

hard to realize inexpensive and scalable fabrications.[122] To circumvent this limitation, Hu et al. at UMD fabricated fully delignified and densified wood composed of aligned cellulose nanofibers, which can be employed as a powerful radiative cooling material (Figure 11A).[123] The multiscale fibers and channels, serving as scattering elements, enable highly efficient broadband reflection in the visible light range. What's more, the molecular vibration of the functional groups on cellulose gives rise to intense emissions in the infrared region (Figure 11B). As shown in Figure 11C, the delignified wood is white, which reflects the incident solar energy and avoids heating in the solar spectrum, and the weatherability can be further enhanced after fluorosilane coating without sacrificing the cooling capability (Figure 11D). With this unique material, average cooling powers of 63 W/m^2 and 16 W/m^2 can be achieved during the night and daytime, respectively. It is calculated that around 20−35% energy savings can be achieved for midrise buildings, and the construction structures in hot regions generally maintain higher energy savings (Figure 11E). The multifunctional radiative cooling wood is attractive for energy-efficient and sustainable buildings for roofing and siding.

In addition to the top-down approach mentioned above, the bottom-up assembly of cellulose fibers has also been explored to fabricate radiative cooling materials. As reported by Chen and co-workers, they fabricated lignocellulosic membranes by vacuum filtration of the delignified cellulose fiber mixed with SiO_2 microspheres, followed by densification via hot pressing (Figure 11F).[124] The 8-fold increase in tensile strength of the cooling membrane (208.5 MPa) in comparison with the pure wood is attributed to the strong interactions between fibers in the compacted cellulose layers composed of a microscale network (Figure 11H). In the proof-of-concept test, the average cooling power is 52 W/m^2, and the subambient temperature decline can reach ∼6 K and ∼8 K during daytime and at night (Figure 11G), respectively. As shown in the radar plot in Figure 11I, such a cooling lignocellulosic membrane demonstrates appealing features in terms of mechanical properties, sustainability, cost, manufacturing, and cooling performance, making it an attractive structural material with substantially reduced carbon emissions and energy consumption.

6. TRANSPARENT WOOD

Transparent wood (TW) is an emerging material with added light and thermal management functionalities, first reported by Fink in 1992, and then rediscovered by the University of Maryland and KTH separately in 2016.[74,125] Transparent wood materials are prepared from wood by delignification or bleaching followed by infiltration of a polymer with a refractive index (RI)

https://doi.org/10.1021/acs.chemrev.2c00450
Chem. Rev. 2023, 123, 1843−1888

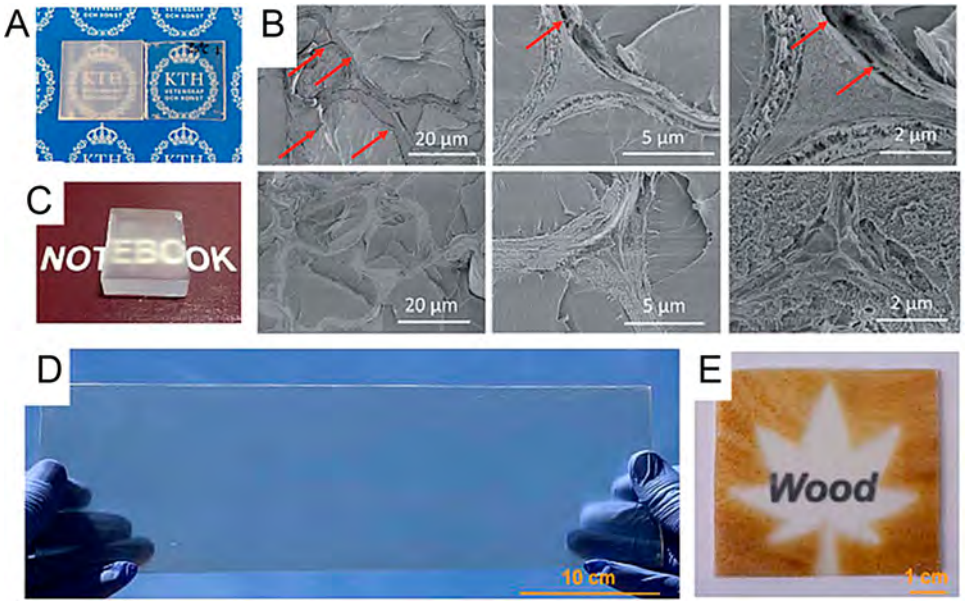

Figure 13. (A) Photograph showing nonacetylated transparent wood (left) and acetylated transparent wood (right).[126] (B) Scanning electron microscopy (SEM) images of nonacetylated (top) and acetylated (bottom) transparent wood: the latter shows no interface debonding gaps. (C) Picture of a 7 mm thick transparent wood. (A–C) Reproduced with permission from ref 126. Copyright 2018 Royal Society of Chemistry. (D,E) A large-scale sheet (400 mm × 110 mm × 1 mm) of transparent wood prepared from wood cut along the longitudinal (i.e., along the fiber) direction and transparent wood along the transverse (i.e., perpendicular to the fiber) direction, patterned with a "tree leaf" shape.[83] Reproduced with permission from ref 83. Copyright 2021 American Association for the Advancement of Science.

that matches that of the scaffold (Figure 12A). Transparent wood is a promising energy-saving building material, with the potential to reduce indoor energy consumption by enabling better thermal insulation and offering comfortable indoor lighting.

Compared to glass, TW exhibits lower thermal conductivity, higher impact strength, and lower density. Therefore, it has potential applications in smart buildings. Characteristic optical properties of transparent wood are transmittance (which measures the loss of energy transport, including that due to absorption and scattering, Figure 12B) and haze (which measures the loss of information, such as imaging content). Compared to many other transparent scattering materials, which are homogeneous or have purely random structures, the strong inhomogeneous and anisotropic scattering in transparent wood makes the characterization of its transmittance and haze significantly different and challenging and makes the material itself a great candidate as a structural "light diffuse" layer for solar cells, lighting systems, and buildings, where it can perform the same function as frosted glass. At short distances from objects, the transparency of relatively thin transparent wood samples is comparable with that of glass, plastics, and cellulose-based nanopaper. However, compared to more conventional transparent or translucent materials, transparent wood reveals a strong anisotropic optical behavior (Figure 12C–H).

Ensuring proper interface compatibilization between the wood scaffold and the impregnating polymer helps to reduce the number of total refractive index variations at interfaces and thus to minimize the overall scattering. In other words, reducing debond gaps to a minimum is of great importance for the optical properties of transparent wood (Figure 13A,B). It is noteworthy that this problem can be reduced by acetylating the wood scaffold, which also allows the preparation of centimeter-thick transparent wood (Figure 13C).[126]

Wood does not transmit visible light efficiently, and it is fundamentally opaque. The extinction of light inside wood happens mostly due to absorption (by lignin) and scattering (by cellulose fibers). Making transparent wood, that is, increasing the transmission of light through wood, requires removing the chromophores of lignin (bleaching), or even lignin itself (delignification), as well as reducing light scattering from the cellulose scaffold. Bleaching and delignification can be achieved by a variety of methods, mostly involving the degradation of lignin using oxidizers (e.g., hypochlorite, chlorite, peracids, and hydrogen peroxide) or reducing agents (such as hydrosulfite). Temperature, time, and reactant concentration, as well as wood species and sample thickness, all influence the process. The reduction of light scattering can be achieved by filling the lumina with materials having a refractive index RI comparable with that of cellulose (which is on average around 1.5). In a seminal 1992 paper, Fink proposed to impregnate (also by the aid of vacuum) a bleached wood scaffold with partially polymerized (meth)-acrylate (e.g., methyl methacrylate) or vinyl (e.g., styrene, *N*-vinylcarbazole) monomers, and then complete the polymerization in situ.[127] Poly(methyl methacrylate) (PMMA) has a RI ≈ 1.49, for poly(styrene) is around 1.6, and that of poly(*N*-vinylcarbazole) is even higher (RI ≈ 1.69). Fink also suggested that colored or fluorescent transparent wood could be obtained by dispersing pigments or luminescent materials in the polymerizing mixture. This method, originally described to facilitate the microscopic observation of wood anatomical features, has become widely adopted to prepare transparent wood materials for engineering applications.[74,125] UV-triggered polymerization approaches are now used alongside more conventional thermal initiation systems, and several other polymers have been used for impregnation, with a clear tendency toward biobased ones. Although PMMA is still the most popular, epoxy or thiol–ene resins are on the rise,[128,129] as well as poly(vinyl alcohol).[130] Toward more "green" transparent

https://doi.org/10.1021/acs.chemrev.2c00450
Chem. Rev. 2023, 123, 1843–1888

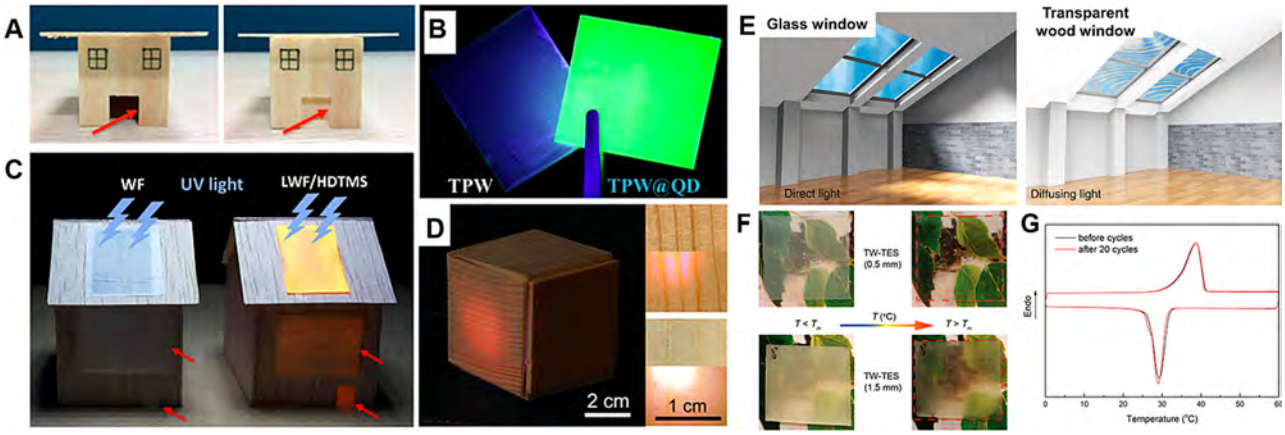

Figure 14. (A) Model house with (left) a native wood roof, where indoor is dark, and (right) transparent wood roof, where indoor is bright.[135] Reproduced with permission from ref 135. Copyright 2017 John Wiley and Sons. (B) Transparent (TPW, left) and luminescent transparent (TPW@QD, right) plywood with isotropic light-emitting characteristics, under UV light irradiation. TPW@QD contains green-emitting CdSe/ZnS quantum dots.[137] Reproduced with permission from ref 137. Copyright 2018 Elsevier. (C) Picture showing model houses with uniform indoor illumination achieved using delignified densified wood panels, native and luminescent, when exposed to a UV light source.[149] Reproduced with permission from ref 149. Copyright 2020 American Chemical Society. (D) Luminescent native wood membranes.[150] Reproduced with permission from ref 150. Copyright 2022 Royal Society of Chemistry. (E) Schematic scene showing the light distribution inside a building by applying a conventional glass ceiling (left) and a transparent "aesthetic wood" window (right).[82] Reproduced with permission from ref 82. Copyright 2020 Springer Nature. (F,G) Thermoresponsive transparent wood (TW-TES). Images showing, for 0.5 mm and 1.5 mm thick specimens, that the transparency can be tuned by varying the temperature, and differential scanning calorimetry (DSC) curves of temperature-responsive transparent wood (TW-TES) before and after thermal cycling, indicating good thermal reliability after 20 cycles.[138] Reproduced with permission from ref 138. Copyright 2019 American Chemical Society.

wood, it is noteworthy to mention the use of acrylic acid-choline chloride,[131] limonene acrylate,[132] and chitosan.[133] Due to the large amount incorporated in the wood scaffold, the physicochemical characteristics of the impregnating polymer have a great influence on the mechanical, other than the optical, properties of transparent wood. TW with different degrees of flexibility or rigidity has been described. It is noteworthy that a TW with programmable shape-memory ability has been recently developed by introducing epoxy-based vitrimers (dynamic covalently cross-linked polymers) into 2 mm-thick delignified wood.[134] In such composite, shape programming and recovery was achieved within 30 min by transesterification, respectively at 150 and 60 °C.

Notable progress has been made also to improve and up-scale the fabrication of transparent wood as well as unravel its complex optical properties. However, delignification, removing up to 30 wt % of wood tissue, weakens the wood structure and makes the handling and fabrication of large samples challenging and impractical. As a solution, selective removal of chromophores (bleaching), preserving the aromatic lignin structure and thus mechanical properties and hydrophobicity, has been proposed. These approaches use alkaline hydrogen peroxide instead of peracids or chlorine-based oxidants. With the "lignin-retaining method" proposed by Li et al.,[135] up to 80 wt % of the lignin was preserved, leading to better mechanical properties after refractive index matching by impregnation with PMMA. Xia et al. reported an alternative method, which does not require the complete immersion of wood in the bleaching mixture.[83,136] Instead, alkaline hydrogen peroxide is brushed on the surface of the wood and is then subjected to irradiation with UV or solar light. Compared to immersion methods, the processing time is strongly reduced (1−6.5 h instead of 4−14 h) (Figure 13D,E).

Over the past few years, several additional ways to improve the thermal and optical properties of TW, such as the incorporation of phase-change materials (PCMs), thermo-, photo-, and electrochromic materials, fluorescent, phosphorescent, and ultraviolet-shielding materials, have been described to promote its use in the building sector (Figure 14A,B).[137] Phase change materials (PCMs) are temperature-responsive materials that can reversibly store or release thermal energy by changing their molecular arrangements from one physical state to another. For organic PCMs such as polyethylene glycol, fatty alcohols, paraffins, and fatty acids, phase changes are governed by the crystallization and melting of their long chains. Crystal formation and melting also influence the light scattering behavior of the material. Therefore, composites of PCMs with wood are explored for temperature-control systems with switchable optical properties (Figure 14F,G).[138] However, for physically incorporated PCMs, the solid−liquid phase transition can be associated with leakage. This problem can be solved by incorporating PCM moieties into copolymers, as proposed by Qiu et al.[139] Impregnating a delignified wood scaffold with a styrene-butyl acrylate copolymer containing 5% of octadecane side chains resulted in TW with the conveniently low latent heat of melting and crystallization (7.20 ± 0.22 J g^{-1} and 6.41 ± 0.54 J g^{-1}, respectively), low thermal conductivity (~0.19 W m^{-1} K^{-1}; for comparison, conventional glass has ~1.2 W m^{-1} K^{-1}) as well as low thermal diffusivity (~0.1 mm^2 s^{-1}).

Another approach for improving the thermal properties of TW is to reduce its transparency to near-infrared (NIR) radiation. This has been achieved by impregnating delignified wood with a polymer matrix containing nanoparticles able to absorb (e.g., cesium tungstate Cs_xWO_3,[140] antimony-doped tin oxide Sb-SnO_2[141]) or reflect (vanadium dioxide VO_2) NIR light. The temperature-mediated reversible metal−semiconductor phase transition in VO_2 is accompanied by a large decrease in NIR transmittance. The phase transition temperature of pure VO_2 is around 68 °C but can be lowered to room temperature, *e.g.*, by doping with tungsten (W-VO_2),[142,143] so that visible light is (partially) allowed to travel through the composite, while IR

https://doi.org/10.1021/acs.chemrev.2c00450
Chem. Rev. 2023, 123, 1843−1888

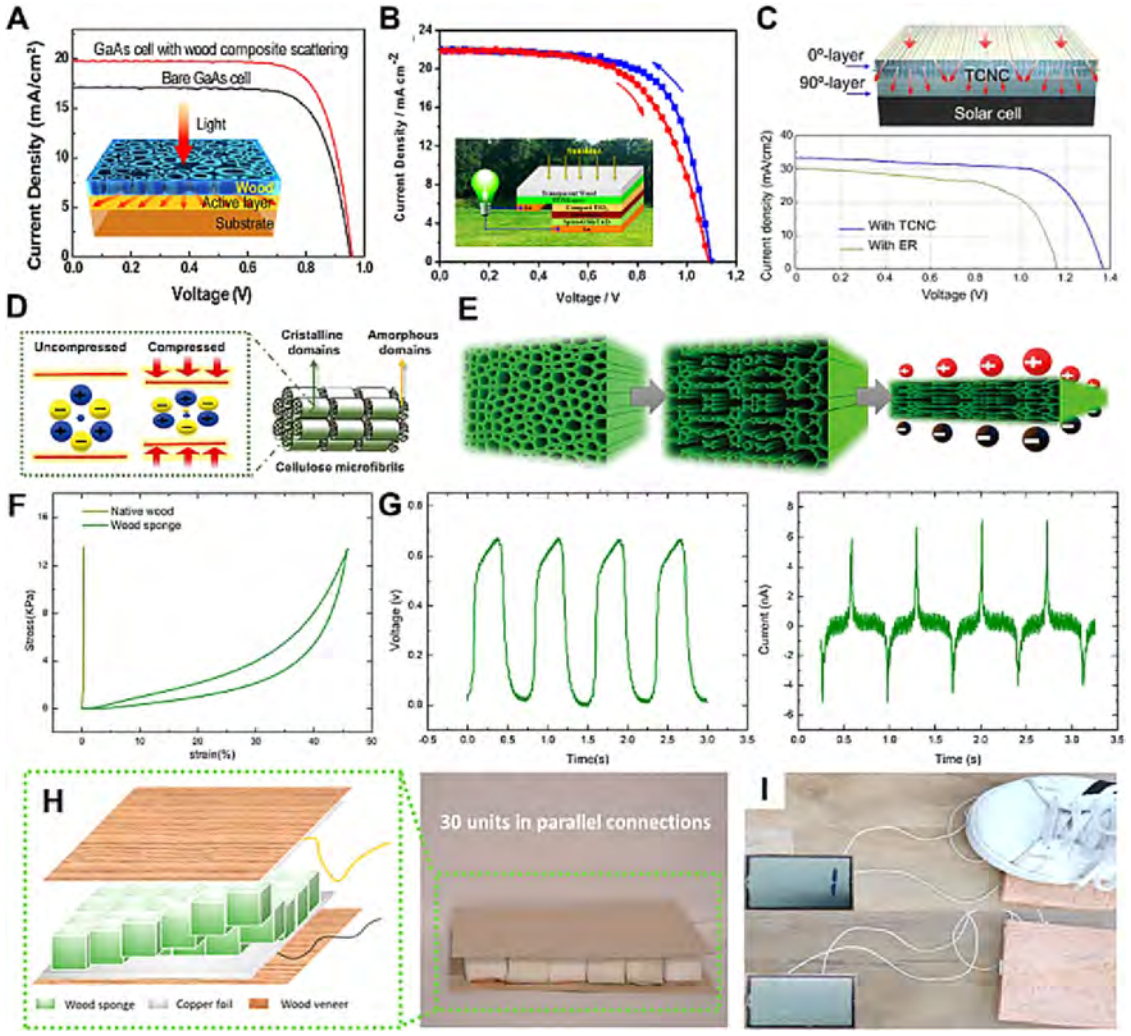

Figure 15. (A) Schematic representation and current density−voltage curves for a GaAs cell with the transparent wood coating (red line) and without (black line).[128] Reproduced with permission from ref 128. Copyright 2016 Elsevier. (B) Schematic representation of a solar cell based on transparent wood and its current density−voltage curves.[154] Reproduced with permission from ref 154. Copyright 2019 American Chemical Society. (C) Transparent cellulose nanofibrils composite as a light management layer for solar cells.[155] Reproduced with permission from ref 155. Copyright 2020 Springer Nature. (D,E) Schematic representations of the piezoelectric effect originating from the deformation of crystalline cellulose domains in wood and wood sponge.[160] Reproduced with permission from ref 160. Copyright 2021 American Association for the Advancement of Science. (F) Demonstration (tensile test) of enhanced compressibility of wood sponge compared to native wood.[161] (G) Voltage (left) and current (right) output of a wood sponge under a constant stress of 13.3 kPa. (H) Schematic representation (left) and picture (right) of a large-scale piezoelectric wood sponge nanogenerator. (I) Demonstration of a wood sponge nanogenerator powering a liquid crystal display (LCD) when pressed by a foot. (F−I) Reproduced with permission from ref 161. Copyright 2020 American Chemical Society.

light is reflected away. It is important to note that all these nanoparticles give intrinsic colors to the TW, and the fact that their phase transitions are usually accompanied by a visible color change.

Nevertheless, because TW which can change color upon different stimuli could be desirable for "smart windows" applications,[144] several studies discussed the incorporation in TW of a variety of organic and inorganic materials for thermo- (e.g., ODB dyes,[145] the already mentioned VO_2) and photochromic (especially using spyropyran dyes composites).[146] An electrochromic transparent wood device was also reported, made by sandwiching a gel electrolyte between two poly(3,4-ethylenedioxythiophene):poly(styrenesulfonate) (PEDOT:PSS)-coated TW electrodes, one functionalized with the electrochromic dye ECP-magenta and the other with a colorless charge-storage polymer (MCCP). A magenta-to-clear color change was then obtained upon the application of a relatively low voltage (0.8 V).

A highly undesirable color change is one challenge, which accompanies the prolonged exposition of transparent wood to ultraviolet radiation ("yellowing"). Exposure to UV−C strongly affects the color and transmittance of transparent wood in a matter of days. Upon irradiation, TW acquires a yellow color, which darkens with increasing exposure time due to the reactivation of chromophores of residual lignin as well as the degradation of the impregnating polymer.[147] To allow the application of transparent wood in buildings, e.g., as windows and roofs, it is of great importance to increase its resistance against environmental degradation (especially the UV light-induced one) and yellowing.

Luminescent wood is a highly promising material for indoor lighting. The incorporation of fluorescent, phosphorescent, or electroluminescent moieties inside wood could allow the design

https://doi.org/10.1021/acs.chemrev.2c00450
Chem. Rev. 2023, 123, 1843−1888

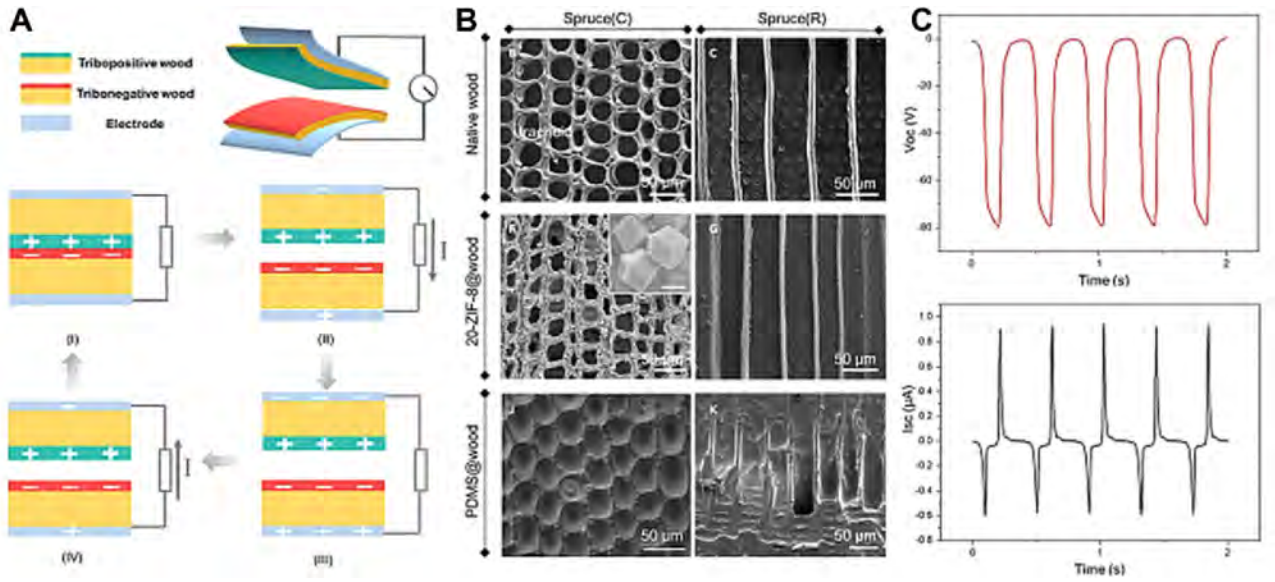

Figure 16. (A) Schematic representation and working mechanism of a functionalized triboelectric wood nanogenerator.[170] (B) Scanning electron microscopy (SEM) images of cross-cut (left) and radial-cut (right) spruce wood: native and after functionalization with in situ-grown ZIF-8 or with PDMS, to make wood respectively more tribopositive and more tribonegative. The inset shows the morphology of ZIF-8 grown on wood (scale bar: 500 nm). (C) Voltage (left) and current (right) output of a large-scale (20 tribowood units, each 2 cm × 3.5 cm) triboelectric wood nanogenerator under a contact force of 50 N. (A−C) Reproduced with permission from ref 170. Copyright 2021 Cell Press.

of panels and displays for smart building applications. Luminescent wood was first mentioned in a 1992 Fink's paper, obtained by dispersing inorganic phosphors in the impregnating polymer matrix, an approach reinvestigated decades later.[148] Since then, many reports have been published on the incorporation of quantum dots in transparent or delignified and densified wood scaffolds (Figure 14B,C).[149,150] An interesting approach to fabricating luminescent wood, which does not require delignification nor refractive index matching because it takes advantage of direct light transmission through the wood ("shine-through"), has been recently reported (Figure 14D).[151]

Despite the technological relevance that optoelectronic wood devices can have for smart buildings, only a few reports are available on this subject. Delignified wood impregnated with poly(acrylic acid) and a mixture of fluorophores, obtained from the hydrothermal treatment of citric acid and urea, was used as a white light-emitting layer converting the UV emission from a conventional LED chip.[152] The assembly of electroluminescent devices was reported by sandwiching a conventional inorganic phosphor (copper-doped zinc sulfide, ZnS:Cu) between two layers of transparent wood, whose surface was made conductive by spray-coating silver nanowires. The resulting devices were claimed to have superior performance compared to more conventional paper and plastic substrates, especially in terms of resistance against humidity and temperature changes.[153,154]

7. ENERGY-CONVERSION WOOD

In addition to contributing to reduced energy consumption, wood materials can also be useful for energy conversion. Transparent wood has been used as a broadband light management layer to enhance the trapping of photons inside the active layer in a standard gallium arsenide solar cell (Figure 15A).[128] More recently, transparent wood was used as a substrate for a low temperature (<150 °C)-processed perovskite solar cell (Figure 15B).[155] In these reports, transparent wood was obtained from radial-cut veneer, which is easier to delignify and impregnate and with good optical properties, but rather limited in size. To alleviate this problem, a two-layer transparent wood with channels oriented perpendicular (0/90°) to each other, obtained from rotary-cut veneer, was proposed to increase the performance of a conventional silicon solar cell (Figure 15C).[156] Nevertheless, the challenges associated with long-time exposure of transparent wood to intense light sources have not yet been taken into account, which limits the real-world applicability of these systems. It is noteworthy that the application of luminescent transparent wood for luminescent solar concentrators (LSCs) has been suggested but not yet demonstrated in practice.

Another very promising direction is represented by wood nanogenerators. Nanogenerators are devices able to harvest low-grade energy, for example, from small temperature gradients, vibrations, or mechanical movement, and to convert it directly into useful electricity by taking advantage of pyro-, piezo-, triboelectric, or other electromechanical coupling effects.[157] The electrical output can vary depending on the device design and the efficiency of the active materials used, but triboelectric nanogenerators (TENGs) can generate very high voltages (up to the kV range) and currents (up to the mA range). Large-scale nanogenerators are especially relevant as point-of-use power sources in smart buildings, for example, as energy-harvesting floorings. Conventional nanogenerators make use of highly efficient but expensive, often toxic, inorganic materials (such as barium titanate, lead zirconium titanate, chalcogenide semiconductors, etc.), but several promising biobased substitutes have been already described, including wood-based ones.

Thanks to the uniaxial orientation and monoclinic symmetry of semi-crystalline cellulose fibrils, wood is a piezoelectric material, i.e., can generate a measurable, although small, electrical output when subjected to mechanical stress (Figure 15D).[158,159] Recently, it was demonstrated that this piezoelectric output can be increased by increasing wood compressibility through delignification (Figure 15D, E).[160,161] Selective removal of lignin from balsa wood using biological or

https://doi.org/10.1021/acs.chemrev.2c00450
Chem. Rev. 2023, 123, 1843−1888

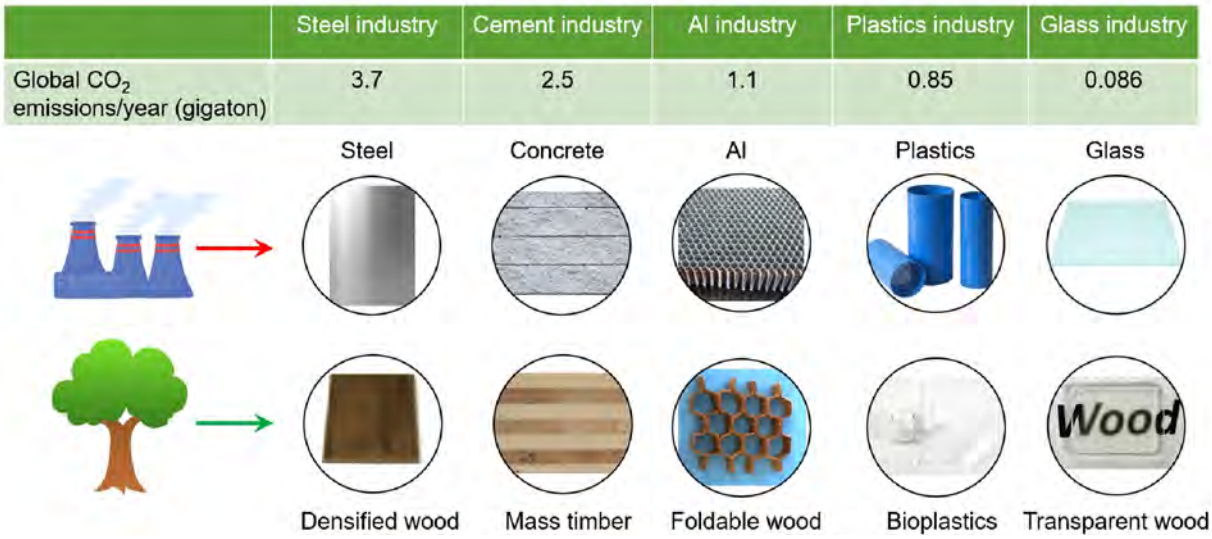

Figure 17. Average CO_2 emission values from different construction-relevant industrial sectors.

chemical (acetic acid−hydrogen peroxide mixture)[161] means resulted in highly compressible wood sponges, with a piezoelectric output ≥85 times higher than native wood (Figure 15F−I). However, the limited electrical output (voltage 0.69 V, current 7.1 nA, and peak power density 0.6 nW cm^{-2} for a 15 × 15 × 14 mm^3 sponge under a pressure of 13.3 kPa) and problematic scalability (chemical delignification is much faster than the biological one, hours instead of weeks, but requires a freeze-drying step) of the process make this approach more suitable for small-scale applications (e.g., for sensing).

Triboelectric wood nanogenerators, thanks to notably higher electrical outputs, are more suitable for large-scale applications. In recent years the development of biobased triboelectric materials, especially using polysaccharides such as cellulose, has generated a huge research interest.[162] However, extensive and complicated modification steps are often required to produce materials with sufficient performance, reducing their overall sustainability. Wood, as a state-of-art material for floorings and wall panels, is a very promising yet challenging substrate for the design of triboelectric nanogenerators. Native wood has negligible triboelectric properties, due to the antistatic properties of lignin and the relatively low polarizability of cellulose.[163,164] Conventionally, delignification and coupling with more efficient (but less sustainable) triboelectric materials such as fluorinated polymers (PTFE, FEP) are exploited to increase the output.[165,166] Functionalization with aminosilanes and fluorinated silanes has also been reported to make delignified densified wood respectively more tribopositive and tribonegative.[167] A nanogenerator made with a fluoropolymer (FEP) tribonegative electrode and a counter electrode made with delignified wood impregnated with single-walled carbon nanotubes (SWCNTs) has been claimed to allow energy harvesting and gas sensing at the same time.[168] Exposure to ppm amounts of ammonia gas resulted in a decrease of the electrical output which, coupled with good resistance against humidity and low temperatures, makes such nanogenerator potentially useful in smart packaging, to help detect spoilage of high-protein foods. Applications for smart buildings are on the rise too, with self-powered wood devices (mainly sensors) being proposed as smart home control systems.[169] Nevertheless, generating energy just by walking or tapping on a wooden floor or desk is an enticing technological opportunity. Recently, triboelectric flooring was obtained, without the need for delignification, by functionalizing a wood scaffold with ZIF-8 metal−organic framework (MOF) nanocrystals (making wood more tribopositive) and silicone polymer (PDMS, making wood more tribonegative) (Figure 16). In that study, the advantage was taken of the characteristic features of wood to increase, respectively, the mechanical stability of the ZIF-8 particles and the surface area of the PDMS layer.[170]

Despite the great promises of piezo- and triboelectric wood nanogenerators, several challenges of both fundamental and applicative nature need yet to be addressed. The exact mechanisms of electricity generation in wood materials are still a subject of debate, while new and improved designs are researched with a highly empirical process. From the sustainability point of view, much remains to be done as well. The use of fluoropolymers significantly reduces the positive aspects brought by the use of wood. Also, the recyclability and disposal of these devices are waiting to be consistently addressed.

8. CARBON IMPACT AND RECYCLABILITY OF ENGINEERED WOOD PRODUCTS

Around 3.7 gigatons of CO_2 are emitted annually from the global steel industry, followed by 2.5 gigatons from the cement sector, 1.1 gigatons from the aluminum (Al) industry, 850 million tons from the plastics industry, and 86 million tons from glass manufacturing (Figure 17).[171,172] Specifically, steel-based structural materials have been widely employed for construction applications. Steel is typically manufactured via a high-temperature process that consumes a significant amount of energy (~20 GJ/t for steel) and produces large greenhouse gas emissions (~1.9 t CO_2-eq/t for steel).[173] Considering the 40 million tons of steel used in the construction industry in the United States per year, 76 million tons of greenhouse gases have been emitted, accounting for more than 1% of the U.S. greenhouse gas emissions.

Wood, on the other hand, can be derived from nature directly and used to fabricate mass timber products. During the growth of trees, it is estimated that 1.8 kg of CO_2 can be removed from the atmosphere per kg of dry wood via photosynthesis. Thanks to the advances made so far in wood nanomaterials and

https://doi.org/10.1021/acs.chemrev.2c00450
Chem. Rev. 2023, 123, 1843−1888

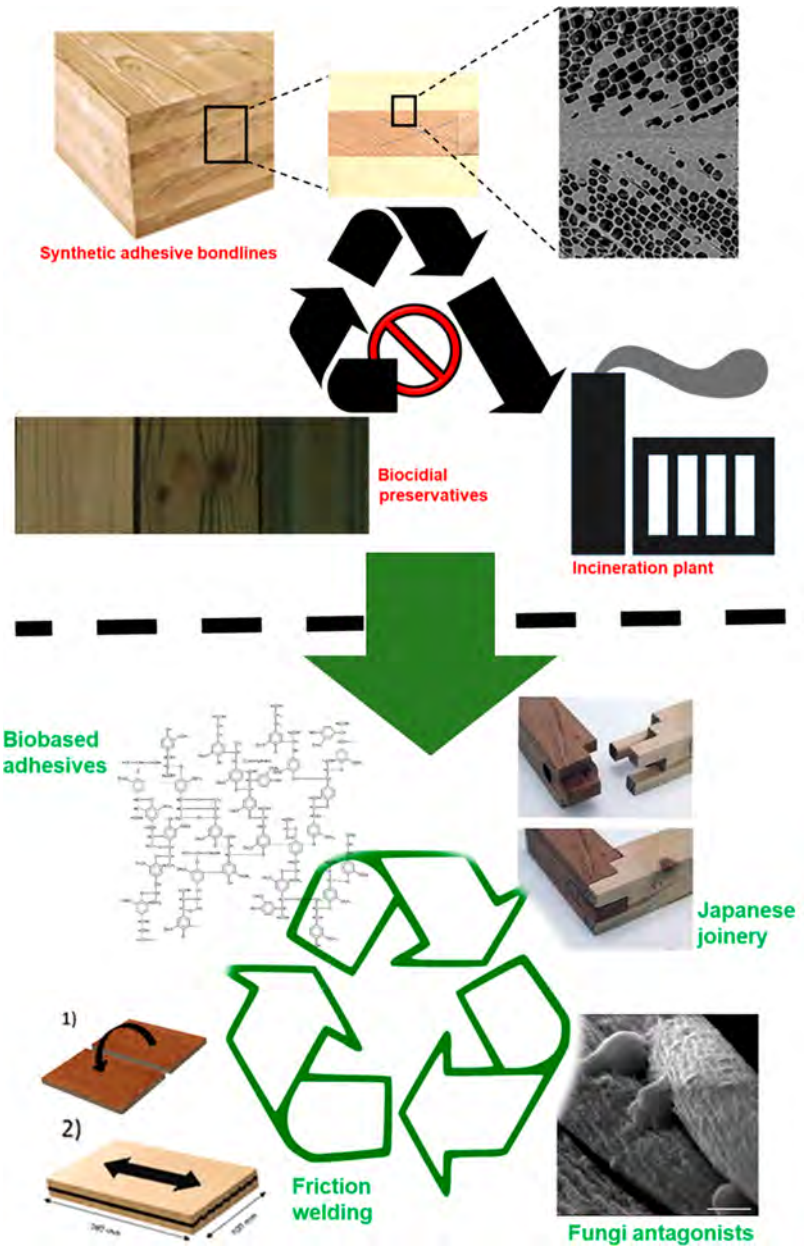

Figure 18. (top) Schematic representation of common factors strongly impeding recycling of wood products. These include the formation of difficult-to-separate wood-based materials with synthetic adhesive bond lines and the use of biocidal preservatives. (bottom) To promote efficient recycling of wood products, the use of biobased (e.g., derived from lignin) and reversible/detachable bonds as well as adhesive-free bonding techniques should go hand-in-hand with the application of nontoxic preservatives. The reality, however, is that those adhesive bonding techniques, which would facilitate recycling, fail in providing the required (wet) stability and durability issues for structural applications still need to be overcome. CLT picture.[176] Reproduced with permission from ref 176. Copyright 2022 Elsevier. SEM image of a bond line in spruce (fiber direction in bonded wood parts different from CLT). Reproduced with permission from ref 177. Copyright 2012 Springer. Pictures of CCA-treated wood.[403] Picture of fungi antagonist.[208] Reproduced with permission from ref 208. Copyright 2008 Elsevier. Picture: Japanese joinery technology: www.spoon-tamago.com.

nanotechnologies, several man-made and energy-intensive building materials commonly used in construction could be, in part or completely, substituted by engineered wood products (Figure 17). Switching from energy-intensive structural materials to more sustainable wood-based products represents an effective approach to reducing embodied emissions from the building sector.

A major obstacle for the construction sector to become more sustainable is the low recycling and reuse of wood-based products. Herein, the biggest barrier to the reuse of structural members is the lack of nondestructive methods to evaluate the structural integrity or locate defects. In Switzerland, for example, the current recycling rate of wood-based products is as low as ~10%.[174] One obvious reason for that is the good calorific value of wood, making its use as an energy source favorable in many cases.[175] However, limitations to recycling a larger amount of engineered wood are also closely connected with established wood treatments, in particular bonding (e.g., adhesives) and protective (e.g., fire-retardancy, wood degradation) purposes.

The vast majority of wood-based products used in the construction sector are bound using synthetic adhesives (Figure 18).[175−177] The development and implementation of materials

https://doi.org/10.1021/acs.chemrev.2c00450
Chem. Rev. 2023, 123, 1843−1888

such as glued laminated timber (glulam) and cross-laminated timber (CLT) would not have been possible without using tailored polycondensation (e.g., PRF) or polyaddition (PUR) adhesives, which can provide a strong and moisture-resistant long-term bond joint between wooden elements.[178,179] However, these properties, which are essential to obtain reliable structures are strong hinders against their efficient recycling. One reason is that the separation of the thermoset adhesives from wood after the end of life of a wood product is a very complicated and, in the current conditions, uneconomical process. Moreover, due to the porous nature of wood, the adhesive layer is not confined to the wood surface, instead, it penetrates into the cell lumina and, in the case of PRF or MUF, even into the wood cell walls.[180] Hence, besides the challenge of separating the wood elements leaving intact the bulk while removing the adhesive from the surface, it is necessary to consider the near-surface interphase region in which wood and adhesive are tightly interwoven at the micro- and nanoscale.[181]

The detrimental effects of established bonding processes on the recyclability of wood products are currently tackled by different research approaches working at different length scales (Figure 18). Synthetic adhesives or metal fasteners exemplify a few practical obstacles to separating and recycling wood products from building deconstruction. To address the challenge of disassembling structural connections, some have investigated traditional wood joinery as an alternative to both adhesive and mechanical fasteners in structural connections. The effectiveness and practicality of joinery without adhesives or fasteners, however, are limited by several factors. The tolerances required to fit and assemble components, for example, generally produce connections that lack stiffness.[182] Others have attempted to develop connection alternatives by conversion of wood components into adhesives based on the degradation of the wood surface by a CO_2 pulsed laser or through the so-called wood welding process.[183] In the wood welding process, rubbing two wood pieces against each other, with a certain frequency and under the application of a certain pressure, results in a high-temperature generation at the interface between the two wooden elements.[184−186] This in turn melts the lignin, which then acts as a glue producing a rigid bond line of high dry strength, all with rather little bulk wood degradation. The major problem against a wider application of this technique is the low wet strength,[187] which excludes any structural application for wood welded materials. Current research activities aim at increasing the wet strength,[188−190] but so far no fully satisfying solution could be found, mainly because of the complexity of the process. For the foreseeable future, therefore, both joinery and wood welding remain niche alternatives to standardized structural connections.

The most promising approach is to change the composition of the adhesives by substituting artificial components with biobased ones. Since ancient times, natural glues based on proteins or polysaccharides have been used for bonding purposes (e.g., gelatin, gluten, dextrin, and starch) and are still used in several applications, for instance, for the gluing of wooden musical instruments. These glues show excellent properties in the dry state but suffer, likewise wood welding connections, from a low or even not-existing wet strength.[184,191,192] Research efforts to increase the cross-linking density of these biobased raw materials are promising,[193] but further progress is needed. Also, lignin, which is obtained in huge amounts as a byproduct of the pulp and paper industry, as well as tannins, are seen as a highly valuable starting material for the development of biobased adhesives.[184,194−197] However, especially lignin residues from pulp and paper production are very heterogeneous in terms of molecular size and functional groups, which also depends on the delignification process applied.[198] As a consequence, elaborate fractionation, depolymerization, and characterization efforts are needed to ensure the quality and reproducibility of lignin components.[199]

Another challenge associated with the development of biobased adhesives is the necessity to increase the cross-linking density, while at the same time reducing the accessibility of −OH groups to achieve a sufficient wet strength of the bond joint. This is already difficult to achieve with an efficient and scalable chemical process, and it becomes even more challenging when the consequences of chemically altering natural products are considered. Such modifications most often lead to materials that, although biobased, have lost their characteristic biodegradability. Whereas favorable for technical applications as, e.g., long-term adhesives, it makes them inappropriate in the context of a circular economy. Hence, together with the biobased adhesive approach, the possibility of a debonding on demand must be introduced to the picture. The research on this subject is still in its infancy but could turn out to be a game-changer, allowing us to overcome the obstacles to the recyclability of wood products.

Besides wood bonding, treatments for modification, and in more recent times also functionalization, can strongly impede the recyclability of wood materials and wood products. While wood modification and preservation treatments serve to improve durability and dimensional stability,[200−202] functionalization serves to enable wood with new properties, opening new fields of applications for wood.[28,203,204] A common feature is that chemical treatments are applied, resulting in often dramatic changes in the chemical composition of the treated wood. The most detrimental in terms of recyclability is the use of various biocide preservatives, whose importance for the durability of timber structures has been reviewed recently.[176] Although health safety issues and environmental concerns have resulted in the prohibition of several chemical compounds and combinations, especially, for use in residential structures, wood impregnated with preservative materials still in use has to be treated as hazardous waste after its end of life. Alternative approaches for wood protection try to prevent the degrading action of specific wood degrading fungi using natural fungi antagonists.[205] Although promising results have been obtained recently, further development is required. Ensuring wood durability is crucial in the context of a global rise in timber building construction as a climate protection measure. A majority of future buildings will be erected in hot and humid climates, favorable conditions not only for the growth of decay fungi but also for termites, which are major threats to wood structures. Research on efficient but environmentally friendly protection against termites is of utmost importance, also given the fact that climate change will favor the spreading of termites around the globe.[206]

Increased durability can be achieved also by wood modification treatments for increased dimensional stability. This is the case of wood acetylation, in which the resulting hydrophobization of the cell wall helps impede fungal attacks.[207] Acetylated wood remains recyclable, while modification treatments with cross-linking polymers appear problematic, in particular when they are not biobased. Similarly, functionalization treatments with inorganic or polymeric compounds will strongly limit the recyclability of functional wood materials as long as green chemistry rules are not strictly applied. These

https://doi.org/10.1021/acs.chemrev.2c00450
Chem. Rev. 2023, 123, 1843−1888

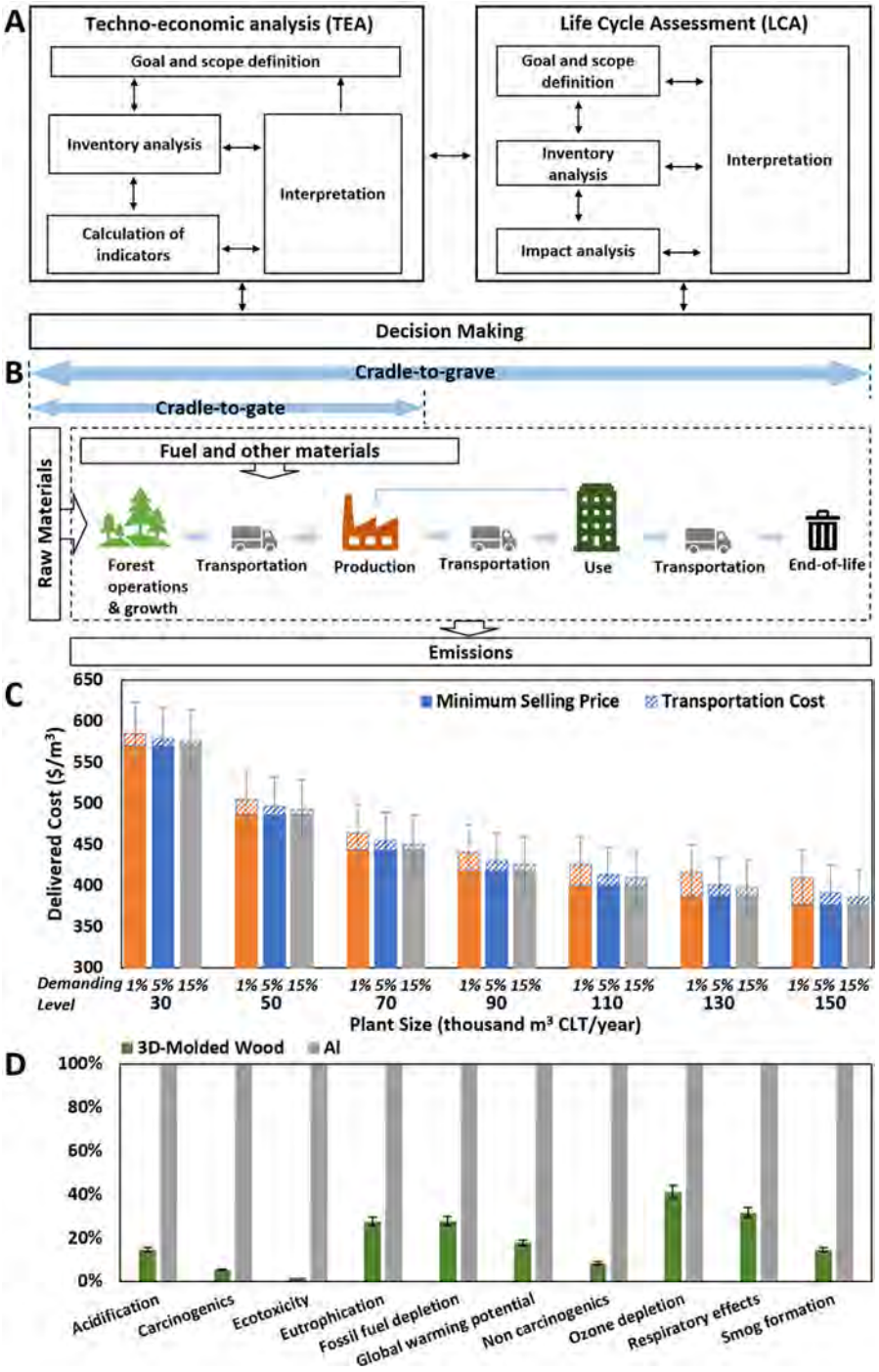

Figure 19. LCA and TEA of engineered wood products. (A) LCA and TEA framework. Reproduced with permission from ref 256. Copyright 2020 Frontiers. (B) The system boundary of LCA for engineered wood products; (C) an example of TEA results (delivered cost including minimum selling price (MSP) and transportation cost) of 1 m^3 CLT (cross-laminated timber) on varied plant capacities and demanding levels.[257] Reproduced with permission from ref 257. Copyright 2022 Tech Science Press. (D) An example of the environmental impacts of 3D-molded wood and aluminum alloy per cubic centimeter per megapascal (normalized to the higher impact material for each environmental impact category).[57] Reproduced with permission from ref 57. Copyright 2021 American Association for the Advancement of Science.

aspects should generate more attention in the future for an advantageous development of this emerging research field.

9. LCA OF ENGINEERED WOOD PRODUCTS

9.1. Basics of LCA on Engineered Wood Products

LCA is a standardized tool to evaluate the environmental impacts of a product or a process throughout its life cycle.[209] As shown in Figure 19A, the LCA framework consists of four main phases, namely the goal and scope definition, Life Cycle Inventory (LCI) analysis, Life Cycle Impact Assessment (LCIA), and Life Cycle Interpretation.[209,210]

The first phase of LCA defines the goal and scope of a study. The scope definition needs an explicit description of the subject to be studied (e.g., an engineered wood product), functional unit, system boundary, data requirements, impact categories

https://doi.org/10.1021/acs.chemrev.2c00450
Chem. Rev. 2023, 123, 1843−1888

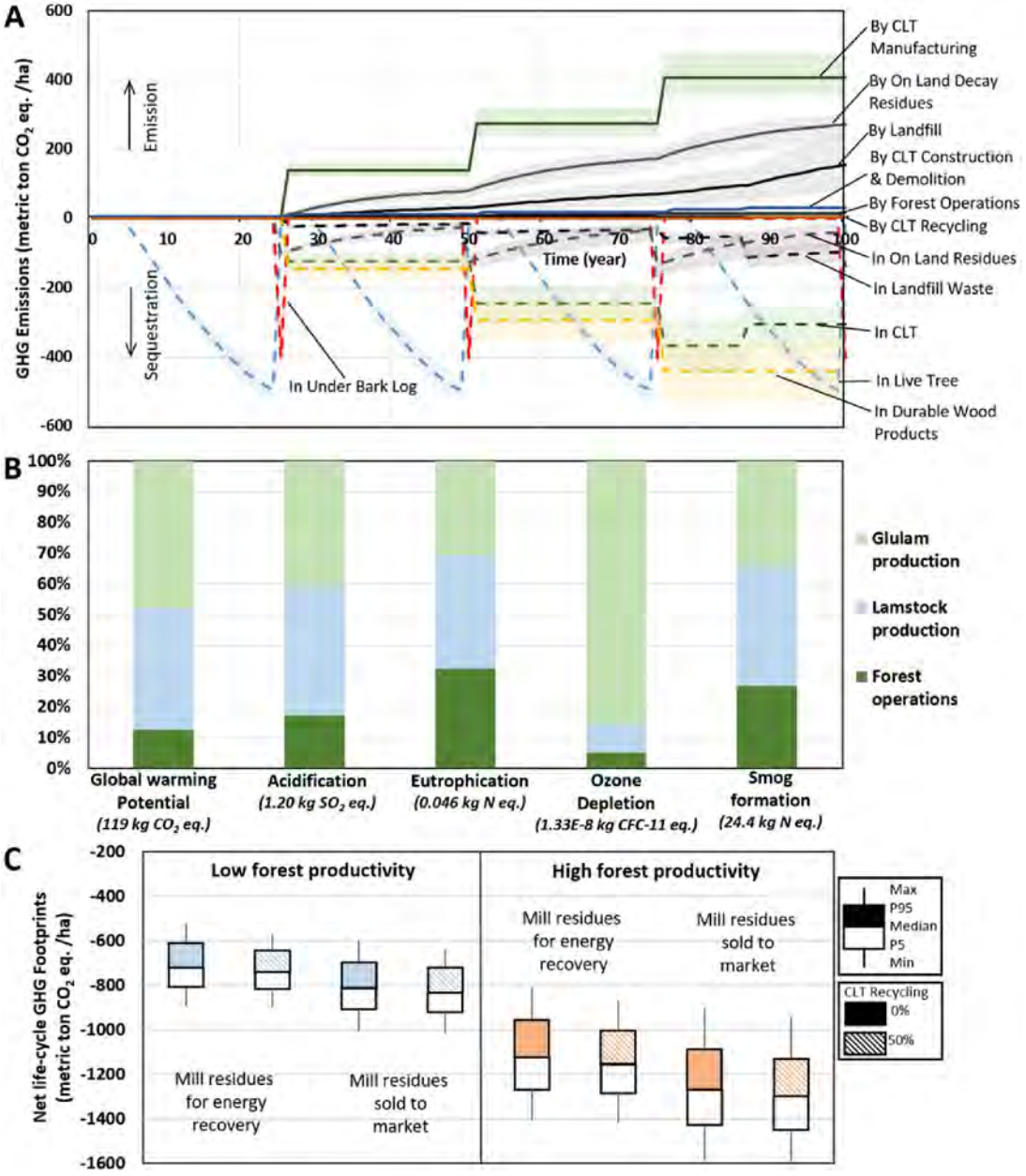

Figure 20. LCA examples of engineered wood products. (A) A dynamic LCA that quantifies carbon flows of a cradle-to-grave CLT system over 100 years.[255] Reproduced with permission from ref 255. Copyright 2020 IOP Publishing. (B) LCA results of 1 m^3 glulam including multiple impact categories.[212] (C) An example of life-cycle GHG emissions of 1 ha forest land for CLT production under varied scenarios of forest management, manufacturing, and end-of-life.[255] Reproduced with permission from ref 255. Copyright 2020 IOP Publishing.

selected, and other scope definition items.[209,211] Previous LCAs of engineered wood products commonly select product-level units as their functional units (e.g., 1 m^3 of wood product, 1000 board feet of wood product). Among those, 1 m^3 of engineered wood products is the most adopted in previous literature.[212−251] Other product-level functional units are related to specific constructional applications (e.g., 1 m^2 of the roof, 30 m^2 of surface decking) to compare with traditional building materials (e.g., steel).[252−254] For example, Petersen and Solberg used 1 m^2 roof as the functional unit to compare the life-cycle energy consumption and greenhouse gas (GHG) emissions of glulam and steel.[252] Besides, stand-level functional units (e.g., 1 ha forest land) can be used to incorporate the effects of forest management strategies and forest yield into the LCA of wood products.[255] Figure 20A and C shows an example from Lan et al., who developed a dynamic LCA for CLT across 100 years in the Southeastern U.S. based on the functional unit of 1-ha forest land. The results demonstrate the substantial impacts of forest productivity on the net GHG emissions of CLT (−954 to −1445 t CO_2 eq/ha for a high forest productivity scenario compared to −609 to −919 t CO_2 eq/ha for a low forest productivity scenario).

The system boundary, which needs to be consistent with the goal of LCA, decides which unit processes should be included within the LCA.[209] Figure 19B shows two typical system boundaries used in LCA studies of engineered wood products, namely cradle-to-gate and cradle-to-grave. The cradle-to-gate system boundary commonly includes raw material extraction, forest operations and growth, transportation, and production. The cradle-to-grave system extends the cradle-to-gate system

https://doi.org/10.1021/acs.chemrev.2c00450
Chem. Rev. 2023, 123, 1843−1888

boundary to cover the use phase and end of life (e.g., landfilling, recycling, reuse, and energy recovery). The cradle-to-gate system boundary is helpful for process design and development, particularly in understanding the impacts of manufacturing, or supply chain-related parameters on environmental impacts. For example, Chen et al. conducted a cradle-to-gate LCA for CLT manufactured in Western Washington and focused on the comparative analysis of varied parameters, including transportation logistics, mill location, and relevant wood species mixes.[242] Results manifest that the location of lumber suppliers and the selection of wood species are important factors in the total environmental impacts.[242] Lu et al. chose the cradle-to-gate system boundary for a comparative LCA of laminated veneer lumber (LVL) made from thinned logs versus mature logs.[258] The results exhibit higher global warming potential (GWP) and embodied energy for LVL from mature logs than thinned logs.[258] González-García et al. conducted a cradle-to-gate LCA for wood hardboard and identified that chemicals, electricity, and production of green chips have large contributions to environmental impacts.[259] Compared to the cradle-to-gate system boundary, the cradle-to-grave system boundary can be useful for understanding the impacts of use and end-of-life design, especially in the context of the circular economy. For example, Nakano et al. performed a cradle-to-grave LCA to assess the life-cycle human health effects of particleboard and medium-density fiberboard.[260] The results indicate that approximately 90% of human health impacts were attributed to the use phase, although their total life-cycle human health impacts were over 90% less than conventional products.[260] End-of-life design is important to the life-cycle results of wood products.[261] Niu et al. conducted a literature review and a streamlined LCA and concluded that prolonging the lifetime of structural materials such as wood by reusing and cascading helps combat climate change and reduce environmental burdens.[262]

The second phase, LCI analysis, collects LCI data (e.g., mass and energy balances, and environmental emissions) based on the goal and scope defined in the first phase.[209,263] The LCI data used in previous engineered wood products LCA mainly come from four sources, namely literature, process-based simulation,[264] databases (e.g., ecoinvent[265] and US LCI database[266]),[242,243,267] and survey data.[213,251,259,268−270] For multi-product systems, system expansion or allocation can be used to determine the environmental burdens associated with individual products.[214,233]

The third phase, life cycle impact assessment (LCIA), calculates the environmental impacts based on the LCI data.[209,210,271] A variety of environmental impacts can be quantified during this phase. Climate change impact, quantified by GWP, is the most commonly used impact category for engineered wood products because engineered wood products are expected to provide benefits in mitigating climate changes by emitting less fossil-based GHG and storing the biogenic carbon as potential carbon sinks.[255] Other impact categories (e.g., ozone depletion, acidification, smog formation, eutrophication, ecotoxicity, human health impact, and resource depletion) can be adopted depending on the goal and scope of the LCA studies. For example, as shown in Figure 19D, Xiao et al. selected 10 different impact categories to compare the total environmental impacts of 3D-molded wood material with aluminum alloy.[57] Besides the selection of impact categories, the selection of LCIA methods is essential. Common impact assessment methods include TRACI (adopted by refs 215,232,233,242,244,272),[273] ReCiPe (used by refs 214,234,254,274),[275] USEtox (employed by refs 226,260,268,276),[277] CML (utilized by refs 215,226,238,268,278,279),[280] and Eco-indicator 99 (applied in refs 218,230,250).[281]

The fourth phase, life cycle interpretation, makes conclusions and recommendations based on the results of LCI or LCIA and identifies significant issues.[209] The interpretation phase also evaluates the LCA for completeness, sensitivity, and consistency, and discusses limitations.[209] Different analytical techniques (e.g., contribution analysis or sensitivity analysis) have been used in this phase to understand the driving factors of environmental impacts and identify improvement opportunities. For example, Echeverria et al. applied contribution analysis to identify the hotspots for environmental impacts of dissolving pulps made from hardwood and softwood and found on-site emissions and chemicals as the main contributors across all dissolving pulp grades.[282] In another LCA study on sustainable bleaching of wood pulp, the upstream burdens of bleaching chemicals contribute to most life-cycle environmental impact categories, and sodium sulfate contributed the most among the chemicals, which reveals the future opportunities to reduce the environmental impacts of pulp bleaching.[283]

9.2. LCAs of Traditional Engineered Wood Products

LCA has been widely employed to quantify the life cycle environmental impacts of traditional engineered wood products, including glulam, I-joist, laminated strand lumber (LSL), LVL, oriented strand board (OSB), plywood, composite board, and other wood products.[213,215,217,230,268,284−286] These studies have used LCA to identify the major contributors to environmental performance. These contributors can be either life cycle stages (e.g., forest operations, panel production, use phase) or processes (e.g., chipping, heat generation, resin application, sawing).[255] As displayed in Figure 20B, Bowers et al. performed a cradle-to-gate LCA on glulam and showed the contribution of each life cycle stage (i.e., forest operation, lamstock production, and glulam production) to six environmental impact categories.[212] The results indicate that GWP and ozone depletion are mostly driven by glulam production, while eutrophication and smog formation are nearly equally contributed by all three life cycle stages. Bergman and Alanya-Rosenbaum studied the life-cycle environmental impacts of I-joist produced in the Pacific Northwest (PNW) and Southeast (SE) U.S., their system contained five life-cycle stages, namely forest operations, LVL production, finger-jointed lumber production, OSB production, and I-joist production.[287] The results show that the LVL production stage accounts for the most contribution (42% in PNW and 55% in SE) in GWP and the I-joist production stage takes over 96% of ozone depletion impact.[287]

LCA has been used to understand the environmental contributions of specific manufacturing processes. González-García et al. developed an LCA for hardboard, including wood preparation, board forming, and board finishing.[259] Across 10 impact categories, wood preparation presents the highest contribution (>50%) to all categories due to the high electricity consumption and the fact that only wood preparation consumes chemicals.[259] Silva et al. developed a cradle-to-gate LCA for medium density particleboard in Brazil and identified the main environmental hotspots to be the use of heavy fuel oil as an energy source and the production of urea-formaldehyde as the adhesive resin.[276] Analyzing the contribution of life cycle stages or processes identifies hotspots and guides future potential research and development for lower environmental impacts.[283]

https://doi.org/10.1021/acs.chemrev.2c00450
Chem. Rev. 2023, 123, 1843−1888

Many studies have developed parametric LCA to quantitatively link decision-making parameters and environmental impact results.[288,289] Such links allow for a better understanding of the environmental consequences of different decision options. Common parameters explored in previous wood products LCA include the use of adhesive resin,[215,226,236,238,272,274,279] energy consumption,[226,228,229,238,258] feedstock selections,[215,268,274,279,285] fuel options,[215,228,232,253,270,272] facility location or transportation distance,[215,251,258,267,268,284] allocation factor,[212−214,219,233,290,291] wood species,[274] and end of life.[215,221,253,260,278,279] Sensitivity analysis is often deployed to analyze the impacts of the parameter change. For example, Puettman et al. used sensitivity analysis in their LCA for OSB production to compare different allocation methods and resin selection.[236] The sensitivity analysis demonstrates that changing the mass allocation method to the economic allocation method increase the results by 16−28%; increasing the use of methylene diphenyl diisocyanate resin and using no phenol formaldehyde resin enlarges the nonrenewable energy consumption but leads to small effects on the total environmental impacts.[236] Khatri et al. deployed sensitivity analysis to investigate the environmental consequences of changing adhesive resin usage, electricity, wood fuel, and transportation distance in LSL manufacturing.[215] This study shows that adhesive usage has a large influence on seven out of nine impact indicators and concludes that "ensuring the optimal adhesive use" can efficiently improve the overall environmental performance.[215] Hence, using parametric LCA to explore and quantify the impacts of different options can support process optimization toward a sustainable direction.

As previous LCA studies are mostly concerned about the climate change impact of GHG emissions, many of them have considered CO_2 sequestration during forest growth and biogenic carbon release at the end of life (e.g., wood waste landfilled or combusted for heat or power generation).[214,246,292] How to account for the climate impact of biogenic carbon emissions is under debate. Many studies have used the carbon-neutral assumption that biogenic carbon emissions will always be offset by carbon uptake during forest growth.[228,253,276,279,293−295] As a result, these studies either only account for fossil-based carbon emissions or use a net zero balance after considering an equal amount of biogenic CO_2 emissions and uptake.[228,253,276,279,293] This carbon-neutral assumption has been challenged by many studies, especially for long-lived wood products.[296,297] Given the long lifetime, wood products provide temporary carbon storage (e.g., decades of years) when they are in use, resulting in a delayed climate impact in terms of biogenic carbon emissions.[298] The longer lifetime, the better, which is one of the reasons why long-lived wood products are recommended as a climate change mitigation strategy by IPCC.[299] As the traditional LCA method is a static approach, most wood products LCA have not considered the delayed climate impact of biogenic emissions. Dynamic LCAs have been developed in recent years, and several studies have shown the importance of incorporating the effect of timing into the carbon footprint analysis of wood products.[300−304] For example, Cardellini et al. developed a dynamic LCA for glulam, whose system boundary includes forest growth, production, use, and end of life.[246] Using the dynamic approach, they estimated the climate impact to be 226%, 406%, and 42% lower than the static approach over 20-, 100-, and 500-year time horizons, respectively.[246] Their results highlight the need for considering the dynamic climate change impact of long-lived wood products that contain biogenic carbon.[246] Another source of carbon emissions/sinks is related to changes in land use and forest management. Although emissions related to these changes are seldomly considered by LCAs of traditional engineered wood, this type of emissions has been reported in LCA studies on woody bioenergy and forest carbon stock.[305−308]

9.3. LCAs of Emerging Wood-Based Materials

Many emerging wood-based products and materials have been developed in recent years, some of them have been commercialized (e.g., CLT) while others have not (e.g., CNC). LCA has been used in combinations of other tools such as green chemistry principle[309] and lean manufacturing[310] to facilitate the early stage design of chemicals, materials, processes, and products that are more environmentally friendly and less resource-intensive. For wood products specifically, many LCAs focus on pinpointing major design parameters that matter most in terms of environmental sustainability to identify improvement directions.[57,255,311,312]

For example, Hu et al. developed 3D moldable wood structural material via cell wall engineering and performed a cradle-to-gate LCA to quantify the environmental performance compared to traditional aluminum alloy.[57] The LCA results identify the energy consumption of the wood treatment as the major contributor. By reducing the delignification time (which reduces energy consumption), the environmental impacts of the 3D-molded wood are largely reduced across all environmental impact categories. Figure 20C shows another example where Lan et al. developed a cradle-to-grave LCA for CLT.[255] Compared to the combustion of mill residues for energy recovery, selling mill residues to produce durable wood products reduces 13% of overall GHG emissions but increases over 145% of fossil-based GHG emissions.[255] Another insight is the benefit of recycling. Recycling 50% of the CLT can lead to a 17−28 t CO_2 eq/ha reduction over 100 years, compared to landfilling case.[255] Santos et al. deployed an LCA to quantify the environmental impacts of a new type of wood product Cross-Insulated Timber (CIT), which is similar to a five-layer CLT panel, but polyurethane rigid foam is used as the inner layer.[312] The study examined different end-of-life scenarios and concluded that end-of-life was a large contributor to the environmental impacts, and the comparison between landfilling and incineration for energy recovery had large uncertainties.[312] The study also investigated the environmental consequences of the optimal design for minimal economic costs (e.g., optimize layer thickness, choose different core layer materials such as polyurethane or insulation cork board core).[312] Their results demonstrate the co-benefits of economically favorable design in lowering the environmental impacts of CIT. Compared to CLT products, CIT has lower impacts in some categories but higher in others, and the comparative conclusions of different designs vary.[312]

9.4. LCAs and Embodied Carbon at the Whole Building Level

The building construction industry (including commercial, residential, and industrial buildings) accounts for 5% of global energy use and 10% of global GHG emissions.[113] Total GHG emissions from the global building sector reached nearly 14Gt in 2019, around 28% is operational carbon and 10% is embodied carbon.[113] A primary source of these emissions is the manufacture of building construction materials such as concrete, steel, and glass. It was the largest knowledge gap concerning embodied carbon in buildings exists at the whole-building level.[313]

https://doi.org/10.1021/acs.chemrev.2c00450
Chem. Rev. 2023, 123, 1843−1888

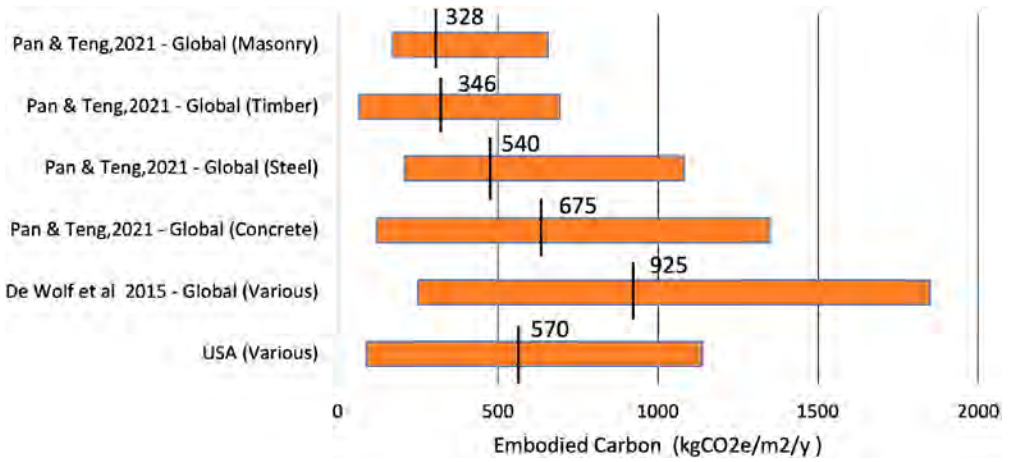

Figure 21. Variation in published embodied carbon results.

Based on limited studies on the whole building embodied carbon assessment (Figure 21). The average life span used in the case studies ranges from 50 to 100, and the average building size is 23615 m^2. The building type included an office building, residential building, educational building, and library. The mean embodied carbon is 570 $kgCO_2/m^2/yr$ in the U.S. As illustrated in Figure 21, the bottom bar represents the embodied carbon of a whole building, ranging from 89 $kgCO_2/m^2/yr$ to 1050 $kgCO_2/m^2/yr$. Also included in Figure 21 are previous studies on global building embodied emission in general and per construction types (masonry, timber, steel, and concrete).[314,315] The average global embodied carbon emission of a whole building is 925 $kgCO_2/m^2/yr$,[314] and masonry building has the lowest mean embodied carbon of 328 $kgCO_2/m^2/yr$, concrete building has the highest mean of 675 $kgCO_2/m^2/yr$, followed by the wood building of 346 $kgCO_2/m^2/yr$ and steel building of 540 $kgCO_2/m^2/yr$.[314] The results demonstrate that, in general, buildings made of wood materials have a much smaller life cycle embodied carbon emission compared to other construction types on a global scale.

The development of embodied carbon is intertwined with the development of LCA methodologies for materials and buildings because embodied carbon is a part of the whole life cycle carbon associated with a building project.[316] In the past two decades, there has been increasing global interest in the analysis of characteristics and the related embodied carbon of large existing building stocks. However, compared to the large body of studies on energy efficiency improvement of the existing building stock, the studies on embodied carbon of building stock are limited. A recent study revealed the majority of existing knowledge of embodied carbon is at the building material and building product level, while only less than 10% of published studies focused on embodied carbon at the whole building level.[313] Two primary causes of limited study on the whole building life cycle embodied carbon include the reliability data of product stages (A1−A3) and availability of data of end-of-life stages (C) because they are highly dependent on the assessor's assumptions of how a building may be used and maintained.[314] In addition, the upstream energy use and carbon emissions resulting from the production of building materials and equipment (A1−A3) are more difficult to measure and track than building operational energy use and emissions. Currently, the data of A1−A3 mainly relies on self-assessment and reporting from manufacturers alone which is not robust and accurate enough, especially for newer and advanced materials such as nanomaterials and materials modified with the use of nanotechnological approaches.

10. TEA OF ENGINEERED WOOD PRODUCTS

10.1. Basics of TEA on Engineered Wood Products

Techno-economic analysis (TEA) is a commonly adopted tool to evaluate the technical performance and economic feasibility of a process, product, or service.[256,257,317−319] TEA can support decision-making processes by providing both technical and economic information.[320] Figure 19A shows the TEA framework proposed by Zimmermann et al., which has similar phrases as the LCA framework and includes goal and scope, inventory, calculation of indicators, and interpretation.[256] The goal and scope definition phase usually includes main questions, intended uses, limitations, audiences of the analysis, system boundary, indicator selection, analysis methods, and other elements.[256] Typical TEA indicators include technical indicators (e.g., energy demand, energy efficiency, conversion rate, material demand, technological maturity, and technological advancement), economic indicators (e.g., capital expenditure, operating expenditure, net present value, internal rate of return, profit, minimum selling price, and life cycle cost), and techno-economic indicators (e.g., technology readiness level).[252,256,257,317−329] For instance, as shown in Figure 19C, Lan et al. used the average delivered cost (minimum selling price plus transportation cost) of CLT as the indicator to explore the impacts of varied plant capacities and CLT demanding levels on the economic performance.[257]

In the inventory phase, the data requirements are defined; technical data (e.g., mass and energy demand and equipment capacity) and economic data (e.g., material price, labor salary, and equipment purchased price) need to be collected and adjusted accordingly depending on the data requirement (e.g., specific year of analysis, region).[256,318] In the calculation phase, based on the prior two phases, the indicators will be calculated to measure the technical and economic performance.[256] In the interpretation phase, the quality, consistency, and robustness of outcomes will be assessed, and conclusions and recommendations will be documented and reported.[256]

10.2. TEA of Traditional Engineered Wood Products

TEA has been applied to analyze the economic feasibility and main economic drivers of traditional engineered wood products. For example, Laufenberg et al. studied the economic perform-

https://doi.org/10.1021/acs.chemrev.2c00450
Chem. Rev. 2023, 123, 1843−1888

ance of LVL and fiber-reinforced wood.[322] The results showed the high contribution of log cost (over 30%) to LVL and the high contribution of glass fiber (over 33%) for fiber-reinforced wood.[322] Balasbaneh et al. estimated the life cycle cost of a single-story building with five building frame material combinations (i.e., hybrid concrete and timber, hybrid steel stud and timber, LVL with steel, glulam with steel, and timber and sandwich steel plate).[324] The results implied that the hybrid concrete and timber scenario was the most expensive due to the high cost in the manufacturing and construction phase.[324] In addition, using engineered wood products (LVL or glulam) had higher costs in the manufacturing and construction phases than timber scenarios, resulting in their higher life cycle costs.[324]

TEA has also been utilized to investigate the impacts of technical parameters and economic parameters on the economic performance of wood products.[257,328,329] Common studied technical parameters include plant capacity,[257,328] energy demand,[257,328] material usage,[257] material loss/efficiency,[257,328] transportation distance,[257,328] feedstock quality,[257,322,330] product grade;[322] economic parameters can include feedstock cost,[257,328,330] material and fuel price,[257,328,330] equipment price,[257,328] internal rate of return or discount rate,[322,328] labor cost,[328,330] maintenance cost,[328] waste disposal cost,[257] and market demand.[257] These analyses of parameter impacts are often coupled with scenario analysis or sensitivity analysis.[252,324]

10.3. TEA of Emerging Wood Materials

TEA can help inform economically attractive designs for emerging products.[257,317] TEA for new technologies often relies on process-based models that provide mass and energy balance data, the foundation of economic analysis. Using process-based models also allows for quantitative linkages between process parameters and economic analysis models, enabling in-depth analysis for a better understanding of the relationships between process/material design and overall economics. Those analyses include scenario analysis, sensitivity analysis, uncertainty analysis, and other needed analyses. For example, Zhang and Lan developed the process-based simulation coupled with economic analysis to study the economic feasibility of CLT produced in the Southern U.S.[257] The scenario analysis results, as shown in Figure 19C, illustrate that expanding the plant capacities from 30 000 to 150 000 m^3 CLT/year decreases the average minimum selling price from $571 to $376/$m^3$ but does not necessarily reduce the delivered cost due to increased transportation cost.[257] Similar trends were reported by Brandt et al.[328] where larger plant capacity reduces the minimum selling price of CLT by 18%.[328] Zhang and Lan also used sensitivity analysis and their results show that the minimum selling price of CLT is susceptible to lumber price change and lumber preparing loss.[257] Wijeyekoon et al. conducted a TEA coupled with risk analysis for co-producing bark briquettes and tannin adhesive from Radiata pine bark in two systems, a standalone plant, and a colocated symbiosis plant.[331] The two process designs were simulated by the process-based models and coupled with a discounted cash flow analysis.[331] The analysis shows that the colocated symbiosis plant has better economic performance due to lower feedstock price, cheaper geothermal energy, and process integration with a future plywood mill (e.g., using tannin as a structural adhesive in the plywood mill).[331] These benefits enabled a 41% reduction in total capital investment. Risk analysis by varying the parameter values, suggests that technical improvement (e.g., increasing tannin yield, decreasing hot water usage) reduces more overall costs than a material price reduction.[331]

11. ENGINEERED WOOD PRODUCTS IN CONTEMPORARY, STATE-OF-THE-ART BUILDINGS

Historically, wood has been a popular choice as the construction material in low-rise buildings and infrastructures (e.g., bridges). Natural, unmodified wood products continue to be used for construction, typically in the form of dimension lumber found in species, grade, and sizes listed in standards like the NDS Supplement.[332] In addition, heavy timber sizes measuring at least 5 in. in each cross-sectional dimension continue to be used for construction, although heavy timber requires larger diameter trees that are less sustainable. For almost a century, engineered wood products have proven to be more efficient and sustainable than heavy timber, by transforming smaller wood constituents into more homogeneous composite structural components. Currently, three primary categories of engineered wood products are used for buildings. The first category includes structural panel products like plywood or oriented strand board (OSB) that are used to sheath floors, roofs, and walls for bracing the framing members and transferring lateral forces, typically generated from wind or seismic events, through the plane of sheathing. The second category includes structural composite lumber, like laminated veneer lumber (LVL). The third category of engineered wood products is known as mass timber, which includes glulam,[333] CLT,[334] nail-laminated timber (NLT),[335] or mass plywood panels (MPP).[336] In contemporary construction, mass timber is the most revolutionary category of engineered wood products because it enables timber construction to span farther and rise taller than conventional light-frame wood structural systems.

11.1. The Rise of Mass Timber Engineered Wood Products and Potential of Modified Wood Enhancements

Modified wood has the potential to significantly improve both strength and stiffness of EWPs, with strategically placed reinforcement. Mass timber is the most revolutionary set of EWPs that has burgeoned over the past decade and made it possible for wood construction to rise to three times the height of conventional light-frame wood construction. Modified wood products, like Superwood,[337] can push the limits of height and spans even further. “Mass timber” defines a class of laminated wood structural products that are glued, nailed, or doweled together to produce structural framing and panels comparable to precast concrete in size but typically at lighter weight.[338] In contrast to heavy timber which requires large-diameter trees to achieve monolithic column and beam sizes, mass timber uses large volumes of dimensional lumber, from smaller-diameter trees, glued together to produce structural components. Laminating lumber makes it possible to surpass the heavy timber sizes, disperses natural defects of wood, and reduces the variability of the mechanical properties[339] so that the effects of an individual lamination are muted relative to the behavior of the whole composite.

Two main types of products have risen to the forefront of the mass timber category in recent construction, glulam, and CLT. Glulam aligns the lumber laminations in the same direction in every layer, whereas CLT typically aligns laminations perpendicular in each new layer. As a result, glulam is most effective for columns, beams, truss members, arches, and other structural frames[333] that need strength and stiffness primarily in

https://doi.org/10.1021/acs.chemrev.2c00450
Chem. Rev. 2023, 123, 1843−1888

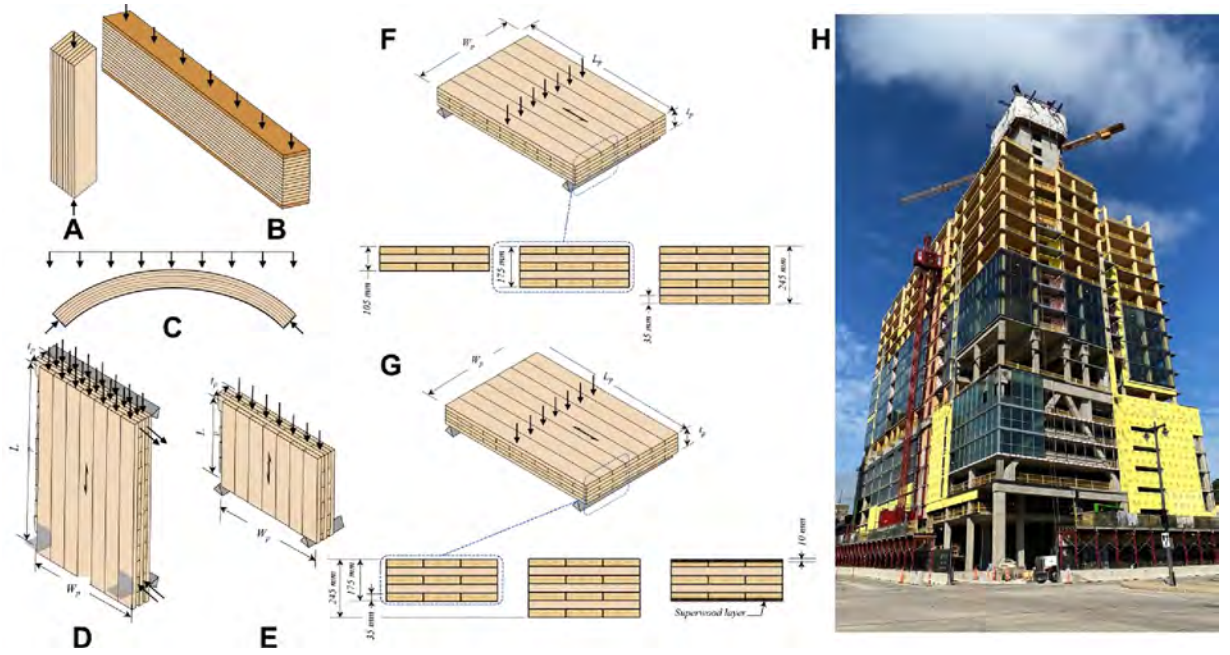

Figure 22. Glulam structural (A) column, (B) beam, and (C) arch components. Arrows represent the directions of the load. Vertically oriented CLT panel in (D) wall and (E) edgewise bending loading configurations. (F) CLT panel in the simple span of flatwise bending along the major strength direction, with standard 3-ply, 5-ply, and 7-ply layups. (G) CLT panel in the simple span of flatwise bending along the major strength direction, with a standard 5-ply layup, standard 7-ply layup, and Superwood-reinforced layup. (H) Construction of Ascent (Milwaukee, WI).

one direction. CLT panels apportion strength and stiffness in orthogonal directions, which serves planar structural elements like slab or wall panels.

Glulam has been used in structures for nearly a century. Glulam is most often manufactured in linear columns and beams but can readily achieve tapered or curved forms by controlling the length, thickness, and placement of laminations. Typical sizes for glulam members range between 65−310 mm (21/2 to 121/4 in.) in width and (51/2 to 601/2 in.) in depth,[340] and larger custom sizes are commonly built by laminating units of standard size. The column configuration of Figure 22A primarily sustains uniform axial stresses, so column layups typically use uniform species and wood grades throughout the glulam cross-section. A similar principle applies to the arch of Figure 22C, which primarily resists the applied loads via uniform axial compression. The beam of Figure 22B, in contrast, varies in stress across the cross-section, under the applied loads. Therefore, beams commonly lay up stiffer and stronger laminations in the top and bottom layers to resist stresses and deformations induced by bending. Because wood is weakest in tension, the tension laminations are carefully graded to improve the modulus of rupture of the beam.[341]

CLT presents similar opportunities to optimize layups, according to loading applications. Figure 22F illustrates one of the most common loading configurations of a simple span CLT panel in flatwise bending. Figure 22F illustrates the general panel width (W_p), length (L_p), and thickness (t_p) parameters. Standard layups of three, five, and seven plies have thicknesses that range between 105 and 245 mm ($4^1/_8$ to $9^5/_8$ in.), as shown in the cross-sectional diagrams of Figure 22F. Loadbearing wall panels, as shown in Figure 22D, are sized only considering the area of laminations with wood fiber oriented parallel to the axial compression loads shown at the top of the wall.[342] Therefore, laminations oriented transversely to the applied axial loads are deemed ineffective in the axial load bearing area yet necessary to provide the flexural resistance that makes the wall panel less susceptible to compression buckling.[343] Openings that are often necessary in wall panels lead to the edgewise bending configuration of Figure 22E. In edgewise bending, the transverse laminations aligned with the minor strength direction of the panel take on primary importance, while the laminations oriented in the vertical, strong direction of the panel contribute a minor amount of stiffness and strength capacity.[344]

Today, this combination of linear glulam and planar CLT mass timber components seems naturally complementary, but each product developed during a different historical era. Originating in 19th century Europe and introduced to the United States in 1930,[345] glulam is still produced on every continent where timber construction is commonplace. The original glues used for glulam timber were based on animal proteins, until the widespread adoption of phenol resorcinol formaldehyde (PRF). From a manufacturing perspective, PRF makes lamination of softwoods easy because it requires only room temperature curing under clamping pressure. Charring glulam adhered with PRF has been widely considered equivalent to solid heavy timber, so concerns over structural wood adhesives had been put to rest, until the development of new products like CLT.[337]

CLT originated in Europe only a few decades ago. CLT has since developed into a solid wood panel with the size and versatility of precast concrete, used in walls and floors, but at significantly less weight and carbon footprint than most concrete panel products.[346] In contrast to glulam, which can be mechanically clamped with manual equipment and incorporate radio-frequency (RF) curing, the wider dimensions of CLT typically require hydraulic presses, polyurethane (PUR)-based adhesives, and digitally controlled manufacturing to feasibly process the volumes of wood required for CLT production. The CLT Handbook provides a concise overview of CLT manufacturing procedures,[347] and the North American *Standard*

https://doi.org/10.1021/acs.chemrev.2c00450
Chem. Rev. 2023, 123, 1843−1888

Table 1. Comparisons of Effective CLT Panel Stiffness, Configured in Flatwise Bending of the Major Strength Direction, Between Standard and Superwood-Reinforced Layups[a]

	Standard		Superwood-Reinforced	Enhanced Superwood Panel Stiffness	
	5-ply	7-ply			
t_p	175 mm	245 mm	175mm	% Difference from standard	
CLT Layup	$EI_{eff,f,0}$ (lb_f-in.^{2}/ft of width)		$EI_{eff,f,0}$ (lb_f-in.^{2}/ft of width)	5-ply	7-ply
E1	440	1089	1037	+136	-4.8
E2	389	963	1006	+159	+4.5
E3	311	769	958	+208	+24.6
E4	440	1089	1037	+136	-4.8
V1	415	1027	1021	+146	-0.6
V2	363	898	990	+173	+10.2
V3	363	899	990	+173	+10.1

[a](1 lb_f = 4.448 N; 1 in. = 25.4 mm.)

for Performance-Rated Cross-Laminated Timber[348] provides detailed specifications regarding steps in the manufacturing process, including testing and quality assurance. While many lamination requirements essentially carry over from glulam standards,[349] the layup of CLT in orthogonal directions and new adhesive choices urged new requirements.

CLT manufacturing commonly used PURs as a laminating adhesive to decrease the clamping and curing times. PUR bonds, however, typically do not maintain integrity under moisture or fire quite as well as PRF adhesives.[350] Delamination of CLT during fire tests led to the mandatory annex B, *Practice for Evaluations Elevated Temperature Performance of Adhesives Used in Cross-Laminated Timber*.[348] Because the scale and costs of such full-scale qualification tests are considerable, Miyamoto et al.[351] developed a small-scale screening test to evaluate whether various adhesive formulations could match the integrity of solid timber when subjected to lap shear loads at temperatures approaching the 300 °C char temperature.

While glulam has been featured in architectural structures for nearly a century, the emergence of CLT panels revitalized mass timber construction. During the early part of the 21st century, the SOFIE project developed a comprehensive research plan for fully panelized CLT building archetypes that culminated in a seismic shake-table test of a 7-story prototype building in Japan.[352] The construction of 9- and 10-story apartments, in East London[353] and Melbourne[354] in the time frame between 2009 and 2011, represented the pinnacle, real-world applications, of this construction archetype, made entirely of CLT panels. Each building respectively claimed a savings of 310[355] and 1645[356] metric tons of carbon dioxide, in terms of carbon sequestered and avoided by using wood in place of steel and concrete.[357]

The global proliferation of CLT has led to increasingly taller timber construction over the past decade. To keep pace with these rapid developments, the 2021 edition of the International Building Code developed new classifications for type IV mass timber structures up to 18 stories tall.[358] A series of full-scale compartment fire tests conducted in ATF laboratories provided a research basis for establishing these code limits.[359] Preferences among commercial architects[360] of North American buildings, however, have trended away from fully panelized CLT structures toward post-and-beam archetypes that support CLT deck panels on glulam framing. As a greater variety of mass timber building schemes emerged, Foster et al.[361] proposed to classify this broad assortment of tall wood construction. To date, the tallest realized mass timber glulam/CLT structures have risen to heights of 18 stories and taller in North America.[362,363]Figure 22H is a photograph of the Ascent building, taken in September 2021 during its construction. The upper 18 stories use mass timber glulam framing and CLT decks that are laterally supported by a reinforced concrete stair-and-elevator service core. This juxtaposition of structural systems exemplifies the efficiency of a hybrid concrete and mass timber superstructure. To expose more of the mass timber frame to view and save on the use of gypsum wallboard that is prescribed for fire protection, 3 h fire tests of glulam columns were conducted at the USDA, Forest Products laboratory, to experimentally determine char rates of glulam columns exposed on four sides.[363] The findings of these 3 h column tests will be the subject of a forthcoming publication and proposed updates to current guidelines for fire endurance calculations.[364]

Despite increased acceptance of mass timber in recent editions of building codes[365] and reference standards,[366] the construction of multistory timber buildings today rarely relies on an entirely wood structure. Reinforced concrete cores are commonly used in multistory buildings, from midrises to skyscrapers, to provide lateral stiffness and robust enclosures for egress.[367] Most wood volume used in this hybrid construction is in the floor systems, which have dual functions. CLT decking panels must transfer gravity loads to the structural frame and act as a diaphragm in the plane of the floor or roof level to transfer lateral loads, typically induced by wind or seismic forces, to vertical "spines" of the building. Full-scale testing of CLT diaphragms and full-scale seismic shake-table testing of two-story mass timber structures have been conducted relatively recently in North America to develop design parameters and validate analysis procedures.[368−371] The two-story mass timber structures of the UC−San Diego shake-table tests swapped three types of CLT shear walls, to develop vertical components of the lateral force-resisting systems. The first CLT shear walls tested avoided damage by rocking controllably, using vertically post-tensioned rods for restraint.[372] The second set of CLT shear

https://doi.org/10.1021/acs.chemrev.2c00450
Chem. Rev. 2023, 123, 1843−1888

walls rocked more passively on sacrificial spring-dampers that demonstrated similar seismic resilience, which would require only replacement of the spring dampers to restore the structure to service postearthquake.[373] The third set of shear walls tested rocked to engage interstitial metal connectors between panels for enhanced ductility.[374] In contrast to the other shear walls that vertically span multiple floors, this shear wall system was developed for platform construction assembly of CLT buildings, which stacks complete floors, and was among the first cohort of new structural systems to develop according to FEMA P695 methodology that requires rigorous assessment of ground motions, numerical analysis methods, test data, design criteria, and peer review, to determine seismic design parameters.[375,376] For a performance-based seismic design option that strives to exceed minimum building code expectations, plans to test the vertically post-tensioned CLT rocking walls in a 10-story shake-table test are underway[377,378] and scheduled to take place in early 2023. While entirely mass timber structures up to 18 stories tall have been recently constructed in low-seismic regions of Europe,[379] research in North America will establish a range of seismic performance options that can be located in regions of moderate and high earthquake risk.

By leveraging the recent advances in both laminated wood products and novel wood modification methods, extended applications of wood-based structural materials can be expected. The Timber Tower Research Project[380] has shown that mass timber could significantly lower the carbon footprint of taller high-rises, but enhancements to fire protection, ductility of connections, reliable glued-in rods, and stiffer floors are needed to realize this vision.[381] As introduced in section 4.1, researchers at the University of Maryland have devised a scalable process that can directly transform natural wood into high-performance Superwood,[72] which features a 10−20-fold increase in strength and stiffness, as well as superb dimensional stability against moisture. Accordingly, Superwood can be incorporated into CLT panels as the top and bottom tension lam,[382] significantly enhancing flexural stiffness of CLT and extending limits of span length. Figure 22G shows a simple span of a CLT panel loaded in flatwise bending in the major strength direction, and Table 1 compares the effective stiffness values in the major direction of standard and Superwood-reinforced layups, as determined using the shear analogy method.[348] For the same 5-ply depth, the Superwood reinforced option increases the stiffness by 136 to 208% over the standard CLT panel. When compared to standard layups of 7-ply CLT, the shallower Superwood-reinforced nearly matches the stiffness of the 7-ply standard. Again, the benefit is greatest in the E3 layup, where the modulus of elasticity of Superwood exceeds the standard lamination by over 6 times. The shallow Superwood-reinforced option is nearly 25% stiffer than the standard 7-ply E3 layup. Therefore, the Superwood-reinforced CLT may span the same distance as a standard 7-ply CLT panel while reducing 70 mm (2−3/4 in.) of floor depth. Adding 10 mm of Superwood layers, as shown in Figure 22G, in other words, adds the stiffness of two standard laminations without adding structure depth.

The enhanced stiffness of Superwood may alternatively lengthen spans while maintaining the depth of a standard CLT panel.[337] For a uniformly loaded simple span floor of standard 175 mm depth, the Superwood-reinforced panel can span 25% longer than the standard E3 panel layup. Through more development of chemical processes and adhesive formulations, there is ample opportunity to further enhance the fire endurance, stiffness, and connection ductility of CLT structures. Ultimately, this may improve the sustainability of mass timber construction to an even greater extent, by allowing for more wood substitution of conventional materials.

11.2. Limitation of Engineered Wood Products in Current Applications

Architects have generally expressed a favorable outlook on engineered wood products[383,384] and mass timber[360] in particular. Despite recent growth in height achieved by mass timber structures, engineered wood products must overcome challenges associated with durability and fire risks to continue expanding limits. In addition, wood structural systems generally lack the stiffness and ductility of reinforced concrete and steel alternatives that have been developed over decades of research. For sustainability, replacing floor construction with timber alternatives has the maximum effect of reducing environmental impact because floor construction typically accounts for the bulk of building materials in a multistory building.[385] Therefore, mass timber floor structures have the greatest potential to enhance the sustainability of buildings in the current marketplace. The building envelope typically accounts for the next greatest amount of building materials in a multistory building. Here, wood substitutions are more challenging because of durability and fire concerns, although there is precedent for both residential and commercial use of wood-based composite[386] and chemically modified wood products such as acetylated wood.[387]

Anywhere wood products may be wet because of direct exposure to the elements or breaches of the building envelope merits careful consideration of moisture control.[388] Wetting during construction, furthermore, may have lasting impacts on durability, and the drying performance of the building component in a real construction site has been investigated in a few case studies.[389] A recent study about multistory mass timber buildings equipped with moisture sensors shows CLT roof and floor panels covered with vapor-impermeable membrane dried slower than glulam columns exposed to indoor air.[390] The time it takes to completely dry CLT structures wetted during construction has not been conclusively determined and should be further studied, also to evaluate the possible size change induced by different drying speeds.

Because almost all construction materials suffer damage from prolonged exposure to fire, fire resistance is one of the major concerns for all kinds of buildings. The 2015 National Design Standard for Wood Construction[332] updated the fire design provision chapter by adding the CLT char rate equation to calculate fire resistance. While wood poses unique fire risks because it is combustible, wood also has uniquely inherent fire protection. Charring forms an insulating layer that slows the rates of burn and lowers the temperature behind the charred front. The 2021 International Building Code (IBC)[365] included new provisions for mass timber construction that allow the buildings to be up to 18 stories in height with gypsum wallboard on all timber elements. To fulfill prescriptive code requirements, wooden buildings need sprinkler fire suppression systems, just like current nonwooden high-rise buildings and gypsum wallboard, encapsulation of all timber elements to meet the maximum fire-resistance rating. Driven by strong demand in the marketplace to aesthetically feature wood structural components in the North American marketplace, there are ongoing efforts to examine the fire performance of mass timber where greater amounts of CLT and glulam are exposed to view.[391−394]

https://doi.org/10.1021/acs.chemrev.2c00450
Chem. Rev. 2023, 123, 1843−1888

For improved structural performance, mass timber systems in particular need greater stiffness and ductility to overcome the limitations of the natural materials. This may be accomplished with chemical modifications to the wood materials or by novel connection detailing. Glued-in steel rods have long been proposed as a detailing solution for mass timber that could add stiffness and ductility to connections.[381,395] In addition, glued-in rods would facilitate the interface of wood with concrete structural materials that can be site-cast around the metal rods. Reliability of the installation and the ability to withstand fire and water infiltration, however, have impeded the implementation of glued-in rods on an industrial scale. Glued-in rods, therefore, pose one major area where advances in adhesive chemistry formulations may help expand the use of timber structural products. Durability, fire, and structural performance are interrelated, so approaching these challenges from a chemical perspective may lead to solutions that will enhance the performance of wood products and, in turn, improve the sustainability of building construction.

12. CONCLUSION AND PERSPECTIVES

A total of >10 billion metric tons of CO_2 removal is achievable at a global scale by trees.[1] This removal constitutes 25% of the global CO_2 emissions in 2019.[1] Therefore, widespread implementation of engineered wood products is needed to maximize carbon storage in buildings. Herein, the development of advanced products with enhanced properties hinges on a fundamental study of the process−structure−property relationships of natural and engineered wood. The complex structure of wood highly depends on the wood species and growth environment, providing a wide variety of material choices. However, this complexity also presents a challenge in investigating this material. The robust cell walls of wood are composed of three biopolymer components (cellulose fibrils, hemicelluloses, and lignin), which are interwoven and bonded to form a natural fibril-based composite. Therefore, the performance and characteristics of wood are governed by the alignment of the cellulose fibrils as well as their interactions with lignin/hemicelluloses. Keeping the alignment of cellulose fibrils in the anisotropic wood is crucial to achieving outstanding properties (e.g., aligned cellulose fibrils have more contact areas providing high mechanical strength, and aligned channels can enable rapid ion transport). In this regard, in situ wood modification can open nanoscale pores within the cell walls and/or modify the molecular cellulose chains while maintaining the overall anisotropic structure of wood.

Environmentally friendly, economically competitive, and sustainable wood materials require novel processes and manufacturing of advanced wood structures. The products, feedstocks, and manufacturing processes should follow the principles of green chemistry, taking into account recyclability and environmental benignity across the life cycle of the raw wood materials and chemicals used.[396] In this aspect, in situ chemical and physical processes can be used to manipulate the chemical structures and spatial distributions of the three components (lignin, hemicelluloses, and cellulose) in different types of feedstocks (e.g., wood chips, thin veneer, and bulk wood timber) to achieve the desired structures, properties, and performance of the advanced wood products. Guided by green chemistry principles in the selection of feedstocks, chemicals, solvents, and processes, green processes that use lower amounts of resources and generate minimal wastes but high-value coproducts can be developed.[397] What is more, manufacturing science and technology should be studied to realize green, scalable, and closed-loop mass production of advanced wood products. To achieve this goal, system-level analysis and optimization of wood treatment and manufacturing can be conducted from a sustainability and life cycle perspective. Different environmental impact categories (e.g., GHG emissions including CO_2, human health impact, energy consumption, and resource depletion) and production costs can be considered simultaneously through multicriteria decision analysis (MCDA) to guide the process and manufacturing design toward the most economically competitive and environmentally beneficial direction.

To advance/develop new innovative engineered wood products, a fundamental understanding of the wood chemistry relying on multiscale, multicomponent characterization is needed. With the development of high-resolution characterization tools, both in situ and ex situ, structural and dynamic characterizations can be carried out at length scales from subangstrom to submicrometer. For example, the structure of cellulose in wood, including its crystallinity, crystal structure and polymorphism, and preferred orientation of fibril crystals, can be analyzed using wide-angle X-ray scattering (WAXS).[398] Nanoscale structures, such as the shape and size of the microfibrils and fibril bundles, the packing and alignment of the fibril structures, etc., can be characterized by small-angle X-ray scattering (SAXS).[399] By leveraging the nondestructive X-ray computed tomography (CT) technique with machine learning for image recognition, automatic and accelerated wood characterization, and identification have been achieved.[400] Cryogenic electron microscopy (cryo-EM), which has been widely used in biological science, can be used to visualize the cellulose structure and provide detailed information about the cell wall structure.[401] The information derived from these analytic tools is crucial for controlling the in situ processing parameters, which lays the foundation for boosting the performance of the final engineered wood and maximizing its carbon sequestration capability.

Emerging artificial intelligence (AI) and machine learning (ML) technologies can also be used to build a data-driven discovery platform for the process−structure−property study of advanced engineered wood. The current advances in ML and data science not only promote the prediction of specific properties of engineered wood but also uncover complex process−structure−property correlations. Data mining methods can also be utilized to search large data sets to identify effective, reduced, data-driven descriptors that affect the targeted property of advanced wood materials. Within the drastically lower-dimensional parameter space, we can use the emergent active learning concept along with ML algorithms to locate desired wood species and suitable processing parameters to uncover the correlation between the processing, structure, and properties of the resulting engineered wood and enable rapid manufacturing of high-performance advanced wood materials.

Understanding the potential environmental, economic, and societal implications of new wood technologies across their life cycles is therefore essential to maximize the potential benefits and minimize risks. LCA and TEA analyses have demonstrated powerful capabilities in advancing such knowledge. Previous LCA and TEA studies have identified key process and supply chain parameters that drive the environmental impact and economic feasibility of wood products, informing material and process optimization toward sustainability.[311] However, previous studies have rarely considered social impacts. Furthermore, only a few studies have incorporated the dynamics of

https://doi.org/10.1021/acs.chemrev.2c00450
Chem. Rev. 2023, 123, 1843−1888

forest and management strategies for forest ecosystems. Future research should focus on developing holistic sustainability assessment tools, such as life cycle sustainability assessment,[402] and incorporating forest-specific dynamics (e.g., carbon and market dynamics) into the material-level and product-level assessment.

Finally, the following specific needs related to engineered wood products should be taken into consideration for future perspectives in this emerging field.

(1) Chemical wastes, such as black liquor, will be generated in the fabrication processes of many wood products. How to optimize the delignification/modification procedures and achieve waste-free/closed-loop manufacturing without compromising performance remains a grand challenge.

(2) The insufficient diffusion of chemicals into the microstructure of wood may impede the large-scale fabrication of engineered wood products. Moreover, manufacturing challenges in reproducibility, performance uniformity, and scaling to meet industry needs should be addressed by considering the existence of knots and other defects in wood.

(3) Despite the decent performance of some engineered wood materials, moisture-dependent swelling and shrinkage will result in dimensional instability and irreversible deformation/cracking. Additional treatments, such as heating, painting, finishing, and surface modifications should be used and evaluated to diminish such adverse effects and prolong the lifespan of engineered wood-based products exposed to the weather.

(4) The dominant adhesives used in conventional wood products, such as formaldehyde-based resin, tend to release volatile organic compounds or even cancerogenic gases during the manufacturing or service life of products. Green and durable adhesives are needed without sacrificing the recyclability, reusability, and functionality of the final products.

(5) The biodegradability of engineered wood products could also be an impediment, resulting in excessively fast degradation under direct exposure to weather elements. More research is needed to strike the balance between durability during service life and biodegradability for disposal.

(6) Evaluations of the antifungal, antitermite, fire-resistant, and moisture-resistant properties per applicable building codes or performance standards are required before the rollout of novel wood products.

(7) Accurate, nondestructive, and low-cost methods have yet to be developed to comprehensively monitor the performance/characteristics of engineered wood over time using. Meanwhile, similar assessments that are reliable and easily implemented are needed to evaluate damaged and deteriorated wood products.

(8) It is necessary to achieve sufficient retention of carbon storage over the service life of wood products and minimize end-of-life emissions where possible by designing wood materials for reuse, repurposing, and/or recycling.

AUTHOR INFORMATION

Corresponding Author

Liangbing Hu − *Department of Materials Science and Engineering, University of Maryland, College Park, Maryland 20742, United States; Center for Materials Innovation, University of Maryland, College Park, Maryland 20742, United States;* orcid.org/0000-0002-9456-9315; Email: binghu@umd.edu

Authors

Yu Ding − *Department of Materials Science and Engineering, University of Maryland, College Park, Maryland 20742, United States*

Zhenqian Pang − *Department of Mechanical Engineering, University of Maryland, College Park, Maryland 20742, United States*

Kai Lan − *Center for Industrial Ecology, Yale School of the Environment, Yale University, New Haven, Connecticut 06511, United States*

Yuan Yao − *Center for Industrial Ecology, Yale School of the Environment, Yale University, New Haven, Connecticut 06511, United States;* orcid.org/0000-0001-9359-2030

Guido Panzarasa − *Wood Materials Science, Institute for Building Materials, ETH Zürich, 8093 Zürich, Switzerland; WoodTec Group, Cellulose & Wood Materials, Empa, 8600 Dübendorf, Switzerland;* orcid.org/0000-0003-1044-0491

Lin Xu − *Department of Materials Science and Engineering, University of Maryland, College Park, Maryland 20742, United States*

Marco Lo Ricco − *US Department of Agriculture (USDA) Forest Products Laboratory, Madison, Wisconsin 53726, United States*

Douglas R. Rammer − *US Department of Agriculture (USDA) Forest Products Laboratory, Madison, Wisconsin 53726, United States*

J. Y. Zhu − *US Department of Agriculture (USDA) Forest Products Laboratory, Madison, Wisconsin 53726, United States*

Ming Hu − *School of Architecture, Planning and Preservation, University of Maryland, College Park, Maryland 20742, United States;* orcid.org/0000-0003-2583-1161

Xuejun Pan − *Department of Biological Systems Engineering, University of Wisconsin—Madison, Madison, Wisconsin 53706, United States;* orcid.org/0000-0002-6859-9342

Teng Li − *Department of Mechanical Engineering, University of Maryland, College Park, Maryland 20742, United States;* orcid.org/0000-0001-6252-561X

Ingo Burgert − *Wood Materials Science, Institute for Building Materials, ETH Zürich, 8093 Zürich, Switzerland; WoodTec Group, Cellulose & Wood Materials, Empa, 8600 Dübendorf, Switzerland;* orcid.org/0000-0003-0028-072X

Complete contact information is available at: https://pubs.acs.org/10.1021/acs.chemrev.2c00450

Notes

The authors declare no competing financial interest.

Biographies

Yu Ding is a postdoctoral associate in Prof. Liangbing Hu's group at the University of Maryland, College Park. He received his B.S. degree in Chemistry from Nankai University (2012) and a doctoral degree in Materials Science and Engineering from the University of Texas at Austin (2018). His research is mainly focused on cellulose-based biomaterials for construction and energy applications.

https://doi.org/10.1021/acs.chemrev.2c00450
Chem. Rev. 2023, 123, 1843−1888

Zhenqian Pang received his B.S. degree from the Huazhong University of Science and Technology, Wuhan, China, and his Ph.D. degree from the Institute of Mechanics, Chinese Academy of Sciences, Beijing, China. Currently, he is a postdoctoral researcher at the Department of Mechanical Engineering, University of Maryland, College Park, USA, and his research focuses on the properties of composites of carbon and cellulose.

Kai Lan is a postdoc associate at the Center for Industrial Ecology, Yale School of the Environment, Yale University. He received his Ph.D. degree in Forest Biomaterials from North Carolina State University, a master's degree in Mechanical Engineering from the University of Michigan Ann Arbor, and a bachelor's degree in Mechanical Engineering from Shanghai Jiao Tong University, China. His research interests include developing modeling tools to evaluate and advance the systems related to sustainable energy and materials.

Yuan Yao is an Assistant Professor of Industrial Ecology and Sustainable Systems at the Yale School of the Environment, Yale University. She received her Ph.D. degree in Chemical Engineering from Northwestern University in the United States and a B.S. degree in Metallurgical Engineering from Northeastern University in China. Her research focuses on understanding the potential environmental impacts of biomass-derived products, materials, and chemicals. She uses interdisciplinary approaches in industrial ecology, sustainable engineering, and data analytics to support industrial and policy decisions for a sustainable bioeconomy.

Guido Panzarasa is a group leader ("Active and Adaptive Wood Materials") at the Institute of Building Materials (Department of Civil, Environmental, and Geomatic Engineering), ETH Zürich (Switzerland). He joined in 2020 the Wood Materials Science laboratory led by Prof. Ingo Burgert to continue and perfect his studies on advanced material synthesis and modification by systems chemistry-based approaches. He received his Ph.D. in Chemical Sciences in 2016 from the University of Eastern Piedmont "Amedeo Avogadro" (Italy) under the supervision of Dr. Katia Sparnacci.

Lin Xu is a postdoctoral associate in Prof. Liangbing Hu's group at the University of Maryland, College Park. He received his B.S. degree in Physics from Tsinghua University (2014) and a doctoral degree in Materials Science and Engineering from the Massachusetts Institute of Technology (2021). His research is mainly focused on cellulose-based biomaterials for energy applications.

Marco Lo Ricco is a USDA, Forest Service, Forest Products Laboratory (FPL) researcher with 15 years of professional structural engineering experience, in buildings of all types, and over 5 years of R&D in testing and analyzing full-scale rocking CLT wall system that resulted in a U.S. patent for a wood-based seismic isolation system. He is focused on development of mass timber structures for more sustainable and resilient construction that can mitigate a variety of hazards.

Douglas R. Rammer is a USDA, Forest Service, Forest Products Laboratory (FPL) researcher with over 25 years of experience in timber building design. He is FPL's technical representative on the National Design Specification for Wood Construction and ANSI committees that develop the performance standards for Glued Laminated and Cross-Laminated Timber.

J. Y. Zhu is a lead scientist at the USDA Forest Service, Forest Products Laboratory, Madison, Wisconsin. He holds an adjunct position at the Department of Biological Systems Engineering, University of Wisconsin—Madison. His research interest covers a broad area of wood utilization for producing biofuels, biochemicals, and biomaterials including fibers and cellulose nanomaterials. His research ranges from laboratory studies to commercial-scale demonstrations. The SPORL process that he coinvented and developed was successfully applied for the world's first woody-biojet commercial flight by preprocessing 60 tons of softwood forest residue.

Ming Hu is an Associate Professor at the School of Architecture, Planning and Preservation, University of Maryland, USA. Her research activities center on how to decarbonize the built environment through net zero impact and healthy building design and to understand how the (smart) technologies might be employed to reduce the impact from built environment to ecosystem. Dr. Hu has an extensive background in high-performance building design and life cycle assessment and has engaged in applied building technology research for over 14 years. Her first book, titled *Net Zero Building: Predicated and Unintended Consequences*, was released in April 2019 through Routledge. Her second book, *Healthy Built Environment and Smart Technologies*, was published in September 2020.

Xuejun Pan is the Vilas Distinguished Achievement Professor in the Department of Biological Systems Engineering at the University of Wisconsin—Madison. He earned his B.E., M.S., and Ph.D. degrees in Chemical Engineering at Tianjin University of Science and Technology, China, and a Ph.D. degree in Applied Bioscience at Hokkaido University, Japan. He conducted postdoctoral research at the Institute of Paper Science and Technology (Georgia Tech), University of Minnesota, and University of British Columbia before joining the University of Wisconsin—Madison in 2006. His research interest is in the chemistry of plant cell wall components (cellulose, lignin, and hemicelluloses) and their conversion to chemicals, fuels, and materials.

Teng Li is currently the Keystone Professor in the Clark School of Engineering at the University of Maryland, College Park, US, where he directs the Laboratory for Advanced Sustainable Materials and Technology. He received his Ph.D. degree in Engineering Science from Harvard University in 2006, following earlier studies at Princeton University and Tsinghua University. His research interests focus on mechanics of sustainable materials, machine learning enabled material discovery, low dimensional materials, energy materials, soft materials and biomaterials, flexible electronics, and nanoelectronics.

Ingo Burgert received a diploma in Wood Science and Technology at the University of Hamburg, Germany, in 1995, followed by a doctoral degree in 2000. From 2000 to 2003, he was postdoc at the University of Natural Resources and Life Sciences (BOKU), Vienna, Austria. From 2003 to 2011, he was a research group leader at the Max Planck Institute of Colloids and Interfaces in the Department of Biomaterials, Potsdam, Germany. Since 2011, he has been a professor of Wood Materials Science at ETH−Swiss Federal Institute of Technology, Zurich, and group leader at Empa−Swiss Federal Laboratories for Materials Science and Technology, Dübendorf, Switzerland.

Liangbing Hu received his B.S. in Physics from the University of Science and Technology of China in 2002, where he worked on colossal magnetoresistance (CMR) materials for three years. He did his Ph.D. (2002−2007) at UCLA, focusing on carbon-nanotube-based nanoelectronics. In 2006, he joined Unidym, Inc., as a cofounding scientist, leading the development of roll-to-roll printed carbon nanotube films and device integration in touch screens, LCDs, flexible OLEDs, and solar cells. He did his postdoc at Stanford University from 2009−2011, where he worked on various energy storage technologies using nanomaterials/nanostructures. Currently, he is a Herbert Rabin Distinguished Professor at the University of Maryland, College Park. His research group focuses on materials innovations, device integration, and manufacturing, with ongoing research activities on electrified ultrahigh-temperature synthesis, energy storage beyond Li-ion batteries, and novel wood nanotechnologies.

https://doi.org/10.1021/acs.chemrev.2c00450
Chem. Rev. 2023, 123, 1843−1888

ACKNOWLEDGMENTS

L.H. acknowledges funding from the Advanced Research Projects Agency−Energy (ARPA-E), U.S. Department of Energy, under award DE-AR0001025 and DE-AR0001485, the Department of Energy's Building Technologies Office (BTO) through the Small Business Innovation Research Program under contract DE-SC0018820, and the Department of Energy's Office of Energy Efficiency & Renewable Energy (EERE) through the Buildings Energy Efficiency Frontiers & Innovation Technologies (BENEFIT) Program under contract DE-EE0009702, and the University of Maryland A. James Clark School of Engineering. T.L. and L.H. acknowledge the support of U.S. National Science Foundation (grant nos. 1362256 and 1936452). X.P. acknowledges the research funding from USDA NIFA (WIS05013). Z.P. and T.L. acknowledge the University of Maryland supercomputing resources (http://hpcc.umd.edu) and Maryland Advanced Research Computing Center (MARCC) made available for conducting the research reported in this work. Y.Y. acknowledges funding from Yale University and the U.S. National Science Foundation. This material is based upon work supported by the National Science Foundation under grant no. 2038439. Any opinions, findings, and conclusions or recommendations expressed in this material are those of the author(s) and do not necessarily reflect the views of the National Science Foundation.

REFERENCES

(1) Harris, N. L.; Gibbs, D. A.; Baccini, A.; Birdsey, R. A.; de Bruin, S.; Farina, M.; Fatoyinbo, L.; Hansen, M. C.; Herold, M.; Houghton, R. A.; et al. Global Maps of Twenty-First Century Forest Carbon Fluxes. *Nat. Clim. Change* **2021**, *11*, 234−240.

(2) *Highlights of the Findings of the U.S. Global Change Research Program Climate Science Special Report*; U.S. Global Change Research Program, 2017; https://science2017.globalchange.gov/chapter/executive-summary/#fig-2013 (accessed 2022-03-13).

(3) Crowther, T. W.; Glick, H. B.; Covey, K. R.; Bettigole, C.; Maynard, D. S.; Thomas, S. M.; Smith, J. R.; Hintler, G.; Duguid, M. C.; Amatulli, G.; et al. Mapping Tree Density at a Global Scale. *Nature* **2015**, *525*, 201−205.

(4) Nordby, A. S.; Shea, A. D. Building Materials in the Operational Phase. *J. Ind. Ecol.* **2013**, *17*, 763−776.

(5) *Paris Agreement*; United Nations, 2015; https://unfccc.int/sites/default/files/english_paris_agreement.pdf (accessed 2022-03-08).

(6) Streiff, L.*NASA Satellites Help Quantify Forests' Impacts on Global Carbon Budget*; National Aeronautics and Space Administration, February 3, 2021; https://www.nasa.gov/feature/goddard/2021/nasa-satellites-help-quantify-forests-impacts-on-the-global-carbon-budget (accessed on 2022-03-02).

(7) Ververis, C.; Georghiou, K.; Christodoulakis, N.; Santas, P.; Santas, R. Fiber Dimensions, Lignin and Cellulose Content of Various Plant Materials and Their Suitability for Paper Production. *Ind. Crops. Prod.* **2004**, *19*, 245−254.

(8) Li, T.; Chen, C.; Brozena, A. H.; Zhu, J. Y.; Xu, L.; Driemeier, C.; Dai, J.; Rojas, O. J.; Isogai, A.; Wågberg, L.; et al. Developing Fibrillated Cellulose as a Sustainable Technological Material. *Nature* **2021**, *590*, 47−56.

(9) Šturcová, A.; Davies, G. R.; Eichhorn, S. J. Elastic Modulus and Stress-Transfer Properties of Tunicate Cellulose Whiskers. *Biomacromolecules* **2005**, *6*, 1055−1061.

(10) Zhu, J. Y.; Agarwal, U. P.; Ciesielski, P. N.; Himmel, M. E.; Gao, R.; Deng, Y.; Morits, M.; Österberg, M. Towards Sustainable Production and Utilization of Plant-Biomass-Based Nanomaterials: a Review and Analysis of Recent Developments. *Biotechnol. Biofuels* **2021**, *14*, 114.

(11) Iglesias, M. C.; Gomez-Maldonado, D.; Via, B. K.; Jiang, Z.; Peresin, M. S. Pulping Processes and Their Effects on Cellulose Fibers and Nanofibrillated Cellulose Properties: A Review. *Forest Prod. J.* **2020**, *70*, 10−21.

(12) Keplinger, T.; Wittel, F. K.; Rüggeberg, M.; Burgert, I. Wood Derived Cellulose Scaffolds—Processing and Mechanics. *Adv. Mater.* **2021**, *33*, 2001375.

(13) Frey, M.; Widner, D.; Segmehl, J. S.; Casdorff, K.; Keplinger, T.; Burgert, I. Delignified and Densified Cellulose Bulk Materials with Excellent Tensile Properties for Sustainable Engineering. *ACS Appl. Mater. Interfaces* **2018**, *10*, 5030−5037.

(14) Hildebrandt, J.; Hagemann, N.; Thrän, D. The Contribution of Wood-Based Construction Materials for Leveraging a Low Carbon Building Sector in Europe. *Sustain. Cities Soc.* **2017**, *34*, 405−418.

(15) Scheller, H. V.; Ulvskov, P. Hemicelluloses. *Annu. Rev. Plant Biol.* **2010**, *61*, 263−289.

(16) Toumpanaki, E.; Shah, D. U.; Eichhorn, S. J. Beyond What Meets the Eye: Imaging and Imagining Wood Mechanical-Structural Properties. *Adv. Mater.* **2021**, *33*, 2001613.

(17) Wang, X.; Pang, Z.; Chen, C.; Xia, Q.; Zhou, Y.; Jing, S.; Wang, R.; Ray, U.; Gan, W.; Li, C.; et al. All-Natural, Degradable, Rolled-Up Straws Based on Cellulose Micro- and Nano-Hybrid Fibers. *Adv. Funct. Mater.* **2020**, *30*, 1910417.

(18) Ray, U.; Zhu, S.; Pang, Z.; Li, T. Mechanics Design in Cellulose-Enabled High-Performance Functional Materials. *Adv. Mater.* **2021**, *33*, 2002504.

(19) Fang, Z.; Li, B.; Liu, Y.; Zhu, J.; Li, G.; Hou, G.; Zhou, J.; Qiu, X. Critical Role of Degree of Polymerization of Cellulose in Super-Strong Nanocellulose Films. *Matter* **2020**, *2*, 1000−1014.

(20) Dinwoodie, J. M.*Timber: Its Nature and Behaviour*; CRC Press, 2000.

(21) Calvo-Flores, F. G.; Dobado, J. A. Lignin as Renewable Raw Material. *ChemSusChem* **2010**, *3*, 1227−1235.

(22) Jin, Z.; Katsumata, K. S.; Lam, T. B. T.; Iiyama, K. Covalent Linkages Between Cellulose and Lignin in Cell Walls of Coniferous and Nonconiferous Woods. *Biopolymers* **2006**, *83*, 103−110.

(23) Eriksson, Ö.; Goring, D. A. I.; Lindgren, B. O. Structural Studies on the Chemical Bonds Between Lignins and Carbohydrates in Spruce Wood. *Wood Sci. Technol.* **1980**, *14*, 267−279.

(24) Lam, T. B. T.; Iiyama, K. Characteristics of Senescent Straw Cell Walls of Dwarf, Semidwarf, and Normal Strains of Rice (Oryza Sativa) Plants. *J. Wood Sci.* **2000**, *46*, 376−380.

(25) Zhao, X.; Qi, F.; Liu, D. In *Nanotechnology for Bioenergy and Biofuel Production*; Rai, M., da Silva, S. S., Eds.; Springer International: Cham, 2017.

(26) Košíková, B.; Ebringerová, A. Lignin-Carbohydrate Bonds in a Residual Soda Spruce Pulp Lignin. *Wood Sci. Technol.* **1994**, *28*, 291−296.

(27) Youssefian, S.; Rahbar, N. Molecular Origin of Strength and Stiffness in Bamboo Fibrils. *Sci. Rep.* **2015**, *5*, 11116.

(28) Chen, C. J.; Kuang, Y. D.; Zhu, S. Z.; Burgert, I.; Keplinger, T.; Gong, A.; Li, T.; Berglund, L.; Eichhorn, S. J.; Hu, L. B. Structure-Property-Function Relationships of Natural and Engineered Wood. *Nat. Rev. Mater.* **2020**, *5*, 642−666.

(29) Ren, K.; Xia, Q.; Liu, Y.; Cheng, W.; Zhu, Y.; Liu, Y.; Yu, H. Wood/Polyimide Composite via a Rapid Substitution Compositing Method for Extreme Temperature Conditions. *Compos. Sci. Technol.* **2021**, *207*, 108698.

(30) Zhou, S.; Jin, K.; Buehler, M. J. Understanding Plant Biomass via Computational Modeling. *Adv. Mater.* **2021**, *33*, 2003206.

(31) Zhu, H.; Zhu, S.; Jia, Z.; Parvinian, S.; Li, Y.; Vaaland, O.; Hu, L.; Li, T. Anomalous Scaling Law of Strength and Toughness of Cellulose Nanopaper. *Proc. Natl. Acad. Sci. U.S.A.* **2015**, *112*, 8971−8976.

(32) Hou, Y.; Guan, Q.-F.; Xia, J.; Ling, Z.-C.; He, Z.; Han, Z.-M.; Yang, H.-B.; Gu, P.; Zhu, Y.; Yu, S.-H.; et al. Strengthening and Toughening Hierarchical Nanocellulose via Humidity-Mediated Interface. *ACS Nano* **2021**, *15*, 1310−1320.

(33) Williams, K. S.; Andzelm, J. W.; Dong, H.; Snyder, J. F. DFT Study of Metal Cation-Induced Hydrogelation of Cellulose Nanofibrils. *Cellulose* **2014**, *21*, 1091−1101.

(34) Wang, R.; Chen, C.; Pang, Z.; Wang, X.; Zhou, Y.; Dong, Q.; Guo, M.; Gao, J.; Ray, U.; Xia, Q.; et al. Fabrication of Cellulose-Graphite Foam via Ion Cross-linking and Ambient-Drying. *Nano Lett.* **2022**, *22*, 3931−3938.
(35) Roy, C.; Budtova, T.; Navard, P. Rheological Properties and Gelation of Aqueous Cellulose-NaOH Solutions. *Biomacromolecules* **2003**, *4*, 259−264.
(36) Jeong, K.; Jeong, H. J.; Lee, G.; Kim, S. H.; Kim, K. H.; Yoo, C. G. Catalytic Effect of Alkali and Alkaline Earth Metals in Lignin Pyrolysis: A Density Functional Theory Study. *Energy Fuels* **2020**, *34*, 9734−9740.
(37) Li, T. EML Webinar Overview: Advanced Materials Toward a Sustainable Future—Mechanics Design. *Extreme Mech. Lett.* **2021**, *42*, 101107.
(38) Dong, H.; Snyder, J. F.; Tran, D. T.; Leadore, J. L. Hydrogel, Aerogel and Film of Cellulose Nanofibrils Functionalized with Silver Nanoparticles. *Carbohydr. Polym.* **2013**, *95*, 760−767.
(39) Ciolacu, D.; Rudaz, C.; Vasilescu, M.; Budtova, T. Physically and Chemically Cross-Linked Cellulose Cryogels: Structure, Properties and Application for Controlled Release. *Carbohydr. Polym.* **2016**, *151*, 392−400.
(40) Ralph, J.; Lapierre, C.; Boerjan, W. Lignin Structure and Its Engineering. *Curr. Opin. Biotechnol.* **2019**, *56*, 240−249.
(41) Chakar, F. S.; Ragauskas, A. J. Review of Current and Future Softwood Kraft Lignin Process Chemistry. *Ind. Crops. Prod.* **2004**, *20*, 131−141.
(42) Sinko, R.; Keten, S. Traction-Separation Laws and Stick-Slip Shear Phenomenon of Interfaces Between Cellulose Nanocrystals. *J. Mech Phys. Solids* **2015**, *78*, 526−539.
(43) Jin, K.; Qin, Z.; Buehler, M. J. Molecular Deformation Mechanisms of the Wood Cell Wall Material. *J. Mech Behav Biomed Mater.* **2015**, *42*, 198−206.
(44) Chen, C.; Song, J.; Cheng, J.; Pang, Z.; Gan, W.; Chen, G.; Kuang, Y.; Huang, H.; Ray, U.; Li, T.; et al. Highly Elastic Hydrated Cellulosic Materials with Durable Compressibility and Tunable Conductivity. *ACS Nano* **2020**, *14*, 16723−16734.
(45) Tang, H.; Butchosa, N.; Zhou, Q. A Transparent, Hazy, and Strong Macroscopic Ribbon of Oriented Cellulose Nanofibrils Bearing Poly(ethylene glycol). *Adv. Mater.* **2015**, *27*, 2070−2076.
(46) Han, X.; Ye, Y.; Lam, F.; Pu, J.; Jiang, F. Hydrogen-Bonding-Induced Assembly of Aligned Cellulose Nanofibers into Ultrastrong and Tough Bulk Materials. *J. Mater. Chem. A* **2019**, *7*, 27023−27031.
(47) Li, Z.; Xia, W. Coarse-Grained Modeling of Nanocellulose Network Towards Understanding the Mechanical Performance. *Extreme Mech. Lett.* **2020**, *40*, 100942.
(48) Ray, U.; Pang, Z.; Li, T. Mechanics of Cellulose Nanopaper Using a Scalable Coarse-Grained Modeling Scheme. *Cellulose* **2021**, *28*, 3359−3372.
(49) López, C. A.; Bellesia, G.; Redondo, A.; Langan, P.; Chundawat, S. P. S.; Dale, B. E.; Marrink, S. J.; Gnanakaran, S. MARTINI Coarse-Grained Model for Crystalline Cellulose Microfibers. *J. Phys. Chem. B* **2015**, *119*, 465−473.
(50) Ramezani, M. G.; Golchinfar, B. Mechanical Properties of Cellulose Nanocrystal (CNC) Bundles: Coarse-Grained Molecular Dynamic Simulation. *J. Compos. Sci.* **2019**, *3*, 57.
(51) Eichhorn, S. J. Stiff as a Board: Perspectives on the Crystalline Modulus of Cellulose. *ACS Macro Lett.* **2012**, *1*, 1237−1239.
(52) Šturcová, A.; Eichhorn, S. J.; Jarvis, M. C. Vibrational Spectroscopy of Biopolymers Under Mechanical Stress: Processing Cellulose Spectra Using Bandshift Difference Integrals. *Biomacromolecules* **2006**, *7*, 2688−2691.
(53) Tanpichai, S.; Quero, F.; Nogi, M.; Yano, H.; Young, R. J.; Lindström, T.; Sampson, W. W.; Eichhorn, S. J. Effective Young's Modulus of Bacterial and Microfibrillated Cellulose Fibrils in Fibrous Networks. *Biomacromolecules* **2012**, *13*, 1340−1349.
(54) Shishehbor, M.; Zavattieri, P. D. Effects of Interface Properties on the Mechanical Properties of Bio-Inspired Cellulose Nanocrystal (CNC)-based Materials. *J. Mech Phys. Solids* **2019**, *124*, 871−896.
(55) Warguła, Ł.; Wojtkowiak, D.; Kukla, M.; Talaśka, K. Symmetric Nature of Stress Distribution in the Elastic-Plastic Range of Pinus L. Pine Wood Samples Determined Experimentally and Using the Finite Element Method (FEM). *Symmetry* **2021**, *13*, 39.
(56) Luimes, R. A.; Suiker, A. S. J.; Verhoosel, C. V.; Jorissen, A. J. M.; Schellen, H. L. Fracture Behaviour of Historic and New Oak Wood. *Wood Sci. Technol.* **2018**, *52*, 1243−1269.
(57) Xiao, S.; Chen, C.; Xia, Q.; Liu, Y.; Yao, Y.; Chen, Q.; Hartsfield, M.; Brozena, A.; Tu, K.; Eichhorn, S. J.; et al. Lightweight, Strong, Moldable Wood via Cell Wall Engineering as a Sustainable Structural Material. *Science* **2021**, *374*, 465−471.
(58) Cheng, J.; Jia, Z.; Li, T. A Constitutive Model of Microfiber Reinforced Anisotropic Hydrogels: with Applications to Wood-Based Hydrogels. *J. Mech Phys. Solids* **2020**, *138*, 103893.
(59) Pan, X.; Arato, C.; Gilkes, N.; Gregg, D.; Mabee, W.; Pye, K.; Xiao, Z.; Zhang, X.; Saddler, J. Biorefining of Softwoods Using Ethanol Organosolv Pulping: Preliminary Evaluation of Process Streams for Manufacture of Fuel-Grade Ethanol and Co-Products. *Biotechnol. Bioeng.* **2005**, *90*, 473−481.
(60) Iakovlev, M.; van Heiningen, A. Efficient Fractionation of Spruce by SO_2-Ethanol-Water Treatment: Closed Mass Balances for Carbohydrates and Sulfur. *ChemSusChem* **2012**, *5*, 1625−1637.
(61) Zhou, H.; Tan, L.; Fu, Y.; Zhang, H.; Liu, N.; Qin, M.; Wang, Z. Rapid Nondestructive Fractionation of Biomass (≤15 min) by using Flow-Through Recyclable Formic Acid toward Whole Valorization of Carbohydrate and Lignin. *ChemSusChem* **2019**, *12*, 1213−1221.
(62) Pan, X.; Sano, Y. Fractionation of Wheat Straw by Atmospheric Acetic Acid Process. *Bioresour. Technol.* **2005**, *96*, 1256−1263.
(63) Shuai, L.; Questell-Santiago, Y. M.; Luterbacher, J. S. A Mild Biomass Pretreatment Using Γ-Valerolactone for Concentrated Sugar Production. *Green Chem.* **2016**, *18*, 937−943.
(64) Cai, C. M.; Zhang, T.; Kumar, R.; Wyman, C. E. THF Co-Solvent Enhances Hydrocarbon Fuel Precursor Yields from Lignocellulosic Biomass. *Green Chem.* **2013**, *15*, 3140−3145.
(65) Brandt, A.; Ray, M. J.; To, T. Q.; Leak, D. J.; Murphy, R. J.; Welton, T. Ionic Liquid Pretreatment of Lignocellulosic Biomass with Ionic Liquid-Water Mixtures. *Green Chem.* **2011**, *13*, 2489−2499.
(66) Shi, J.; Gladden, J. M.; Sathitsuksanoh, N.; Kambam, P.; Sandoval, L.; Mitra, D.; Zhang, S.; George, A.; Singer, S. W.; Simmons, B. A.; et al. One-Pot Ionic Liquid Pretreatment and Saccharification of Switchgrass. *Green Chem.* **2013**, *15*, 2579−2589.
(67) Wang, Z.-K.; Li, H.; Lin, X.-C.; Tang, L.; Chen, J.-J.; Mo, J.-W.; Yu, R.-S.; Shen, X.-J. Novel Recyclable Deep Eutectic Solvent Boost Biomass Pretreatment for Enzymatic Hydrolysis. *Bioresour. Technol.* **2020**, *307*, 123237.
(68) Zhou, M.; Fakayode, O. A.; Ahmed Yagoub, A. E.; Ji, Q.; Zhou, C. Lignin Fractionation from Lignocellulosic Biomass Using Deep Eutectic Solvents and Its Valorization. *Renew. Sust. Energy Rev.* **2022**, *156*, 111986.
(69) Zhu, J.; Chen, L.; Cai, C. Acid Hydrotropic Fractionation of Lignocelluloses for Sustainable Biorefinery: Advantages, Opportunities, and Research Needs. *ChemSusChem* **2021**, *14*, 3031−3046.
(70) Cai, C.; Hirth, K.; Gleisner, R.; Lou, H.; Qiu, X.; Zhu, J. Y. Maleic Acid as a Dicarboxylic Acid Hydrotrope for Sustainable Fractionation of Wood at Atmospheric Pressure and ≤ 100 °C: Mode and Utility of Lignin Esterification. *Green Chem.* **2020**, *22*, 1605−1617.
(71) Chen, L.; Dou, J.; Ma, Q.; Li, N.; Wu, R.; Bian, H.; Yelle, D. J.; Vuorinen, T.; Fu, S.; Pan, X.; Zhu, J. Y. Rapid and Near-Complete Dissolution of Wood Lignin at ≤ 80°C by a Recyclable Acid Hydrotrope. *Sci. Adv.* **2017**, *3*, No. e1701735.
(72) Song, J.; Chen, C.; Zhu, S.; Zhu, M.; Dai, J.; Ray, U.; Li, Y.; Kuang, Y.; Li, Y.; Quispe, N.; et al. Processing Bulk Natural Wood into a High-Performance Structural Material. *Nature* **2018**, *554*, 224−228.
(73) Jia, C.; Chen, C.; Mi, R.; Li, T.; Dai, J.; Yang, Z.; Pei, Y.; He, S.; Bian, H.; Jang, S.-H.; et al. Clear Wood toward High-Performance Building Materials. *ACS Nano* **2019**, *13*, 9993−10001.
(74) Zhu, M.; Song, J.; Li, T.; Gong, A.; Wang, Y.; Dai, J.; Yao, Y.; Luo, W.; Henderson, D.; Hu, L. Highly Anisotropic, Highly Transparent Wood Composites. *Adv. Mater.* **2016**, *28*, 5181−5187.

https://doi.org/10.1021/acs.chemrev.2c00450
Chem. Rev. 2023, 123, 1843−1888

(75) Lu, Y.; He, Q.; Fan, G.; Cheng, Q.; Song, G. Extraction and Modification of Hemicellulose from Lignocellulosic Biomass: A review. *Green Process. Synth.* **2021**, *10*, 779−804.
(76) Li, Z.; Pan, X. Strategies to Modify Physicochemical Properties of Hemicelluloses from Biorefinery and Paper Industry for Packaging Material. *Rev. Environ. Sci. Biotechnol.* **2018**, *17*, 47−69.
(77) Leu, S.-Y.; Zhu, J. Y. Substrate-Related Factors Affecting Enzymatic Saccharification of Lignocelluloses: Our Recent Understanding. *Bioenergy Res.* **2013**, *6*, 405−415.
(78) Zhu, J. Y.; Pan, X. Efficient Sugar Production from Plant Biomass: Current Status, Challenges, and Future Directions. *Renew. Sust. Energy Rev.* **2022**, *164*, 112583.
(79) Song, J.; Chen, C.; Yang, Z.; Kuang, Y.; Li, T.; Li, Y.; Huang, H.; Kierzewski, I.; Liu, B.; He, S.; et al. Highly Compressible, Anisotropic Aerogel with Aligned Cellulose Nanofibers. *ACS Nano* **2018**, *12*, 140−147.
(80) Garemark, J.; Yang, X.; Sheng, X.; Cheung, O.; Sun, L.; Berglund, L. A.; Li, Y. Top-Down Approach Making Anisotropic Cellulose Aerogels as Universal Substrates for Multifunctionalization. *ACS Nano* **2020**, *14*, 7111−7120.
(81) Dence, C. W.; Reeve, D. W.*Pulp Bleaching Principles and Practice*; TAPPI Press, 1996; pp 812−815
(82) Mi, R.; Chen, C.; Keplinger, T.; Pei, Y.; He, S.; Liu, D.; Li, J.; Dai, J.; Hitz, E.; Yang, B.; Burgert, I.; Hu, L. Scalable Aesthetic Transparent Wood for Energy Efficient Buildings. *Nat. Commun.* **2020**, *11*, 3836.
(83) Xia, Q.; Chen, C.; Li, T.; He, S.; Gao, J.; Wang, X.; Hu, L. Solar-Assisted Fabrication of Large-Scale, Patternable Transparent Wood. *Sci. Adv.* **2021**, *7*, No. eabd7342.
(84) Shikinaka, K.; Otsuka, Y. Functional "Permanently Whitened" Lignin Synthesized via Solvent-Controlled Encapsulation. *Green Chem.* **2022**, *24*, 3243−3249.
(85) Rowell, R. M. Understanding Wood Surface Chemistry and Approaches to Modification: A Review. *Polymers* **2021**, *13*, 2558.
(86) Mantanis, G. I. Chemical Modification of Wood by Acetylation or Furfurylation: A Review of the Present Scaled-up Technologies. *BioRes.* **2017**, *12*, 12.
(87) Fox, S. C.; Li, B.; Xu, D.; Edgar, K. J. Regioselective Esterification and Etherification of Cellulose: A Review. *Biomacromolecules* **2011**, *12*, 1956−1972.
(88) Heinze, T.; El Seoud, O. A.; Koschella, A. In *Cellulose Derivatives: Synthesis, Structure, and Properties*; Heinze, T., El Seoud, O. A., Koschella, A., Eds.; Springer International: Cham, 2018.
(89) Li, G.; Shang, Y.; Wang, Y.; Wang, L.; Chao, Y.; Qi, Y. Reaction Mechanism of Etherification of Rice Straw with Epichlorohydrin in Alkaline Medium. *Sci. Rep.* **2019**, *9*, 14307.
(90) Jankauskaitė, V.; Balčiūnaitienė, A.; Alexandrova, R.; Buškuvienė, N.; Žukienė, K. Effect of Cellulose Microfiber Silylation Procedures on the Properties and Antibacterial Activity of Polydimethylsiloxane. *Coatings* **2020**, *10*, 567.
(91) Klemm, D.; Stein, A. Silylated Cellulose Materials in Design of Supramolecular Structures of Ultrathin Cellulose Films. *J. Macromol. Sci. A* **1995**, *32*, 899−904.
(92) Goussé, C.; Chanzy, H.; Cerrada, M. L.; Fleury, E. Surface Silylation of Cellulose Microfibrils: Preparation and Rheological Properties. *Polymer* **2004**, *45*, 1569−1575.
(93) Yu, H.-Y.; Chen, R.; Chen, G.-Y.; Liu, L.; Yang, X.-G.; Yao, J.-M. Silylation of Cellulose Nanocrystals and Their Reinforcement of Commercial Silicone Rubber. *J. Nanopart. Res.* **2015**, *17*, 361.
(94) Petzold, K.; Koschella, A.; Klemm, D.; Heublein, B. Silylation of Cellulose and Starch - Selectivity, Structure Analysis, and Subsequent Reactions. *Cellulose* **2003**, *10*, 251−269.
(95) Sterman, S.; Marsden, J. G. Silane Coupling Agents. *Ind. Eng. Chem.* **1966**, *58*, 33−37.
(96) Abdelmouleh, M.; Boufi, S.; ben Salah, A.; Belgacem, M. N.; Gandini, A. Interaction of Silane Coupling Agents with Cellulose. *Langmuir* **2002**, *18*, 3203−3208.
(97) Es-haghi, H.; Mirabedini, S. M.; Imani, M.; Farnood, R. R. Preparation and Characterization of Pre-Silane Modified Ethyl Cellulose-Based Microcapsules Containing Linseed Oil. *Colloids Surf. A: Physicochem. Eng. Asp.* **2014**, *447*, 71−80.
(98) Thakur, M. K.; Gupta, R. K.; Thakur, V. K. Surface Modification of Cellulose Using Silane Coupling Agent. *Carbohydr. Polym.* **2014**, *111*, 849−855.
(99) Leung, A. C. W.; Hrapovic, S.; Lam, E.; Liu, Y.; Male, K. B.; Mahmoud, K. A.; Luong, J. H. T. Characteristics and Properties of Carboxylated Cellulose Nanocrystals Prepared from a Novel One-Step Procedure. *Small* **2011**, *7*, 302−305.
(100) Isogai, A.; Saito, T.; Fukuzumi, H. TEMPO-Oxidized Cellulose Nanofibers. *Nanoscale* **2011**, *3*, 71−85.
(101) Liimatainen, H.; Visanko, M.; Sirviö, J. A.; Hormi, O. E. O.; Niinimaki, J. Enhancement of the Nanofibrillation of Wood Cellulose through Sequential Periodate-Chlorite Oxidation. *Biomacromolecules* **2012**, *13*, 1592−1597.
(102) Li, N.; Bian, H.; Zhu, J. Y.; Ciesielski, P. N.; Pan, X. Tailorable Cellulose II Nanocrystals (CNC II) Prepared in Mildly Acidic Lithium Bromide Trihydrate (MALBTH). *Green Chem.* **2021**, *23*, 2778−2791.
(103) Sirvio, J.; Hyvakko, U.; Liimatainen, H.; Niinimaki, J.; Hormi, O. Periodate Oxidation of Cellulose at Elevated Temperatures Using Metal Salts as Cellulose Activators. *Carbohydr. Polym.* **2011**, *83*, 1293−1297.
(104) Kim, U.-J.; Kuga, S. Ion-Exchange Chromatography by Dicarboxyl Cellulose Gel. *J. Chromatogr. A* **2001**, *919*, 29−37.
(105) Wu, M.; Kuga, S. Cationization of Cellulose Fabrics by Polyallylamine Binding. *J. Appl. Polym. Sci.* **2006**, *100*, 1668−1672.
(106) Bengtsson, M.; Gatenholm, P.; Oksman, K. The Effect of Crosslinking on the Properties of Polyethylene/Wood Flour Composites. *Compos. Sci. Technol.* **2005**, *65*, 1468−1479.
(107) He, X.; Xiao, Z.; Feng, X.; Sui, S.; Wang, Q.; Xie, Y. Modification of Poplar Wood with Glucose Crosslinked with Citric Acid and 1,3-Dimethylol-4,5-Dihydroxy Ethyleneurea. *Holzforschung* **2016**, *70*, 47−53.
(108) Wang, D.; Ling, Q.; Nie, Y.; Zhang, Y.; Zhang, W.; Wang, H.; Sun, F. In-Situ Cross-Linking of Waterborne Epoxy Resin Inside Wood for Enhancing Its Dimensional Stability, Thermal Stability, and Decay Resistance. *ACS Appl. Polym. Mater.* **2021**, *3*, 6265−6273.
(109) Zainal, S. H.; Mohd, N. H.; Suhaili, N.; Anuar, F. H.; Lazim, A. M.; Othaman, R. Preparation of Cellulose-Based Hydrogel: a Review. *J. Mater. Res. Technol.* **2021**, *10*, 935−952.
(110) Du, H.; Liu, W.; Zhang, M.; Si, C.; Zhang, X.; Li, B. Cellulose Nanocrystals and Cellulose Nanofibrils Based Hydrogels for Biomedical Applications. *Carbohydr. Polym.* **2019**, *209*, 130−144.
(111) Roy, D.; Semsarilar, M.; Guthrie, J. T.; Perrier, S. Cellulose Modification by Polymer Grafting: a Review. *Chem. Soc. Rev.* **2009**, *38*, 2046−2064.
(112) Ragauskas, A. J.; Beckham, G. T.; Biddy, M. J.; Chandra, R.; Chen, F.; Davis, M. F.; Davison, B. H.; Dixon, R. A.; Gilna, P.; Keller, M.; et al. Lignin Valorization: Improving Lignin Processing in the Biorefinery. *Science* **2014**, *344*, 1246843.
(113) Global Status Report for Buildings and Construction; Global Alliance for Buildings and Construction, UN Environment Programme, Oct 19, 2021; https://globalabc.org/resources/publications/2021-global-status-report-buildings-and-construction (accessed 2022-03-13).
(114) Sotayo, A.; Bradley, D.; Bather, M.; Sareh, P.; Oudjene, M.; El-Houjeyri, I.; Harte, A. M.; Mehra, S.; O'Ceallaigh, C.; Haller, P.; et al. Review of State of the Art Of Dowel Laminated Timber Members and Densified Wood Materials as Sustainable Engineered Wood Products for Construction and Building Applications. *Dev. Built Environ.* **2020**, *1*, 100004.
(115) Gan, W.; Chen, C.; Wang, Z.; Song, J.; Kuang, Y.; He, S.; Mi, R.; Sunderland, P. B.; Hu, L. Dense, Self-Formed Char Layer Enables a Fire-Retardant Wood Structural Material. *Adv. Funct. Mater.* **2019**, *29*, 1807444.
(116) Kuljich, S.; Cáceres, C. B.; Hernández, R. E. Steam-Bending Properties of Seven Poplar Hybrid Clones. *Int. J. Mater. Form.* **2015**, *8*, 67−72.

https://doi.org/10.1021/acs.chemrev.2c00450
Chem. Rev. 2023, 123, 1843−1888

(117) Qin, Y. A Review on the Development of Cool Pavements to Mitigate Urban Heat Island Effect. *Renew. Sust. Energy Rev.* **2015**, *52*, 445−459.
(118) Li, T.; Song, J.; Zhao, X.; Yang, Z.; Pastel, G.; Xu, S.; Jia, C.; Dai, J.; Chen, C.; Gong, A.; et al. Anisotropic, Lightweight, Strong, and Super Thermally Insulating Nanowood with Naturally Aligned Nanocellulose. *Sci. Adv.* **2018**, *4*, No. eaar3724.
(119) Gan, W.; Chen, C.; Wang, Z.; Pei, Y.; Ping, W.; Xiao, S.; Dai, J.; Yao, Y.; He, S.; Zhao, B.; et al. Fire-Resistant Structural Material Enabled by an Anisotropic Thermally Conductive Hexagonal Boron Nitride Coating. *Adv. Funct. Mater.* **2020**, *30*, 1909196.
(120) Li, D.; Huang, C. Thermal Insulation Performances of Carbonized Sawdust Packed Bed for Energy Saving In Buildings. *Energy Build.* **2022**, *254*, 111625.
(121) Xu, J.; Yang, T.; Xu, X.; Guo, X.; Cao, J. Processing Solid Wood into a Composite Phase Change Material for Thermal Energy Storage by Introducing Silica-Stabilized Polyethylene Glycol. *Compos. - A: Appl. Sci. Manuf.* **2020**, *139*, 106098.
(122) Raman, A. P.; Anoma, M. A.; Zhu, L.; Rephaeli, E.; Fan, S. Passive Radiative Cooling Below Ambient Air Temperature Under Direct Sunlight. *Nature* **2014**, *515*, 540−544.
(123) Li, T.; Zhai, Y.; He, S.; Gan, W.; Wei, Z.; Heidarinejad, M.; Dalgo, D.; Mi, R.; Zhao, X.; Song, J.; et al. A Radiative Cooling Structural Material. *Science* **2019**, *364*, 760−763.
(124) Chen, Y.; Dang, B.; Fu, J.; Wang, C.; Li, C.; Sun, Q.; Li, H. Cellulose-Based Hybrid Structural Material for Radiative Cooling. *Nano Lett.* **2021**, *21*, 397−404.
(125) Li, Y.; Fu, Q.; Yu, S.; Yan, M.; Berglund, L. Optically Transparent Wood from a Nanoporous Cellulosic Template: Combining Functional and Structural Performance. *Biomacromolecules* **2016**, *17*, 1358−1364.
(126) Li, Y.; Yang, X.; Fu, Q.; Rojas, R.; Yan, M.; Berglund, L. Towards Centimeter Thick Transparent Wood Through Interface Manipulation. *J. Mater. Chem. A* **2018**, *6*, 1094−1101.
(127) Fink, S. Transparent Wood - A New Approach in the Functional Study of Wood Structure. *Holzforschung* **1992**, *46*, 403−408.
(128) Zhu, M.; Li, T.; Davis, C. S.; Yao, Y.; Dai, J.; Wang, Y.; AlQatari, F.; Gilman, J. W.; Hu, L. Transparent and Haze Wood Composites for Highly Efficient Broadband Light Management in Solar Cells. *Nano Energy* **2016**, *26*, 332−339.
(129) Höglund, M.; Johansson, M.; Sychugov, I.; Berglund, L. A. Transparent Wood Biocomposites by Fast UV-Curing for Reduced Light-Scattering through Wood/Thiol-ene Interface Design. *ACS Appl. Mater. Interfaces* **2020**, *12*, 46914−46922.
(130) Subba Rao, A. N.; Nagarajappa, G. B.; Nair, S.; Chathoth, A. M.; Pandey, K. K. Flexible Transparent Wood Prepared from Poplar Veneer and Polyvinyl Alcohol. *Compos. Sci. Technol.* **2019**, *182*, 107719.
(131) Wang, M.; Li, R.; Chen, G.; Zhou, S.; Feng, X.; Chen, Y.; He, M.; Liu, D.; Song, T.; Qi, H. Highly Stretchable, Transparent, and Conductive Wood Fabricated by in Situ Photopolymerization with Polymerizable Deep Eutectic Solvents. *ACS Appl. Mater. Interfaces* **2019**, *11*, 14313−14321.
(132) Montanari, C.; Ogawa, Y.; Olsén, P.; Berglund, L. A. High Performance, Fully Bio-Based, and Optically Transparent Wood Biocomposites. *Adv. Sci.* **2021**, *8*, 2100559.
(133) Van Hai, L.; Muthoka, R. M.; Panicker, P. S.; Agumba, D. O.; Pham, H. D.; Kim, J. All-Biobased Transparent-Wood: a New Approach and Its Environmental-Friendly Packaging Application. *Carbohydr. Polym.* **2021**, *264*, 118012.
(134) Wang, K.; Dong, Y.; Ling, Z.; Liu, X.; Shi, S. Q.; Li, J. Transparent Wood Developed by Introducing Epoxy Vitrimers into a Delignified Wood Template. *Compos. Sci. Technol.* **2021**, *207*, 108690.
(135) Li, Y.; Fu, Q.; Rojas, R.; Yan, M.; Lawoko, M.; Berglund, L. Lignin-Retaining Transparent Wood. *ChemSusChem* **2017**, *10*, 3445−3451.
(136) Xia, Q.; Chen, C.; Yao, Y.; He, S.; Wang, X.; Li, J.; Gao, J.; Gan, W.; Jiang, B.; Cui, M.; et al. In Situ Lignin Modification toward Photonic Wood. *Adv. Mater.* **2021**, *33*, 2001588.
(137) Fu, Q.; Yan, M.; Jungstedt, E.; Yang, X.; Li, Y.; Berglund, L. A. Transparent Plywood as a Load-Bearing and Luminescent Biocomposite. *Compos. Sci. Technol.* **2018**, *164*, 296−303.
(138) Montanari, C.; Li, Y.; Chen, H.; Yan, M.; Berglund, L. A. Transparent Wood for Thermal Energy Storage and Reversible Optical Transmittance. *ACS Appl. Mater. Interfaces* **2019**, *11*, 20465−20472.
(139) Qiu, Z.; Wang, S.; Wang, Y.; Li, J.; Xiao, Z.; Wang, H.; Liang, D.; Xie, Y. Transparent Wood with Thermo-Reversible Optical Properties Based on Phase-Change Material. *Compos. Sci. Technol.* **2020**, *200*, 108407.
(140) Yu, Z.; Yao, Y.; Yao, J.; Zhang, L.; Chen, Z.; Gao, Y.; Luo, H. Transparent Wood Containing Csxwo3 Nanoparticles for Heat-Shielding Window Applications. *J. Mater. Chem. A* **2017**, *5*, 6019−6024.
(141) Qiu, Z.; Xiao, Z.; Gao, L.; Li, J.; Wang, H.; Wang, Y.; Xie, Y. Transparent Wood Bearing a Shielding Effect to Infrared Heat and Ultraviolet via Incorporation of Modified Antimony-Doped Tin Oxide Nanoparticles. *Compos. Sci. Technol.* **2019**, *172*, 43−48.
(142) Liu, S.; Tso, C. Y.; Lee, H. H.; Du, Y. W.; Yu, K. M.; Feng, S.-P.; Huang, B. Self-Densified Optically Transparent VO_2 Thermochromic Wood Film for Smart Windows. *ACS Appl. Mater. Interfaces* **2021**, *13*, 22495−22504.
(143) Zhang, L.; Wang, A.; Zhu, T.; Chen, Z.; Wu, Y.; Gao, Y. Transparent Wood Composites Fabricated by Impregnation of Epoxy Resin and W-Doped VO_2 Nanoparticles for Application in Energy-Saving Windows. *ACS Appl. Mater. Interfaces* **2020**, *12*, 34777−34783.
(144) Höglund, M.; Garemark, J.; Nero, M.; Willhammar, T.; Popov, S.; Berglund, L. A. Facile Processing of Transparent Wood Nanocomposites with Structural Color from Plasmonic Nanoparticles. *Chem. Mater.* **2021**, *33*, 3736−3745.
(145) Zhu, X.; Liu, Y.; Dong, N.; Li, Z. Fabrication and Characterization of Reversible Thermochromic Wood Veneers. *Sci. Rep.* **2017**, *7*, 16933.
(146) Wang, L.; Liu, Y.; Zhan, X.; Luo, D.; Sun, X. Photochromic Transparent Wood for Photo-Switchable Smart Window Applications. *J. Mater. Chem. C* **2019**, *7*, 8649−8654.
(147) Wachter, I.; Štefko, T.; Rantuch, P.; Martinka, J.; Pastierová, A. Effect of UV Radiation on Optical Properties and Hardness of Transparent Wood. *Polymers* **2021**, *13*, 2067.
(148) Yang, H.; Chao, W.; Wang, S.; Yu, Q.; Cao, G.; Yang, T.; Liu, F.; Di, X.; Li, J.; Wang, C.; et al. Self-Luminous Wood Composite for Both Thermal and Light Energy Storage. *Energy Stor. Mater.* **2019**, *18*, 15−22.
(149) Li, Y.; Yu, S.; Veinot, J. G. C.; Linnros, J.; Berglund, L.; Sychugov, I. Luminescent Transparent Wood. *Adv. Opt. Mater.* **2017**, *5*, 1600834.
(150) Fu, Q.; Tu, K.; Goldhahn, C.; Keplinger, T.; Adobes-Vidal, M.; Sorieul, M.; Burgert, I. Luminescent and Hydrophobic Wood Films as Optical Lighting Materials. *ACS Nano* **2020**, *14*, 13775−13783.
(151) Ritter, M.; Burgert, I.; Panzarasa, G. Shine-through Luminescent Wood Membranes. *Mater. Adv.* **2022**, *3*, 1767−1771.
(152) Bi, Z.; Li, T.; Su, H.; Ni, Y.; Yan, L. Transparent Wood Film Incorporating Carbon Dots as Encapsulating Material for White Light-Emitting Diodes. *ACS Sustain. Chem. Eng.* **2018**, *6*, 9314−9323.
(153) Zhang, T.; Yang, P.; Li, Y.; Cao, Y.; Zhou, Y.; Chen, M.; Zhu, Z.; Chen, W.; Zhou, X. Flexible Transparent Sliced Veneer for Alternating Current Electroluminescent Devices. *ACS Sustain. Chem. Eng.* **2019**, *7*, 11464−11473.
(154) Zhang, T.; Yang, P.; Chen, M.; Yang, K.; Cao, Y.; Li, X.; Tang, M.; Chen, W.; Zhou, X. Constructing a Novel Electroluminescent Device with High-Temperature and High-Humidity Resistance based on a Flexible Transparent Wood Film. *ACS Appl. Mater. Interfaces* **2019**, *11*, 36010−36019.
(155) Li, Y.; Cheng, M.; Jungstedt, E.; Xu, B.; Sun, L.; Berglund, L. Optically Transparent Wood Substrate for Perovskite Solar Cells. *ACS Sustain. Chem. Eng.* **2019**, *7*, 6061−6067.
(156) Zou, W.; Wang, Z.; Sun, D.; Ji, X.; Zhang, P.; Zhu, Z. Transparent Cellulose Nanofibrils Composites with Two-layer Delignified Rotary-cutting Poplar Veneers (0°-layer and 90°-layer) for Light Acquisition of Solar Cell. *Sci. Rep.* **2020**, *10*, 1947.

https://doi.org/10.1021/acs.chemrev.2c00450
Chem. Rev. 2023, 123, 1843−1888

(157) Wang, Z. L. On the First Principle Theory of Nanogenerators from Maxwell's Equations. *Nano Energy* **2020**, *68*, 104272.
(158) Fukada, E. Piezoelectricity of Wood. *J. Phys. Soc. Jpn.* **1955**, *10*, 149−154.
(159) Fukada, E. Piezoelectricity as a Fundamental Property of Wood. *Wood Sci. Technol.* **1968**, *2*, 299−307.
(160) Sun, J.; Guo, H.; Schädli, G. N.; Tu, K.; Schär, S.; Schwarze, F. W. M. R.; Panzarasa, G.; Ribera, J.; Burgert, I. Enhanced Mechanical Energy Conversion with Selectively Decayed Wood. *Sci. Adv.* **2021**, *7*, No. eabd9138.
(161) Sun, J.; Guo, H.; Ribera, J.; Wu, C.; Tu, K.; Binelli, M.; Panzarasa, G.; Schwarze, F. W. M. R.; Wang, Z. L.; Burgert, I. Sustainable and Biodegradable Wood Sponge Piezoelectric Nanogenerator for Sensing and Energy Harvesting Applications. *ACS Nano* **2020**, *14*, 14665−14674.
(162) Torres, F. G.; De-la-Torre, G. E. Polysaccharide-Based Triboelectric Nanogenerators: A Review. *Carbohydr. Polym.* **2021**, *251*, 117055.
(163) Özel, M.; Demir, F.; Aikebaier, A.; Kwiczak-Yiğitbaşı, J.; Baytekin, H. T.; Baytekin, B. Why Does Wood Not Get Contact Charged? Lignin as an Antistatic Additive for Common Polymers. *Chem. Mater.* **2020**, *32*, 7438−7444.
(164) Zhou, J.; Wang, H.; Du, C.; Zhang, D.; Lin, H.; Chen, Y.; Xiong, J. Cellulose for Sustainable Triboelectric Nanogenerators. *Adv. Energy Sustainability Res.* **2022**, *3*, 2100161.
(165) Luo, J.; Wang, Z.; Xu, L.; Wang, A. C.; Han, K.; Jiang, T.; Lai, Q.; Bai, Y.; Tang, W.; Fan, F. R.; Wang, Z. L. Flexible and Durable Wood-Based Triboelectric Nanogenerators for Self-Powered Sensing in Athletic Big Data Analytics. *Nat. Commun.* **2019**, *10*, 5147.
(166) Hao, S.; Jiao, J.; Chen, Y.; Wang, Z. L.; Cao, X. Natural Wood-Based Triboelectric Nanogenerator as Self-Powered Sensing for Smart Homes and Floors. *Nano Energy* **2020**, *75*, 104957.
(167) Bang, J.; Moon, I. K.; Jeon, Y. P.; Ki, B.; Oh, J. Fully Wood-Based Green Triboelectric Nanogenerators. *Appl. Surf. Sci.* **2021**, *567*, 150806.
(168) Cai, C.; Mo, J.; Lu, Y.; Zhang, N.; Wu, Z.; Wang, S.; Nie, S. Integration of a Porous Wood-Based Triboelectric Nanogenerator and Gas Sensor for Real-Time Wireless Food-Quality Assessment. *Nano Energy* **2021**, *83*, 105833.
(169) Shi, X.; Luo, J.; Luo, J.; Li, X.; Han, K.; Li, D.; Cao, X.; Wang, Z. L. Flexible Wood-Based Triboelectric Self-Powered Smart Home System. *ACS Nano* **2022**, *16*, 3341−3350.
(170) Sun, J.; Tu, K.; Büchele, S.; Koch, S. M.; Ding, Y.; Ramakrishna, S. N.; Stucki, S.; Guo, H.; Wu, C.; Keplinger, T.; et al. Functionalized Wood with Tunable Tribopolarity for Efficient Triboelectric Nanogenerators. *Matter* **2021**, *4*, 3049−3066.
(171) Huang, L.; Krigsvoll, G.; Johansen, F.; Liu, Y.; Zhang, X. Carbon Emission of Global Construction Sector. *Renew. Sust. Energy Rev.* **2018**, *81*, 1906−1916.
(172) Li, Y. L.; Han, M. Y.; Liu, S. Y.; Chen, G. Q. Energy Consumption and Greenhouse Gas Emissions by Buildings: A Multi-Scale Perspective. *Build Environ* **2019**, *151*, 240−250.
(173) Sun, W.; Wang, Q.; Zhou, Y.; Wu, J. Material and Energy Flows of the Iron and Steel Industry: Status Quo, Challenges and Perspectives. *Applied Energy* **2020**, *268*, 114946.
(174) Gauch, M. M. C.; Hincapié, I.; Hörler, R.; Böni, H.*Projekt MatCH—Material—und Energieressourcen Sowie Umweltauswirkungen der Baulichen Infrastruktur der Schweiz*; Empa, 2016.
(175) Telmo, C.; Lousada, J. Heating Values of Wood Pellets from Different Species. *Biomass & Bioenergy* **2011**, *35*, 2634−2639.
(176) Ayanleye, S.; Udele, K.; Nasir, V.; Zhang, X.; Militz, H. Durability and Protection of Mass Timber Structures: A Review. *J. Build. Eng.* **2022**, *46*, 103731.
(177) Hass, P.; Wittel, F. K.; Mendoza, M.; Herrmann, H. J.; Niemz, P. Adhesive Penetration in Beech Wood: Experiments. *Wood Sci. Technol.* **2012**, *46*, 243−256.
(178) Custodio, J.; Broughton, J.; Cruz, H. A Review of Factors Influencing the Durability of Structural Bonded Timber Joints. *Int. J. Adhes. Adhes.* **2009**, *29*, 173−185.
(179) Stoeckel, F.; Konnerth, J.; Gindl-Altmutter, W. Mechanical Properties of Adhesives for Bonding Wood-A Review. *Int. J. Adhes. Adhes.* **2013**, *45*, 32−41.
(180) Konnerth, J.; Gindl, W. Mechanical Characterisation of Wood-Adhesive Interphase Cell Walls by Nanoindentation. *Holzforschung* **2006**, *60*, 429−433.
(181) Kamke, F. A.; Lee, J. N. Adhesive Penetration in Wood - A Review. *Wood Fiber Sci.* **2007**, *39*, 205−220.
(182) Fang, D. M.; Moradei, J.; Brutting, J.; Fscher, A.; Landez, D. K.; Shao, B. S.; Sherrow-Groves, N.; Fivet, C.; Mueller, C.*60th Anniversary Symposium of the International-Association-for-Shell-and-Spatial-Structures (IASS Symposium)/9th International Conference on Textile Composites and Inflatable Structures (Structural Membranes), Barcelona, Spain*, 2019; pp 2911−2918.
(183) Dolan, J. A.; Sathitsuksanoh, N.; Rodriguez, K.; Simmons, B. A.; Frazier, C. E.; Renneckar, S. Biocomposite Adhesion Without Added Resin: Understanding the Chemistry of The Direct Conversion of Wood into Adhesives. *RSC Adv.* **2015**, *5*, 67267−67276.
(184) Pizzi, A. Recent Developments in Eco-Efficient Bio-Based Adhesives for Wood Bonding: Opportunities and Issues. *J. Adhes. Sci. Technol.* **2006**, *20*, 829−846.
(185) Stamm, B.; Natterer, J.; Navi, P. Joining Wood by Friction Welding. *Holz Als Roh-und Werkst.* **2005**, *63*, 313−320.
(186) Hahn, B.; Stamm, B.; Weinand, Y. Linear Friction Welding of Spruce Boards: Experimental Investigations on Scale Effects Due to Humidity Evaporation. *Wood Sci. Technol.* **2014**, *48*, 855−871.
(187) Vaziri, M.; Lindgren, O.; Pizzi, A.; Mansouri, H. R. Moisture Sensitivity of Scots Pine Joints Produced by Linear Frictional Welding. *J. Adhes. Sci. Technol.* **2010**, *24*, 1515−1527.
(188) Amirou, S.; Pizzi, A.; Delmotte, L. Citric Acid as Waterproofing Additive in Butt Joints Linear Wood Welding. *Eur. J. Wood Wood Prod.* **2017**, *75*, 651−654.
(189) Mansouri, H. R.; Omrani, P.; Pizzi, A. Improving the Water Resistance of Linear Vibration-Welded Wood Joints. *J. Adhes. Sci. Technol.* **2009**, *23*, 63−70.
(190) Pizzi, A.; Zhou, X.; Navarrete, P.; Segovia, C.; Mansouri, H. R.; Placentia Pena, M. I.; Pichelin, F. Enhancing Water Resistance of Welded Dowel Wood Joints by Acetylated Lignin. *J. Adhes. Sci. Technol.* **2013**, *27*, 252−262.
(191) Kaufmann, M.; Kolbe, J.; Vallee, T. Hardwood Rods Glued into Softwood Using Environmentally Sustainable Adhesives. *J. Adhes.* **2018**, *94*, 991−1016.
(192) Antov, P.; Savov, V.; Neykov, N. Sustainable Bio-Based Adhesives for Eco-Friendly Wood Composites A Review. *Wood Res.* **2020**, *65*, 51−62.
(193) Hemmila, V.; Adamopoulos, S.; Karlsson, O.; Kumar, A. Development of Sustainable Bio-Adhesives for Engineered Wood Panels - A Review. *RSC Adv.* **2017**, *7*, 38604−38630.
(194) Collins, M. N.; Nechifor, M.; Tanasa, F.; Zanoaga, M.; McLoughlin, A.; Strozyk, M. A.; Culebras, M.; Teaca, C. A. Valorization of Lignin in Polymer and Composite Systems for Advanced Engineering Applications - A Review. *Int. J. Biol. Macromol.* **2019**, *131*, 828−849.
(195) Ferdosian, F.; Pan, Z. H.; Gao, G. C.; Zhao, B. X. Bio-Based Adhesives and Evaluation for Wood Composites Application. *Polymers* **2017**, *9*, 70.
(196) Pichelin, F.; Nakatani, M.; Pizzi, A.; Wieland, S.; Despres, A.; Rigolet, S. Structural Beams from Thick Wood Panels Bonded Industrially with Formaldehyde-Free Tannin Adhesives. *Forest Prod. J.* **2006**, *56*, 31−36.
(197) Wang, M. C.; Leitch, M.; Xu, C. B. C. Synthesis of Phenol-Formaldehyde Resol Resins Using Organosolv Pine Lignins. *Eur. Polym. J.* **2009**, *45*, 3380−3388.
(198) Lora, J. H.; Glasser, W. G. Recent Industrial Applications of Lignin: A Sustainable Alternative to Nonrenewable Materials. *J. Polym. Environ.* **2002**, *10*, 39−48.
(199) Sun, Z. H.; Fridrich, B.; de Santi, A.; Elangovan, S.; Barta, K. Bright Side of Lignin Depolymerization: Toward New Platform Chemicals. *Chem. Rev.* **2018**, *118*, 614−678.

https://doi.org/10.1021/acs.chemrev.2c00450
Chem. Rev. 2023, 123, 1843−1888

(200) Hill, C. A. S. Wood Modification: An Update. *BioResources* **2011**, *6*, 918−919.
(201) Militz, H.; Lande, S. Challenges in Wood Modification Technology on The Way to Practical Applications. *Wood Mater. Sci. Eng.* **2009**, *4*, 23−29.
(202) Sandberg, D.; Kutnar, A.; Mantanis, G. Wood Modification Technologies - A Review. *iForest* **2017**, *10*, 895−908.
(203) Berglund, L. A.; Burgert, I. Bioinspired Wood Nanotechnology for Functional Materials. *Adv. Mater.* **2018**, *30*, 1704285.
(204) Zhu, H.; Luo, W.; Ciesielski, P. N.; Fang, Z.; Zhu, J. Y.; Henriksson, G.; Himmel, M. E.; Hu, L. Wood-Derived Materials for Green Electronics, Biological Devices, and Energy Applications. *Chem. Rev.* **2016**, *116*, 9305−9374.
(205) Ribera, J.; Tang, A. M. C.; Schubert, M.; Lam, R. Y. C.; Chu, L. M.; Leung, M. W. K.; Kwan, H. S.; Bas, M. C.; Schwarze, F. In Vitro Evaluation of Antagonistic Trichoderma Strains for Eradicating Phellinus Noxius in Colonised Wood. *J. Trop. Forest Sci.* **2016**, *28*, 457−468.
(206) van Niekerk, P. B.; Marais, B. N.; Brischke, C.; Borges, L. M. S.; Kutnik, M.; Niklewski, J.; Ansard, D.; Humar, M.; Cragg, S. M.; Militz, H. Mapping the Biotic Degradation Hazard of Wood in Europe - Biophysical Background, Engineering Applications, and Climate Change-Induced Prospects. *Holzforschung* **2022**, *76*, 188−210.
(207) Rowell, R. M.; Diekerson, J. P. In *Deterioration and Protection of Sustainable Biomaterials*; Schultz, T. P., Goodell, B., Nicholas, D. D., Eds.; American Chemical Society: Wasington DC, 2014; Vol. *1158*.
(208) Schubert, M.; Fink, S.; Schwarze, F. W. M. R. Evaluation of Trichoderma spp. as a Biocontrol Agent Against Wood Decay Fungi in Urban Trees. *Biol. Control* **2008**, *45*, 111−123.
(209) *ISO 14044:2006 Environmental Management, Life Cycle Assessment, Requirements and Guidelines*; ISO, 2006; https://www.iso.org/standard/38498.html (accessed 2022-03-02).
(210) Lan, K.; Yao, Y. Integrating Life Cycle Assessment and Agent-Based Modeling: A Dynamic Modeling Framework for Sustainable Agricultural Systems. *J. Cleaner Prod.* **2019**, *238*, 117853.
(211) Lan, K.; Yao, Y. Dynamic Life Cycle Assessment of Energy Technologies under Different Greenhouse Gas Concentration Pathways. *Environ. Sci. Technol.* **2022**, *56*, 1395−1404.
(212) Bowers, T.; Puettmann, M.; Ganguly, I.; Eastin, I. Cradle-to-Gate Life-Cycle Impact Analysis of Glued-Laminated (Glulam) Timber: Environmental Impacts from Glulam Produced in the US Pacific Northwest and Southeast. *Forest Prod. J.* **2017**, *67*, 368−380.
(213) Bowers, T.; Puettmann, M.; Ganguly, I.; Eastin, I.*CORRIM Report: Life Cycle Assessment for the Production of Pacific Northwest Glued Laminated Timbers*; Consortium for Research on Renewable Industrial Materials, 2020; https://corrim.org/wp-content/uploads/2020/06/CORRIM-AWC-PNW-Glulam-v2.pdf (accessed 202203-02).
(214) Laurent, A. B.; Menard, J. F.; Lesage, P.; Beauregard, R. Cradle-to-Gate Environmental Life Cycle Assessment of the Portfolio of an Innovative Forest Products Manufacturing Unit. *BioResources* **2016**, *11*, 8981−9001.
(215) Khatri, P.; Sahoo, K.; Bergman, R.; Puettmann, M. Life Cycle Assessment of North American Laminated Strand Lumber (LSL) Production. *Recent Progress in Materials* **2021**, *3*, 1−1.
(216) Jarosch, L.; Zeug, W.; Bezama, A.; Finkbeiner, M.; Thrän, D. A Regional Socio-Economic Life Cycle Assessment of a Bioeconomy Value Chain. *Sustainability* **2020**, *12*, 1259.
(217) Bergman, R. D.; Alanya-Rosenbaum, S.*Cradle-to-Gate Life-Cycle Assessment of Laminated Veneer Lumber (LVL) Produced in the Pacific Northwest Region of the United States*; CORRIM Final Report, Module H2; Forest Service, U.S. Department of Agriculture, 2017; https://www.fpl.fs.usda.gov/documnts/pdf2017/fpl_2017_bergman003.pdf (accessed 2022-03-02).
(218) Ferrari, C. I.Life Cycle Assessment: Environmental Modeling of Plywood and Laminated Veneer Lumber Manufacturing. Master Thesis. Oregon State University, 2000.
(219) Bergman, R. D.; Alanya-Rosenbaum, S.*Cradle-to-Gate Life-Cycle Assessment of Laminated Veneer Lumber Produced in the Southeast Region of the United States*; CORRIM Final Report, Module H2; Forest Service, U.S. Department of Agriculture, 2016; https://www.fpl.fs.usda.gov/documnts/pdf2017/fpl_2017_bergman004.pdf (accessed 2022-03-03).
(220) Bergman, R. D.; Alanya-Rosenbaum, S. Cradle-to-Gate Life-Cycle Assessment of Laminated Veneer Lumber Production in the United States. *Forest Prod. J.* **2017**, *67*, 343−354.
(221) Zimmer, B.; Kairi, M.LCA of Laminated Veneer Lumber Finnforest Study. In *COST Action E9-Life Cycle Assessment on Forestry and Forest Products*; European Commission, 2000.
(222) Bergman, R. D.Life-Cycle Inventory Analysis of Laminated Veneer Lumber Production in the United States,*Proceedings of the 58th International Convention of Society of Wood Science and Technology, 2015, Jackson, WY*, 2015; p 1−14.
(223) Puettmann, M.; Oneil, E.; Wilson, J.; Johnson, L.*Cradle to Gate Life Cycle Assessment of Laminated Veneer Lumber Production from the Southeast*; Consortium for Research on Renewable Industrial Materials, 2013; https://citeseerx.ist.psu.edu/viewdoc/download;jsessionid=5A0B0D2173664C8B008FC36374D7163A?doi=10.1.1.432.7696&rep=rep1&type=pdf (accessed 2022-03-03).
(224) Boscato, G.; Mora, T. D.; Peron, F.; Russo, S.; Romagnoni, P. A New Concrete-Glulam Prefabricated Composite Wall System: Thermal Behavior, Life Cycle Assessment and Structural Response. *J. Build. Eng.* **2018**, *19*, 384−401.
(225) Bergman, R. D.; Alanya-Rosenbaum, S.*Life Cycle Assessment for the Production of PNW Laminated Veneer Lumber*; Consortium for Research on Renewable Industrial Materials, 2020; https://corrim.org/wp-content/uploads/2020/10/CORRIM-AWC-PNW-LVL.pdf (accessed 2022-03-03).
(226) Piekarski, C. M.; de Francisco, A. C.; da Luz, L. M.; Kovaleski, J. L.; Silva, D. A. L. Life Cycle Assessment of Medium-Density Fiberboard (MDF) Manufacturing Process in Brazil. *Sci. Total Environ.* **2017**, *575*, 103−111.
(227) Kouchaki-Penchah, H.; Sharifi, M.; Mousazadeh, H.; Zarea-Hosseinabadi, H. Life Cycle Assessment of Medium-Density Fiberboard Manufacturing Process in Islamic Republic of Iran. *J. Cleaner Prod.* **2016**, *112*, 351−358.
(228) Erdil, M.; Yılgör, N. An Assessment of Carbon Footprint in MDF Manufacturing: A Case Study of Wood Based Panel Production in Turkey. *J. Anatolian Environ. Anim. Sci.* **2020**, *5*, 841−848.
(229) Puettmann, M.; Sinha, A.*Life Cycle Assessment of Mass Ply Panels Produced in Oregon*; WoodLife Environmental Consultants, LLC, 2020; https://frereswood.com/wp-content/uploads/2021/01/Cradle-to-Gate-LCA-of-Oregon-MPP-November-2020-1.pdf (accessed 2022-03-08).
(230) Benetto, E.; Becker, M.; Welfring, J. Life Cycle Assessment of Oriented Strand Boards (OSB): From Process Innovation to Ecodesign. *Environ. Sci. Technol.* **2009**, *43*, 6003−6009.
(231) Puettmann, M.; Oneil, E.; Kline, E.; Johnson, L.*Cradle to Gate Life Cycle Assessment of Oriented Strandboard Production from the Southeast*; Consortium for Research on Renewable Industrial Materials, 2013; https://corrim.org/wp-content/uploads/2018/06/SE-OSB-LCA-May-2013-final.pdf (accessed 2022-03-08).
(232) Kaestner, D.Life Cycle Assessment of the Oriented Strand Board and Plywood Industries in the United States of America. Master Thesis. The University of Tennessee, 2015.
(233) Taylor, A. M.; Bergman, R. D.; Puettmann, M. E.; Alanya-Rosenbaum, S. Impacts of the Allocation Assumption in Life-Cycle Assessments of Wood-Based Panels. *Forest Prod. J.* **2017**, *67*, 390−396.
(234) Ferro, F. S.; Silva, D. A. L.; Rocco Lahr, F. A.; Argenton, M.; González-García, S. Environmental Aspects of Oriented Strand Boards Production. A Brazilian Case Study. *J. Cleaner Prod.* **2018**, *183*, 710−719.
(235) Tucker, S.; England, J.; Hall, M.; May, B.; Mitchell, P.; Tucker, S.; England, J.; Hall, M.; May, B.; Mitchell, P.Life Cycle Assessment of Forest and Wood Products in Australia. *Environmental Design Guide*; Royal Australian Institute of Architects, 2009; Vol. *37*, pp 1−10
(236) Puettman, M.; Kaestner, D.; Taylor, A.*Life Cycle Assessment for the Production of Oriented Strandboard Production*; Consortium for Research on Renewable Industrial Materials, 2019; https://corrim.org/

https://doi.org/10.1021/acs.chemrev.2c00450
Chem. Rev. 2023, 123, 1843−1888

wp-content/uploads/2020/12/CORRIM-AWC-OSB-Final.pdf (accessed 2022-03-09).
(237) Puettmann, M.; Oneil, E.; Wilson, J.; Johnson, L.*Cradle to Gate Life Cycle Assessment of Softwood Plywood Production from the Southeast*; Consortium for Research on Renewable Industrial Materials, 2013; https://citeseerx.ist.psu.edu/viewdoc/download?doi=10.1.1.431.1525&rep=rep1&type=pdf (accessed 2022-03-03).
(238) Jia, L.; Chu, J.; Ma, L.; Qi, X.; Kumar, A. Life Cycle Assessment of Plywood Manufacturing Process in China. *Int. J. Environ. Res. Public Health* **2019**, *16*, 2037.
(239) Gan, K.; Massijaya, M.*Life Cycle Assessment for Environmental Product Declaration of Tropical Plywood Production in Malaysia and Indonesia*; International Tropical Timber Organization, 2014; http://www.itto.int/files/user/pdf/EPD-LCA%20MERANTI%20PLYWOOD-FINAL%20REPORT.pdf (accessed on 2022-03-03).
(240) Wilson, J. B.; Sakimoto, E. T.Gate-to-Gate Life-Cycle Inventory of Softwood Plywood Production,*Wood Fiber Sci.*, **2005**; https://wfs.swst.org/index.php/wfs/article/view/1047 (accessed 2022-03-03).
(241) Ahmad, S.; Sahid, I.; Subramaniam, V.; Muhamad, H.; Mokhtar, A.Life Cycle Inventory for Palm Based Plywood: A Gate-To-Gate Case Study. *AIP Conference Proceedings*, 2013; pp 569−575.
(242) Chen, C. X.; Pierobon, F.; Ganguly, I. Life Cycle Assessment (LCA) of Cross-Laminated Timber (CLT) produced in Western Washington: The role of logistics and wood species mix. *Sustainability* **2019**, *11*, 1278.
(243) Puettmann, M.; Sinha, A.; Ganguly, I.*Life Cyle Assessment of Cross Laminated Timber Produced in Oregon*; Consortium for Research on Renewable Industrial Materials, 2018; https://corrim.org/wp-content/uploads/2019/02/Life-Cycle-Assessment-of-Oregon-Cross-Laminated-Timber.pdf (accessed 2022-03-03).
(244) *A Life Cycle Assessment of Cross-Laminated Timber Produced in Canada*; Athena Sustainable Materials Institute, 2013; http://www.athenasmi.org/resources/publications/ (accessed 2022-03-03).
(245) Vamza, I.; Diaz, F.; Resnais, P.; Radziņa, A.; Blumberga, D. Life Cycle Assessment of Reprocessed Cross Laminated Timber in Latvia. *Environ. Clim. Technol.* **2021**, *25*, 58−70.
(246) Cardellini, G.; Mutel, C. L.; Vial, E.; Muys, B. Temporalis, a Generic Method and Tool for Dynamic Life Cycle Assessment. *Sci. Total Environ.* **2018**, *645*, 585−595.
(247) Puettmann, M.; Oneil, E.; Milota, M.; Johnson, L.*Cradle to Gate Life Cycle Assessment of Softwood Lumber Production from the Pacific Northwest*; College of Information Sciences and Technology, Pennsylvania State University, 2013; https://citeseerx.ist.psu.edu/viewdoc/download?doi=10.1.1.639.6514&rep=rep1&type=pdf (accessed 2022-03-03).
(248) Laurent, A. B.; Gaboury, S.; Wells, J. R.; Bonfils, S.; Boucher, J. F.; Sylvie, B.; D'Amours, S.; Villeneuve, C. Cradle-to-Gate Life-Cycle Assessment of a Glued-Laminated Wood Product from Quebec's Boreal Forest. *Forest Prod. J.* **2013**, *63*, 190−198.
(249) Puettmann, M. E.; Wilson, J. B. Gate-to-Gate Life-Cycle Inventory of Glued-Laminated Timbers Production. *Wood Fiber Sci.* **2005**, *37*, 99−113.
(250) Gámez-García, D. C.; Gómez-Soberón, J. M.; Corral-Higuera, R.; Almaral-Sánchez, J. L.; Gómez-Soberón, M. C.; Gómez-Soberón, L. A. LCA as Comparative Tool for Concrete Columns and Glulam Columns. *J. Sustainable Architect. Civ. Eng.* **2015**, *11*, 21−31.
(251) Bowers, T.; Puettmann, M. E.; Ganguly, I.; Eastin, I. Cradle-to-gate Life-Cycle Impact Analysis of Glued-Laminated (Glulam) Timber: Environmental Impacts from Glulam Produced in the US Pacific Northwest and Southeast. *Forest Prod. J.* **2017**, *67*, 368−380.
(252) Petersen, A. K.; Solberg, B. Greenhouse Gas Emissions, Life-Cycle Inventory and Cost-Efficiency of Using Laminated Wood Instead of Steel Construction. Case: Beams at Gardermoen Airport. *Environ. Sci. Policy* **2002**, *5*, 169−182.
(253) Sandin, G.; Peters, G. M.; Svanström, M. Life Cycle Assessment of Construction Materials: The Influence of Assumptions in End-Of-Life Modelling. *Int. J. Life Cycle Assess.* **2014**, *19*, 723−731.
(254) Balasbaneh, A. T.; Sher, W. Comparative Sustainability Evaluation of Two Engineered Wood-Based Construction Materials: Life Cycle Analysis of CLT versus GLT. *Build. Environ.* **2021**, *204*, 108112.
(255) Lan, K.; Kelley, S. S.; Nepal, P.; Yao, Y. Dynamic Life Cycle Carbon and Energy Analysis for Cross-Laminated Timber in the Southeastern United States. *Environ. Res. Lett.* **2020**, *15*, 124036.
(256) Zimmermann, A. W.; Wunderlich, J.; Müller, L.; Buchner, G. A.; Marxen, A.; Michailos, S.; Armstrong, K.; Naims, H.; McCord, S.; Styring, P.; Sick, V.; Schomacker, R. Techno-Economic Assessment Guidelines for CO_2 Utilization. *Front. Energy Res.* **2020**, *8*, 5.
(257) Zhang, Z.; Lan, K. Understanding the Impacts of Plant Capacities and Uncertainties on the Techno-Economic Analysis of Cross-Laminated Timber Production in the Southern US. *J. Renewable Mater.* **2022**, *10*, 53.
(258) Lu, H. R.; El Hanandeh, A.; Gilbert, B.; Bailleres, H.A Comparative Life Cycle Assessment (LCA) of Alternative Material for Australian Building Construction. *MATEC Web of Conferences*, 2017; pp 1−9.
(259) González-García, S.; Feijoo, G.; Widsten, P.; Kandelbauer, A.; Zikulnig-Rusch, E.; Moreira, M. T. Environmental Performance Assessment of Hardboard Manufacture. *Int. J. Life Cycle Assess.* **2009**, *14*, 456−466.
(260) Nakano, K.; Ando, K.; Takigawa, M.; Hattori, N. Life Cycle Assessment of Wood-Based Boards Produced in Japan and Impact of Formaldehyde Emissions During the Use Stage. *Int. J. Life Cycle Assess.* **2018**, *23*, 957−969.
(261) Tanguay, X.; Essoua Essoua, G. G.; Amor, B. Attributional and Consequential Life Cycle Assessments in A Circular Economy with Integration of a Quality Indicator: a Case Study of Cascading Wood Products. *J. Ind. Ecol.* **2021**, *25*, 1462−1473.
(262) Niu, Y.; Rasi, K.; Hughes, M.; Halme, M.; Fink, G. Prolonging Life Cycles of Construction Materials and Combating Climate Change by Cascading: The Case of Reusing Timber in Finland. *Resour., Conserv. Recycl.* **2021**, *170*, 105555.
(263) Lan, K.; Park, S.; Yao, Y.Key Issue, Challenges, and Status Quo of Models for Biofuel Supply Chain Design. In *Biofuels for a More Sustainable Future: Life Cycle Sustainability Assessment and Multi-Criteria Decision Making*; Elsevier BV, 2019.
(264) Lan, K.; Zhang, B.; Yao, Y. Circular Utilization of Urban Tree Waste Contributes to the Mitigation of Climate Change and Eutrophication. *One Earth* **2022**, *5*, 944−957.
(265) Wernet, G.; Bauer, C.; Steubing, B.; Reinhard, J.; Moreno-Ruiz, E.; Weidema, B. The Ecoinvent Database Version 3 (Part I): Overview and Methodology. *Int. J. Life Cycle Assess.* **2016**, *21*, 1218−1230.
(266) *U.S. Life Cycle Inventory Database*; US National Renewable Energy Laboratory, 2022.
(267) Liu, Y.; Guo, H.; Sun, C.; Chang, W. S. Assessing Cross Laminated Timber (CLT) as an Alternative Material for Mid-Rise Residential Buildings in Cold Regions in China-a Life-Cycle Assessment Approach. *Sustainability* **2016**, *8*, 1047.
(268) Antonio, F.; Lahr, R.; Junior, H. S.; Fiorelli, J.*Non-conventional Building Materials Based on Agro-industrial Wastes*; Tiliform: Bauru, Brazil, 2015.
(269) Bolin, C. A.; Smith, S. Life Cycle Assessment of ACQ-Treated Lumber with Comparison to Wood Plastic Composite Decking. *J. Cleaner Prod.* **2011**, *19*, 620−629.
(270) Kouchaki-Penchah, H.; Sharifi, M.; Mousazadeh, H.; Zarea-Hosseinabadi, H.; Nabavi-Pelesaraei, A. Gate to Gate Life Cycle Assessment of Flat Pressed Particleboard Production in Islamic Republic of Iran. *J. Cleaner Prod.* **2016**, *112*, 343−350.
(271) Lan, K.; Ou, L.; Park, S.; Kelley, S. S.; Yao, Y. Life Cycle Analysis of Decentralized Preprocessing Systems for Fast Pyrolysis Biorefineries with Blended Feedstocks in the Southeastern United States. *Energy Technol.* **2020**, *8*, 1900850.
(272) Sahoo, K.; Bergman, R.; Puettmann, M.*Cradle-to-Gate Life-Cycle Assessment of North American Laminated Strand Lumber Production*; USDA Forest Service, Forest Products Laboratory, 2021;

https://www.fs.usda.gov/treesearch/pubs/63516 (accessed 2022-03-03).
(273) Ryberg, M.; Vieira, M. D.; Zgola, M.; Bare, J.; Rosenbaum, R. K. Updated US and Canadian Normalization Factors for TRACI 2.1. *Clean Technol. Environ. Policy* **2014**, *16*, 329−339.
(274) Pommier, R.; Grimaud, G.; Prinçaud, M.; Perry, N.; Sonnemann, G. LCA (Life Cycle Assessment) of EVP - Engineering Veneer Product: Plywood Glued Using A Vacuum Moulding Technology from Green Veneers. *J. Cleaner Prod.* **2016**, *124*, 383−394.
(275) Huijbregts, M. A.; Steinmann, Z. J.; Elshout, P. M.; Stam, G.; Verones, F.; Vieira, M.; Zijp, M.; Hollander, A.; van Zelm, R. ReCiPe2016: a Harmonised Life Cycle Impact Assessment Method at Midpoint and Endpoint Level. *Int. J. Life Cycle Assess.* **2017**, *22*, 138−147.
(276) Silva, D. A. L.; Lahr, F. A. R.; Garcia, R. P.; Freire, F. M. C. S.; Ometto, A. R. Life Cycle Assessment of Medium Density Particleboard (MDP) Produced in Brazil. *Int. J. Life Cycle Assess.* **2013**, *18*, 1404−1411.
(277) Rosenbaum, R. K.; Bachmann, T. M.; Gold, L. S.; Huijbregts, M. A.; Jolliet, O.; Juraske, R.; Koehler, A.; Larsen, H. F.; MacLeod, M.; Margni, M.; et al. USEtox—the UNEP-SETAC Toxicity Model: Recommended Characterisation Factors for Human Toxicity and Freshwater Ecotoxicity in Life Cycle Impact Assessment. *Int. J. Life Cycle Assess.* **2008**, *13*, 532−546.
(278) Silvestre, J. D.; Pargana, N.; De Brito, J.; Pinheiro, M. D.; Durão, V. Insulation Cork Boards-Environmental Life Cycle Assessment of an Organic Construction Material. *Materials* **2016**, *9*, 394.
(279) Sommerhuber, P. F.; Wenker, J. L.; Rüter, S.; Krause, A. Life Cycle Assessment of Wood-Plastic Composites: Analysing Alternative Materials and Identifying An Environmental Sound End-Of-Life Option. *Resour., Conserv. Recycl.* **2017**, *117*, 235−248.
(280) Guine´e, J. B.; Gorree, M.; Heijungs, R.; Huppes, G.; Kleijn, R.; van Oers, L.; Wegener Sleeswijk, A.; Suh, S.; Udo de Haes, H. A.; de Bruijn H, V., et al.*Handbook on Life Cycle Assessment: Operational Guide to the ISO Standards*; Kluwer Academic Publishers: New York, Boston, Dordrecht, London, Moscow, 2002.
(281) Goedkoop, M.; Spriensma, R.*Eco-indicator 99—A Damage Oriented Method for Life Cycle Impact Assessment*; PRe Consultants, 1999.
(282) Echeverria, D.; Venditti, R.; Jameel, H.; Yao, Y. Process Simulation-Based Life Cycle Assessment of Dissolving Pulps. *Environ. Sci. Technol.* **2022**, *56*, 4578−4586.
(283) Echeverria, D.; Venditti, R.; Jameel, H.; Yao, Y. A General Life Cycle Assessment Framework for Sustainable Bleaching: A Case Study of Peracetic Acid Bleaching of Wood Pulp. *J. Cleaner Prod.* **2021**, *290*, 125854.
(284) Bergman, R. D.Life-Cycle Inventory Analysis of I-Joist Production in the United States. *Proceedings of the 58th International Convention of Society of Wood Science and Technology, Grand Teton National Park, 2015, Jackson Hole, Wyoming*, 2015; p 1−14.
(285) Sahoo, K.; Bergman, R.; Khatri, P. Cradle-to-Grave Life-Cycle Assessment of Cellulosic Fiberboard. *Recent Prog. in Mater.* **2021**, *3*, 1−1.
(286) Puettmann, M.; Kaestner, D.; Taylor, A.*Life Cycle Assessment of Softwood Plywood Production in the US Pacific Northwest*; CORRIM Report, Module D1; Consortium for Research on Renewable Industrial Materials, 2016; https://www.corrim.org/wp-content/uploads/Module-D1-PNW-Plywood.pdf (accessed 2022-03-03).
(287) Bergman, R. D.; Alanya-Rosenbaum, S. Cradle-to-Gate Life-Cycle Assessment of Composite I-Joist Production in the United States. *Forest Prod. J.* **2017**, *67*, 355−367.
(288) Lan, K.Dynamic and Parametric Life Cycle Assessment Modeling Frameworks for Biomass Production and Biomass-Based Products. Ph.D. Dissertation. , North Carolina State University, 2020.
(289) Yao, Y.; Huang, R. A Parametric Life Cycle Modeling Framework for Identifying Research Development Priorities of Emerging Technologies: A Case Study Of Additive Manufacturing. *Procedia CIRP* **2019**, *80*, 370−375.
(290) Bergman, R. D.; Alanya-Rosenbaum, S.*Cradle-to-Gate Life-Cycle Assessment of Composite I-Joists Produced in the Southeast Region of the United*; Consortium for Research on Renewable Industrial Materials, 2017; https://www.fpl.fs.usda.gov/documnts/pdf2017/fpl_2017_bergman001.pdf (accessed 2022-03-03).
(291) Puettman, M.; Kaestner, D.; Taylor, A.*Life Cycle Assessment of Softwood Plywood Production in the US Southeast*; CORRIM Report, Module D2; Consortium for Research on Renewable Industrial Materials, 2016; https://corrim.org/wp-content/uploads/Module-D2-SE-Plywood.pdf (accessed 2022-03-03).
(292) Wilson, J. B.; Dancer, E. R.; Puettmann, M.; Sakimoto, E.*Laminated Veneer Lumber—Pacific Northwest and Southeast*; CORRIM Phase I Final Report, Module H; Consortium for Research on Renewable Industrial Materials, 2004; https://corrim.org/wp-content/uploads/2018/03/laminated-veneer-lumber-pnw-and-se.pdf (accessed 2022-03-03).
(293) González-García, S.; Feijoo, G.; Heathcote, C.; Kandelbauer, A.; Moreira, M. T. Environmental Assessment of Green Hardboard Production Coupled with A Laccase Activated System. *J. Cleaner Prod.* **2011**, *19*, 445−453.
(294) Wilson, J. B.; Dancer, E. R. Gate-to-Gate Life-Cycle Inventory of I-Joist Production. *Wood Fiber Sci.* **2006**, *37*, 85−98.
(295) Wilson, J. B.; Dancer, E. R. Gate-to-Gate Life-Cycle Inventory of Laminated Veneer Lumber Production. *Wood Fiber Sci.* **2005**, *37*, 114−127.
(296) Head, M.; Bernier, P.; Levasseur, A.; Beauregard, R.; Margni, M. Forestry Carbon Budget Models to Improve Biogenic Carbon Accounting in Life Cycle Assessment. *J. Cleaner Prod.* **2019**, *213*, 289−299.
(297) Cowie, A. L.; Berndes, G.; Bentsen, N. S.; Brandão, M.; Cherubini, F.; Egnell, G.; George, B.; Gustavsson, L.; Hanewinkel, M.; Harris, Z. M.; et al. Applying a Science-Based Systems Perspective to Dispel Misconceptions about Climate Effects of Forest Bioenergy. *GCB Bioenergy* **2021**, *13*, 1210−1231.
(298) Iordan, C. M.; Hu, X.; Arvesen, A.; Kauppi, P.; Cherubini, F. Contribution of Forest Wood Products to Negative Emissions: Historical Comparative Analysis from 1960 to 2015 in Norway, Sweden and Finland. *Carbon Balance Manage.* **2018**, *13*, 12.
(299) IPCC*Climate Change 2013: The Physical Science Basis. Contribution of Working Group I to the Fifth Assessment Report of IPCC the Intergovernmental Panel on Climate Change*; Cambridge University Press: Cambridge; New York, 2014.
(300) Head, M.; Levasseur, A.; Beauregard, R.; Margni, M. Dynamic Greenhouse Gas Life Cycle Inventory and Impact Profiles of Wood Used in Canadian Buildings. *Build. Environ.* **2020**, *173*, 106751.
(301) Pittau, F.; Lumia, G.; Heeren, N.; Iannaccone, G.; Habert, G. Retrofit as a Carbon Sink: The Carbon Storage Potentials of the EU Housing Stock. *J. Cleaner Prod.* **2019**, *214*, 365−376.
(302) Pingoud, K.; Ekholm, T.; Savolainen, I. Global Warming Potential Factors and Warming Payback Time as Climate Indicators of Forest Biomass Use. *Mitig. Adaptat. Strat. Gl.* **2012**, *17*, 369−386.
(303) Faraca, G.; Tonini, D.; Astrup, T. F. Dynamic Accounting of Greenhouse Gas Emissions from Cascading Utilisation of Wood Waste. *Sci. Total Environ.* **2019**, *651*, 2689−2700.
(304) Levasseur, A.; Lesage, P.; Margni, M.; Samson, R. Biogenic Carbon and Temporary Storage Addressed with Dynamic Life Cycle Assessment. *J. Ind. Ecol.* **2013**, *17*, 117−128.
(305) Levasseur, A.; Lesage, P.; Margni, M.; Brandão, M.; Samson, R. Assessing Temporary Carbon Sequestration and Storage Projects Through Land Use, Land-Use Change and Forestry: Comparison of Dynamic Life Cycle Assessment with Ton-Year Approaches. *Climatic change* **2012**, *115*, 759−776.
(306) Helin, T.; Sokka, L.; Soimakallio, S.; Pingoud, K.; Pajula, T. Approaches for Inclusion of Forest Carbon Cycle in Life Cycle Assessment-A Review. *GCB Bioenergy* **2013**, *5*, 475−486.
(307) Daystar, J.; Venditti, R.; Kelley, S. S. Dynamic Greenhouse Gas Accounting for Cellulosic Biofuels: Implications of Time Based Methodology Decisions. *Int. J. Life Cycle Assess.* **2017**, *22*, 812−826.

https://doi.org/10.1021/acs.chemrev.2c00450
Chem. Rev. 2023, 123, 1843−1888

(308) Levasseur, A.; Lesage, P.; Margni, M.; Deschenes, L.; Samson, R. Considering Time in LCA: Dynamic LCA and Its Application to Global Warming Impact Assessments. *Environ. Sci. Technol.* **2010**, *44*, 3169−3174.
(309) Zimmerman, J. B.; Anastas, P. T.; Erythropel, H. C.; Leitner, W. Designing for a Green Chemistry Future. *Science.* **2020**, *367*, 397−400.
(310) Cheung, W. M.; Leong, J. T.; Vichare, P. Incorporating Lean Thinking and Life Cycle Assessment to Reduce Environmental Impacts of Plastic Injection Moulded Products. *J. Cleaner Prod.* **2017**, *167*, 759−775.
(311) Yildirim, N. Life Cycle Assessment (LCA) of Nanocellulose Composite Panels (Ncps) Manufactured Using Freeze-Drying Technique. *Turkish J. Forest Res.* **2018**, *5*, 56−63.
(312) Santos, P.; Correia, J. R.; Godinho, L.; Dias, A. M. P. G.; Dias, A. Life Cycle Analysis of Cross-Insulated Timber Panels. *Structures* **2021**, *31*, 1311−1324.
(313) Hu, M.; Esram, N. W. The Status of Embodied Carbon in Building Practice and Research in the United States: A Systematic Investigation. *Sustainability* **2021**, *13*, 12961.
(314) De Wolf, C.; Pomponi, F.; Moncaster, A. Measuring Embodied Carbon Dioxide Equivalent of Buildings: A Review and Critique of Current Industry Practice. *Energy Buildings* **2017**, *140*, 68−80.
(315) Pan, L.; Zhang, T.; Li, W.; Li, Z.; Zhou, C. Sector-Level Evaluation of China's CO_2 Emissions: Trend Evolution and Index Ranking. *J. Clean. Prod.* **2021**, *286*, 125453.
(316) Esram, N. W. H. M.*Knowledge Infrastructure: The Critical Path to Advance Embodied Carbon Building Codes*. American Council for an Energy-Efficient Economy, Washington, DC2021.
(317) Lan, K.; Xu, Y.; Kim, H.; Ham, C.; Kelley, S. S.; Park, S. Techno-Economic Analysis of Producing Xylo-Oligosaccharides and Cellulose Microfibers from Lignocellulosic Biomass. *Bioresour. Technol.* **2021**, *340*, 125726.
(318) Lan, K.; Ou, L.; Park, S.; Kelley, S. S.; English, B. C.; Yu, T. E.; Larson, J.; Yao, Y. Techno-Economic Analysis of Decentralized Preprocessing Systems for Fast Pyrolysis Biorefineries with Blended Feedstocks in the Southeastern United States. *Renewable Sustainable Energy Rev.* **2021**, *143*, 110881.
(319) Lan, K.; Park, S.; Kelley, S. S.; English, B. C.; Yu, T. H. E.; Larson, J.; Yao, Y. Impacts of Uncertain Feedstock Quality on the Economic Feasibility of Fast Pyrolysis Biorefineries with Blended Feedstocks and Decentralized Preprocessing Sites in the Southeastern United States. *GCB Bioenergy* **2020**, *12*, 1014−1029.
(320) Mahmud, R.; Moni, S. M.; High, K.; Carbajales-Dale, M. Integration of Techno-Economic Analysis and Life Cycle Assessment for Sustainable Process Design - A Review. *J. Cleaner Prod.* **2021**, *317*, 128247.
(321) Persson, M.; Wogelberg, S.Analytical Models of Prestressed and Reinforced Glulam Beams: A Competitive Analysis of Strengthened Glulam Beams. Master Thesis. Chalmers University of Technology, 2011.
(322) Laufenberg, T. L.; Rowlands, R. E.; Krueger, G. P. Economic Feasibility of Synthetic Fiber Reinforced Laminated Veneer Lumber (Lvl). *Forest Prod. J.* **1984**, *34*, 15−22.
(323) Toksoy, D.; Çolakoğlu, G.; Aydin, I.; ÇOlak, S.; Demirkir, C. Technological and Economic Comparison of the Usage of Beech and Alder Wood in Plywood and Laminated Veneer Lumber Manufacturing. *Build. Environ.* **2006**, *41*, 872−876.
(324) Balasbaneh, A. T.; Marsono, A. K. B.; Khaleghi, S. J. Sustainability Choice of Different Hybrid Timber Structure for Low Medium Cost Single-Story Residential Building: Environmental, Economic and Social Assessment. *J. Build. Eng.* **2018**, *20*, 235−247.
(325) Adeeb, E.; Kim, T. W.; Sohn, C. H. Cost-Benefit Analysis of Medium-Density Fiberboard Production by Adding Fiber from Recycled Medium-Density Fiberboard. *Forest Prod. J.* **2019**, *68*, 414−418.
(326) Xie, X.; Luo, M.; Hu, S. Green Assessment Method for Industrial Technology: A Case Study of the Saline Lake Industry. *ACS Sustainable Chem. Eng.* **2022**, *10*, 1544−1553.
(327) Peters, M. S.; Timmerhaus, K. D.; West, R. E.*Plant Design and Economics for Chemical Engineers*; McGraw-Hill: New York, 2003.
(328) Brandt, K.; Wilson, A.; Bender, D.; Dolan, J. D.; Wolcott, M. P. Techno-Economic Analysis for Manufacturing Cross-Laminated Timber. *BioResources* **2019**, *14*, 7790−7804.
(329) Bédard, P.; Fournier, F.; Gagnon, S.; Gingras, A.; Lavoie, V.; Robichaud, F.*Manufacturing Cross-Laminated Timber (CLT) Technological and Economic Analysis*; Quebec Wood Export Bureau, 2010; https://library.fpinnovations.ca/en/permalink/fpipub39323 (accessed 2022-03-12).
(330) Spelter, B. H. Plywood Mill Economics. *Plywood Panel World* **1988**, *1988*, 18−20.
(331) Wijeyekoon, S.; Suckling, I.; Fahmy, M.; Hall, P.; Bennett, P. Techno-Economic Analysis of Tannin and Briquette Co-Production from Bark Waste: A Case Study Quantifying Symbiosis Benefits in Biorefinery. *Biofuels, Bioprod. Biorefin.* **2021**, *15*, 1332−1344.
(332) *National Design Specification for Wood Construction with Commentary*; American Wood Council: Leesburg, VA, 2018.
(333) *Glulam Product Guide*; APA—The Engineered Wood Association: Tacoma, WA, 2017; Vol. *X440E*.
(334) *CLT Handbook: Cross-Laminated Timber*, U.S. ed.; Karacabeyli, E., Douglas, B., Eds.; U.S. Department of Agriculture, Forest Service, Forest Products Laboratory, and Binational Softwood Lumber Council (BSLC): Pointe-Claire, Quebec, 2013.
(335) Foit, J.; Minard, A.; Jacobs, A. T.; Boyle, I.; Epp, L.; Bergen, N.; Brown, B.; Finch, G.; Shane, C.; Gerard, R.et al.*Nail-Laminated Timber: U.S. Design and Construction Guide*, v1.0;2017.
(336) *Mass Ply Design and Construction Guide*; Freres Engineered Wood: Lyons, OR, 2022.
(337) Hu, L.; Zhu, M.; Song, J.Strong and Tough Structural Wood Materials, and Methods for Fabricating and Use Thereof. US Patent Application B011130252, 2018.
(338) Harte, A. M. Mass Timber—The Emergence of a Modern Construction Material. *J. Struct. Integr. Maint.* **2017**, *2*, 121−132.
(339) Zahn, J. J.; Rammer, D. R. Design of Glued Laminated Timber Columns. *J. Struct. Eng.* **1995**, *121*, 1789−1794.
(340) *National Design Specification Design Values for Wood Construction*; American Wood Council: Leesburg, VA, 2018.
(341) Senalik, C. A.; Farber, B.*Commercial Lumber, Round Timbers, and Ties*; General Technical Report FPL-GTR-282; Forest Service, U.S. Department of Agriculture, 2021; Chapter 6, pp 1−25.
(342) Ross, L. A.; Gagnon, S.; Keith, E. In *CLT Handbook: Cross-Laminated Timber, U.S. ed.*; Karacabeyli, E.; Douglas, B., Eds.; U.,S. Department of Agriculture, Forest Service, Forest Products Laboratory, and Binational Softwood Lumber Council (BSLC): Pointe-Claire, Quebec, Canada, 2013.
(343) Senalik, C. A.; Farber, B.*Mechanical Properties of Wood*; General Technical Report FPL-GTR-282; Forest Service, U.S. Department of Agriculture, 2021; Chapter 5, 1−46.
(344) Danielsson, H.; Serrano, E. Cross Laminated Timber at In-Plane Beam Loading - Prediction of Shear Stresses in Crossing Areas. *Eng. Struct.* **2018**, *171*, 921−927.
(345) Rhude, A. J. Structural Glued Laminated Timber: History of Its Origins and Early Development. *Forest Prod. J.* **1996**, *46*, 15.
(346) Mohammad, M.; Gagnon, S.; Douglas, B. K.; Podesto, L. *Wood Des. Focus* **2012**, *22*, 3−12.
(347) Yeh, B.; Kretschmann, D.; Wang, B. J. In *CLT Handbook: Cross-Laminated Timber*, U.S. ed.; Karacabeyli, E., Douglas, B., Eds.; U.S. Department of Agriculture, Forest Service, Forest Products Laboratory, and Binational Softwood Lumber Council (BSLC): Pointe-Claire, Quebec, Canada, 2013.
(348) *Standard for Performance-Rated Cross-Laminated Timber*; ANSI/APA PRG 320; APA—The Engineered Wood Association: Tacoma, WA, 2018.
(349) *Standard Specification for Structural Glued Laminated Timber of Softwood Species*; ANSI 117; APA—The Engineered Wood Association: Tacoma, WA, 2020.
(350) Lehringer, C.; Gabriel, J.*Materials and Joints in Timber Structures*; Dordrecht, 2014; pp 405−420.

https://doi.org/10.1021/acs.chemrev.2c00450
Chem. Rev. 2023, 123, 1843−1888

(351) Miyamoto, B.; Bechle, N. J.; Rammer, D. R.; Zelinka, S. L. A Small-Scale Test to Examine Heat Delamination in Cross Laminated Timber (CLT). *Forests* **2021**, *12*, 232.
(352) Ceccotti, A.; Sandhaas, C.; Okabe, M.; Yasumura, M.; Minowa, C.; Kawai, N. SOFIE project - 3D Shaking Table Test on A Seven-Storey Full-Scale Cross-Laminated Timber Building. *Earthq. Eng. Struct. Dyn.* **2013**, *42*, 2003−2021.
(353) Gröndahl, M. In *The New York Times: Science*; The New York Times Company: New York, 2012; Vol. *2021*.
(354) *Perkins + Will Survey of International Tall Wood Buildings*; Forestry Innovation Investment and Binational Softwood Lumber Council, 2014.
(355) *Cross-Laminated Timber: Structural Principles*; Timber Research and Development Association, 2009.
(356) Durlinger, B.; Crossin, E.; Wong, J. P.*Life Cycle Assessment of a Cross Laminated Timber Building*; Forest & Wood Products Australia Limited, 2013.
(357) Cadorel, X.; Crawford, R.*Life Cycle Analysis of Cross Laminated Timber in Buildings: A Review*; The Architectural Science Association (ANZAScA), 2018.
(358) Showalter, J. B. In *Building Safety Journal*; International Code Council: Washington DC, 2020.
(359) Zelinka, S. L.; Hasburgh, L. E.; Bourne, K. J.; Tucholski, D. R.; Ouellette, J. P.; Kochkin, V.*Compartment Fire Testing of a Two-Story Mass Timber Building*; United States Department of Agriculture, Forest Service, Forest Products, 2018.
(360) Laguarda Mallo, M. F.; Espinoza, O. Awareness, Perceptions and Willingness to Adopt Cross-Laminated Timber by the Architecture Community in the United States. *J. Clean. Prod.* **2015**, *94*, 198−210.
(361) Foster, R. M.; Reynolds, T.; Ramage, M. Proposal for Defining a Tall Timber Building. *J. Struct. Eng.* **2016**, *142*, 02516001.
(362) Fast, P.; Jackson, R. In *STRUCTURE magazine*; C3 Ink: Reedsburg, WI, **2017**; Vol. *24*.
(363) Fernandez, A.; Komp, J.; Peronto, J. Ascent-Challenges and Advances of Tall Mass Timber Construction. *Int. J. High-Rise Build* **2020**, *9*, 235−244.
(364) *Calculating the Fire Resistance of Wood Members and Assemblies*; Technical Report 10; *American Wood Council*, 2021.
(365) *2021 International Building Code*; International Code Council, Incorporated: Country Club Hills, IL, 2020.
(366) *National Design Specification Supplement (NDS) Design Values for Wood Construction*, 2018 ed.; American Wood Council: Leesburg, VA, 2017.
(367) Taranath, B. S.*Reinforced Concrete Design of Tall Buildings*; CRC Press, 2009.
(368) Beairsto, C.; Gupta, R.; Miller, T. H. Monotonic and Cyclic Behavior of CLT Diaphragms. *Pract. Period. Struct. Des. Constr.* **2022**, *27*, 04021085.
(369) Bhardwaj, B.; Pang, W.; Rammer, D.; Amini, M. O.; Pryor, S. E.Experimental Performance Testing of Cantilever Cross-Laminated Timber (CLT) Diaphragm under in-Plane Shear. *World Conference on Timber Engineering, Santiago, Chile, August*, 2021.
(370) Line, P.; Nyseth, S.; Waltz, N. Full-Scale Cross-Laminated Timber Diaphragm Evaluation. II: CLT Diaphragm Connection Tests. *J. Struct. Eng.* **2022**, *148*, 04022038.
(371) Line, P.; Nyseth, S.; Waltz, N. Full-Scale Cross-Laminated Timber Diaphragm Evaluation. I: Design and Full-Scale Diaphragm Testing. *J. Struct. Eng.* **2022**, *148*, 04022037.
(372) Pei, S.; van de Lindt, J. W.; Barbosa, A. R.; Berman, J. W.; McDonnell, E.; Daniel Dolan, J.; Blomgren, H.-E.; Zimmerman, R. B.; Huang, D.; Wichman, S. Experimental Seismic Response of a Resilient 2-Story Mass-Timber Building with Post-Tensioned Rocking Walls. *J. Struct. Eng.* **2019**, *145*, 04019120.
(373) Blomgren, H.-E.; Pei, S.; Jin, Z.; Powers, J.; Dolan, J. D.; van de Lindt, J. W.; Barbosa, A. R.; Huang, D. Full-Scale Shake Table Testing of Cross-Laminated Timber Rocking Shear Walls with Replaceable Components. *J. Struct. Eng.* **2019**, *145*, 04019115.
(374) van de Lindt, J. W.; Furley, J.; Amini, M. O.; Pei, S.; Tamagnone, G.; Barbosa, A. R.; Rammer, D.; Line, P.; Fragiacomo, M.; Popovski, M. Experimental Seismic Behavior of A Two-Story CLT Platform Building. *Eng. Struct.* **2019**, *183*, 408−422.
(375) *Quantification of Building Seismic Performance Factors*; FEMA P-695; Federal Emergency Management Agency: Washington DC, 2009.
(376) van de Lindt, J. W.; Amini, M. O.; Rammer, D.; Line, P.; Pei, S.; Popovski, M. Seismic Performance Factors for Cross-Laminated Timber Shear Wall Systems in the United States. *J. Struct. Eng.* **2020**, *146*, 04020172.
(377) Pei, S.; Dolan, J.; Zimmerman, R.; McDonnell, E.; Popovski, P.From Testing to Codification: Post-tensioned Cross Laminated Timber Rocking Walls. In *Proceedings of the International Network for Timber Engineering Research (INTER)*; National Science Foundation, 2019.
(378) Ryan, K. L.; Pei, S.; Hutchinson, T.*Shake Table Testing of a 10-story Mass Timber Building with Nonstructural Components*; National Science Foundation, 2022.
(379) Abrahamsen, R.Mjøstårnet−Construction of an 81 m Tall Timber Building. *Internationales Holzbau-Forum IHF*, 2017.
(380) *Timber Tower Research Project, Skidmore, Owings & Merrill, LLP*; Softwood Lumber Board, 2014.
(381) Steiger, R.; Serrano, E.; Stepinac, M.; Rajčić, V.; O'Neill, C.; McPolin, D.; Widmann, R. Strengthening of Timber Structures with Glued-In Rods. *Constr Build Mater.* **2015**, *97*, 90−105.
(382) *Revolutionary Technology, Millions Of Years Old. Discover How the Latest Breakthroughs in Wood Can Help You and the World*; Inventwood, LLC: College Park, MD, 2020; www.inventwood.com.
(383) Kitek Kuzman, M.; Klarić, S.; Pirc Barčić, A.; Vlosky, R. P.; Janakieska, M. M.; Grošelj, P. Architect Perceptions of Engineered Wood Products: An Exploratory Study of Selected Countries in Central and Southeast Europe. *Constr Build Mater.* **2018**, *179*, 360−370.
(384) Markström, E.; Kuzman, M. K.; Bystedt, A.; Sandberg, D.; Fredriksson, M. Swedish Architects View of Engineered Wood Products in Buildings. *J. Clean. Prod.* **2018**, *181*, 33−41.
(385) Arehart, J. H.; Srubar III, W. V.; Pomponi, F.; D'Amico, B. Embodied Energy and Carbon Emissions of DOE Prototype Buildings from a Life Cycle Perspective. *ASHRAE Trans.* **2020**, *126*, 38−47.
(386) Ivanović-Šekularac, J.; Čikić-Tovarović, J.; Šekularac, N. Application of Wood as an Element of Façade Cladding in Construction and Reconstruction of Architectural Objects to Improve Their Energy Efficiency. *Energy Build.* **2016**, *115*, 85−93.
(387) Sandberg, D.; Kutnar, A.; Mantanis, G. Wood modification technologies - a review. *iForest - Biogeosciences and Forestry* **2017**, *10*, 895−908.
(388) Pei, S.; Rammer, D.; Popovski, M.; Williamson, T.; Line, P.; van de Lindt, J. W.An Overview of CLT Research and Implementation in North America. In *WCTE 2016, World Conference on Timber Engineering August 22−25, 2016, Vienna*, 2016.
(389) Chang, S. J.; Wi, S.; Kang, S. G.; Kim, S. Moisture Risk Assessment of Cross-Laminated Timber Walls: Perspectives on Climate Conditions and Water Vapor Resistance Performance of Building Materials. *Build Environ* **2020**, *168*, 106502.
(390) Pei, S.; Stogdill, J.; Glass, S. V.; Zelinka, S.; Kordziel, S.; Tabares-Velasco, P. C. Long-Term Moisture Monitoring Results of an Eight-Story Mass Timber Building in the Pacific Northwest. *J. Archit. Eng.* **2021**, *27*, 06021002.
(391) Barber, D. Fire Safety of Mass Timber Buildings with CLT in USA. *Wood Fiber Sci.* **2018**, *50*, 83−95.
(392) Wiesner, F.; Bisby, L. A.; Bartlett, A. I.; Hidalgo, J. P.; Santamaria, S.; Deeny, S.; Hadden, R. M. Structural Capacity in Fire of Laminated Timber Elements in Compartments with Exposed Timber Surfaces. *Eng. Struct.* **2019**, *179*, 284−295.
(393) Hadden, R. M.; Bartlett, A. I.; Hidalgo, J. P.; Santamaria, S.; Wiesner, F.; Bisby, L. A.; Deeny, S.; Lane, B. Effects of Exposed Cross Laminated Timber on Compartment Fire Dynamics. *Fire Saf. J.* **2017**, *91*, 480−489.
(394) Wade, C.; Spearpoint, M.; Fleischmann, C.; Baker, G.; Abu, A. Predicting the Fire Dynamics of Exposed Timber Surfaces in Compartments Using A Two-Zone Model. *Fire Technol.* **2018**, *54*, 893−920.

https://doi.org/10.1021/acs.chemrev.2c00450
Chem. Rev. 2023, 123, 1843−1888

(395) Tlustochowicz, G.; Serrano, E.; Steiger, R. State-of-the-Art Review on Timber Connections with Glued-In Steel Rods. *Mater. Struct.* **2011**, *44*, 997−1020.
(396) Gilbertson, L. M.; Zimmerman, J. B.; Plata, D. L.; Hutchison, J. E.; Anastas, P. T. Designing Nanomaterials to Maximize Performance and Minimize Undesirable Implications Guided by the Principles of Green Chemistry. *Chem. Soc. Rev.* **2015**, *44*, 5758.
(397) Anastas, P.; Eghbali, N. Green Chemistry: Principles and Practice. *Chem. Soc. Rev.* **2010**, *39*, 301−312.
(398) Fink, H.-P.; Philipp, B.; Paul, D.; Serimaa, R.; Paakkari, T. The Structure of Amorphous Cellulose as Revealed by Wide-Angle X-Ray Scattering. *Polymer* **1987**, *28*, 1265−1270.
(399) Ebeling, T.; Paillet, M.; Borsali, R.; Diat, O.; Dufresne, A.; Cavaillé, J. Y.; Chanzy, H. Shear-Induced Orientation Phenomena in Suspensions of Cellulose Microcrystals, Revealed by Small Angle X-ray Scattering. *Langmuir* **1999**, *15*, 6123−6126.
(400) Kobayashi, K.; Hwang, S.-W.; Okochi, T.; Lee, W.-H.; Sugiyama, J. Non-Destructive Method for Wood Identification Using Conventional X-Ray Computed Tomography Data. *J. Cult. Herit.* **2019**, *38*, 88−93.
(401) Lyczakowski, J. J.; Bourdon, M.; Terrett, O. M.; Helariutta, Y.; Wightman, R.; Dupree, P. Structural Imaging of Native Cryo-Preserved Secondary Cell Walls Reveals the Presence of Macrofibrils and Their Formation Requires Normal Cellulose, Lignin and Xylan Biosynthesis. *Front. Plant Sci.* **2019**, *10*, 1398.
(402) Van Schoubroeck, S.; Thomassen, G.; Van Passel, S.; Malina, R.; Springael, J.; Lizin, S.; Venditti, R. A.; Yao, Y.; Van Dael, M. An Integrated Techno-Sustainability Assessment (TSA) Framework for Emerging Technologies. *Green Chem.* **2021**, *23*, 1700−1715.
(403) Solo-Gabriele, H.; Fleming, L. E.; Townsend, T.; Cai, Y.Disposal Strategies for CCA-Treated Wood. In *2003 RCRA National Meeting: Putting Resource Conservation into RCRA, 12−15 August*, 2003; pp 943−1006.

https://doi.org/10.1021/acs.chemrev.2c00450
Chem. Rev. 2023, 123, 1843−1888